Ana Catarina Freire Moreira

Using Magnetic Resonance Images for planning treatments in External Radiotherapy- validation procedures for planning "*MRI-only*"

Dissertation submitted to Faculdade de Ciências da Universidade do Porto to obtain a Master's degree in Medical Physics

Supervisor: João António Miranda dos Santos, Assessor de Saúde (Física Médica) no Instituto Português de Oncologia Francisco Gentil, EPE e Professor Afiliado da Universidade do Porto (ICBAS)

Co-Supervisor: Joana Borges Lencart e Silva Assessora de Saúde (Directora do Serviço de Física Médica) no Instituto Português de Oncologia Francisco Gentil, EPE

Departamento de Física e Astronomia
Faculdade de Ciências da Universidade do Porto
September 2013

Acknowledgments

During this project I had the support and help of several people, without whom it would have been easy to accomplish my master thesis.

I wish to thank to Dr. João Santos, to accept guide this thesis, for all the support, knowledge and availability expended throughout this project as well as to Dr. Joana Lencart for help in performing the experimental component and have afforded me the opportunity to integrate the field of radiotherapy.

Other important person, who could not fail to thank, is Dr. Helena Pereira, Service director of External Radiotherapy, who authorized this study using data (non-confidential) of the patients.

At Sune K. Buhl of the Department of Oncology (52AA) of Herlev Ringvej University Hospital in Copenhagen, my huge thank you for having given me access to their own version of the script of camouflages the MR images, which served as the basis of one used in this thesis.

I would like to thank the service team of Medical Physics IPO Porto in particular to the Physicist Luís Cunha for his help in adapting the script and, as might be expected, to understand the occupation of his office.

I also wanted to thank the technologists of Radiology and Radiotherapy for understanding and cooperation during the acquisition of CT and MR images. I also thank dosimetrist Fatima Borges helped me some times during the planning steps.

My thanks to all.

Communications

Influence of the organ CT units assignment for MRI only based external radiotherapy treatment planning, *A.C. Moreira, J. Lencart, J.A.M. Santos*, International Conference on Medical Physics (ICMP 2013), Brighton, 31st - 4th September 2013. (POSTER PRESENTATION)

Uso exclusivo de imagens de Ressonância Magnética no plano de tratamento de Radioterapia Externa – "*MRI only*", *A.C. Moreira, J. Lencart, J.A.M. Santos, 1º* Encontro Nacional de Física Médica e Engenharia Biomédica, Instituto Português de Oncologia de Lisboa Francisco Gentil, E.P.E., 7th - 9th November 2013. (POSTER PRESENTATION)

Abstract

In External Radiotherapy (ER) the calculation of the dose distribution is based on the knowledge of interaction between the ionizing radiation and tissue. This interaction depends not only on the geometry and the energy spectrum of the beam but also on the electronic density (related to the attenuation coefficient) geometrical distribution of the various types of tissues. Therefore, computed tomography images (CT) are used as a support for dose distribution calculation, which combine the information of the location of the organs with the information of the electronic density (and attenuation coefficient) of the different tissues.

However, regarding to various soft tissues, which have attenuation coefficients very similar, the CT images have a low contrast resolution between different soft tissues being sometimes difficult to distinguish the borders between organs at risk and tumour.

Some examples are brain, prostate or gynecological tumours. In these cases, and given its high contrast resolution, one uses the image of Magnetic Resonance Imaging (MRI) as an aid in contouring both the organs at risk and the volumes to be treated, using the registration and fusion of CT and MR image sets. If there are already MR images of the patient, presumably their usage will be possible for the delineation of volumes and by the planning system to implement the treatment plan for radiotherapy.

Some studies have already been made on the exclusive use of MR images for the planning of a radiotherapy treatment on brain tumours [Prabhakar *et al*., 2007; Karlsson *et al.*, 2009; Jonsson *et al*., 2010], on which the distribution of the electronic density necessary for the planning is integrated in the MRI using various methods. It is this perspective that governs the objectives of this work.

This procedure is not yet established in common clinical practice nor is part of the External Radiotherapy protocols due to the lack of a universal consensus as to its applicability. Hence the importance of this study as a possible contribution to a future application.

KEYWORDS: External Radiotherapy (ER), Computed Tomography (CT), electronic density, attenuation coefficient, Magnetic Resonance Imaging (MRI).

Resumo

Em Radioterapia Externa (RE) o cálculo de distribuição de dose baseia-se na interação entre a radiação ionizante e os tecidos, interação essa que depende não só da geometria e do espectro de energias do feixe como da densidade eletrónica (relacionada com o coeficiente de atenuação) dos tecidos irradiados. Assim, utilizam-se como suporte para o cálculo, imagens de tomografia computorizada (CT), que aliam a informação da localização dos órgãos à informação da densidade eletrónica (e coeficiente de atenuação) dos diferentes tecidos.

No entanto, no que toca aos diferentes tecidos moles, os quais têm coeficientes de atenuação muito próximos, as imagens de CT têm uma baixa resolução de contraste entre os tecidos moles sendo, por vezes, difícil distinguir as fronteiras entre órgãos de risco e tumor. São exemplo disso, lesões cerebrais, tumores da próstata ou ginecológicos. Nestes casos, e dada a sua elevada resolução de contraste, utiliza-se a imagem de Ressonância Magnética (MR) como auxiliar na marcação, tantos dos órgão de risco como dos volumes a tratar, recorrendo ao registo e fusão dos conjuntos de imagens de CT e MR. Existindo já imagens de MR do doente, é em princípio possível a sua utilização para a marcação dos volumes e utilização pelo sistema de planeamento para a execução do plano de tratamento de Radioterapia.

Já têm sido feitos alguns estudos de utilização apenas de imagens de MR para planeamento de tratamentos de radioterapia a tumores cerebrais [Prabhakar *et al.*, 2007; Karlsson *et al.*, 2009; Jonsson *et al.*, 2010], nos quais as distribuições de densidades eletrónicas necessárias para o planeamento são integradas nas imagens de MR, utilizando vários métodos. É nesta perspetiva que se rege os objetivos deste trabalho.

Este procedimento não está ainda estabelecido na prática clínica nem faz parte dos protocolos de RE por ainda não haver um consenso universal quanto à sua aplicabilidade. Daí a importância da sua realização, com um possível contributo para uma futura aplicação.

PALAVRAS-CHAVE: Radioterapia Externa, Tomografia Computorizada (CT), densidade eletrónica, coeficiente de atenuação, Imagem de Ressonância Magnética (MRI).

Contents

List of figures

Chapter 2

Chapter 3

Chapter 4

Chapter 5

List of tables

Chapter 2

Chapter 3

Chapter 5

List of acronyms

%	Percentage
μ	Linear attenuation coefficient
^{0}	Degrees
2D	Two dimensions
3D	Three dimensions
AAA	Anisotropic Analytical Algorithm
AAPM	American Association of Physicists in Medicine
ACR	American College of Radiology
ALARA	As Low As Reasonable Achievable
B_0	External Magnetic Field
B_1	Magnetic Field
C	Carbon Ion
CE	Compton Effect
cm	centimetres
CT	Computerized Tomography
CTV	Clinical Target Volume
DICOM	Digital Imaging and Communication in Medicine
d_{max}	Maximum Distance
DMLC	Dynamic Multi-Leaf Collimator
DVH	Dose-Volume Histogram
E	Photon Energy
ER	External Radiotherapy
F	Fluor Ion
FID	Free Induction Decay
FRFSE	Fast Relaxation Fast Spin Echo
FSE	Fast Spin Echo
g	grammas
GE	Gradient-Echo
GHz	Giga Hertz
GTV	Gross Tumour Volume
H	Hydrogen proton
H_2O	Water
HU	Hounsfield Units
I	Final intensity of the beam

I_0	Initial intensity of the beam
IORT	Intraoperative Radiation Therapy
ICRU	International Committee on Radiation Units and Measurements
IGRT	Image Guided Radiotherapy
IMAT	Intensity Modulated Arc Therapy
IMRT	Intensity Modulated Radiation Therapy
ITV	Internal Target Volume
IV	Irradiated Volume
KeV	Kilo Electron-Volt
Linac	Linear accelerator
M_0	Total Magnetization
MeV	Mega Electron-Volt
MHz	Mega Hertz
min	Minutes
mm	millimetres
ms	milliseconds
MR	Magnetic Resonance
MRI	Magnetic Resonance Imaging
MSF	Multiple-Static-Field
MU	Monitor Units
M_{xy}	Transversal Magnetization
M_z	Longitudinal Magnetization
Na	Sodium Ion
NEMA	National Electrical Manufactures Association
NMR	Nuclear Magnetic Resonance
OAR	Organ at Risk
P	Phosphor Ion
PACS	Picture Archiving and Communication System
PBC	Pencil Beam Convolution
PDD	Percentage Depth Dose
PE	Photoelectric Effect
PET	Positron Emission Tomography
PTV	Planning Target Volume
RF	Radio Frequency
RTP	Radiotherapy Treatment Planning
RX	X-Rays
SE	Spin-Echo

SOP	Service-Object Pairs
SPECT	Single-Proton Emission Computed Tomography
SSD	Source-Surface Distance
T	Tesla
TE	Echo time
TR	Repetition time
T1	Time Constant of longitudinal relaxation
T2	Time Constant of transversal relaxation
TBI	Total Body Irradiation
TPS	Treatment Planning System
TV	Treated Volume
UID	Unique Identifiers
US	Ultra Sounds
VMAT	Volumetric Modulated Arc Therapy
VOI	Volumes of Interest
w	Larmor Frequency
Z	Atomic number
$\mathbf{Z_{eff}}$	Effective atomic number
$\boldsymbol{x}$	Material thickness
$\boldsymbol{\rho}$	Bulk density of the material

Chapter 1

INTRODUCTION

1. Introduction

Currently, the images obtained by computed tomography (CT) are the ones used in the planning of External Radiotherapy (ER) due to its imaging characteristics in terms of the quality of definition of contours on the anatomy of each patient. However, factors such as the low contrast resolution in tissues with attenuation coefficients too similar, lead to consider whether this will be the best choice for a higher quality images for ER treatment planning.

It is thus recommended the use of magnetic resonance imaging (MRI), which is a method of imaging diagnosis established in clinical practice and which is in increasing progress [Beavis *et al.*, 1998]. Its use in the treatment planning in external radiotherapy brings an added value with regard to the distinction between the tumour and the components of risk, when it comes to soft tissues.

The MRI is based on the interaction of magnetic properties of hydrogen with the application of an external magnetic field and with the production of radio frequency waves, which results in the production of highly detailed images of the human body.

The images obtained by MRI are acquired from the application of nuclear magnetic resonance (NMR). These in turn are dependent upon absorption of radio waves by hydrogen nuclei H (composed of one proton and one neutron), wherein this has an intrinsic nuclear spin which is present in sufficient amounts to enable the production of a beneficial anatomical image since most of the protons existing in the human body (mainly consisting of water) is found in nuclei of water.

The MRI has introduced several benefits on diagnostic imaging that can confer some advantages over the use of CT, as regards its application in the treatment planning in External Radiotherapy (RTP) [Chen *et al.*, 2004a and 2004b; Jonsson *et al.*, 2010; Prabhakar *et al.*, 2007].

The high contrast in the soft tissues, which allows a better definition of the contours of the tumour, is one of the main pre-eminences that derive from its use in planning the treatment, as well as obtaining a multi-planar image.

Compared with the image obtained by computed tomography, MRI avoids any type of patient exposure to ionizing radiation (by most insignificant as this exposure might be), which causes it to be exposed to the minimum possible radiation in the treatment (respecting the ALARA Principle - As Low As Reasonably Achievable). When it comes to a diagnostic image of this idea is important. However for images used

exclusively for planning, exposure to ionizing radiation becomes negligible, taking into account the doses to which the patient will be exposed during the treatment.

For some types of cancer, particularly in soft tissues (such as in the brain, in the prostate or gynecological), the planning based only on MRI may be sufficient. Nevertheless, the disadvantages entailed by the use of the image obtained by MR make the treatment plan in ER be faithfully governed by diagnostic images obtained by CT. Some of these limitations are:

- Artefacts and geometric distortions in the image due to effects associated with the system or induced by subject/body, that change the exact representation of anatomical structures, i.e., the spatial location and relative intensity, leading to inaccuracies in the calculation of the distribution of the dose. The image distortions associated with the system are generated by heterogeneities in the main magnetic field distribution and due to non-linearity of gradient, while the distortions caused by the object are generated by the variations of sensitivity and chemical shift (which happens because the core of the system of spins is surrounded by different chemical environments (molecules) in a chemically heterogeneous object).

- Absence of electron density information of the tissues necessary for dosimetric calculations.

- Nonexistence of signal corresponding to bone structures, namely this structure has an important role serving as a reference in locating other structures due to their high electron density and the respective attenuation coefficients, when it comes to CT images. However, in MRI, as this material is extremely arid in water (rich in hydrogen nuclei) it is not permissible to obtain an anatomical image where it will be easy to observe accurately, for example, the tissue-bone interface recognizing the contour shape, thereby preventing the distinction between tumour and organs at risk.

As stated above, the MRI is a superior modality in the evaluation of tumours in soft tissues while the image obtained by CT provides a better visualization of the tumour in bone regions. In its turn, the CT provides information of electronic density extremely indispensable for the dose calculation.

Thus, there is often the need to aggregate these two techniques to associate the information from each of the sets of images on the treatment plan, then resorting to the fusion of the CT with the MRI.

All these factors lead to a weighting which must be taken into account when you want to optimize the quality of the image obtained, in order to have the most appropriate treatment possible to the needs of the patient.

At the end of the last decade up to today, there have been some studies that claim to prove this situation, in particular, some authors such as Stanescu *et al.* (2006 and 2008), Chen *et al.* (2004a, 2004b and 2007), Dowling *et al*. (2012), among others.

Under a general perspective, Stanescu *et al*. (2006) proposed the application of MR images on the TPS from the "transformation" of these in CT images of brain lesions, i.e., following the acquisition of the MR images one preceded to the segmentation of the anatomical structures in three distinct regions: brain, bone and scalp. Then it was assigned to each of the volumes the values of electronic density on corresponding mass, for example, 1.47 g/cm^3 to 1 g/cm^3 for the brain and the scalp. From here, as the target volumes are marked and have associated the respective information of electronic density, it is then possible to proceed to the calculation of the dose. The results were compared with the results obtained with only the CT images fused with the MRI, and were evaluated based on dose-volume histograms (DVH) and in terms of dose distribution. Stanescu *et al.* (2006) concluded that the proposed 3T MR only based treatment planning procedure performs as well as the standard clinical procedure that relies on both CT and MR studies. MRI simulation can significantly reduce the patient treatment cost and save staff and machine time, and avoid any errors that may be associated with the image fusion process.

Similarly, Chen *et al.* (2004a and 2007) and Dowling *et al.* (2012) applied a similar methodology but in a study of prostate tumours and reached similar conclusions.

As is to be expected, all the studies carried out are always based on CT images to prove the exclusive applicability of the MRI in TPS, which means there is still uncertainty in applying the technique without resorting to the standard technique to make sure that the process is feasible.

In addition, there is still a great difficulty in changing the regulatory structure on which the entire planning system is guided, because there is still a great linking in the use of images obtained by CT, calling into question the legality of this new procedure.

A question must be asked: will the exclusive use of the MRI in the treatment plan in external radiotherapy be feasible and in which pathology it will prevail advantages over CT?

It is starting from this controversy, that the present study is based on trying to demonstrate, by means of tests, that it is possible to employ this technique without resorting to images obtained by Computed Tomography, so that in the near future this procedure be applicable, exclusively, in the system of treatment planning in External Radiotherapy.

1.1 Motivation

The elaboration of a correct clinical diagnosis is an indispensable factor for the treatment of patients. The use of radiological imaging has a fundamental role serving as an auxiliary means of diagnosis and therapy.

When it comes to cancer patients, the production of high quality images which allow a correct and accurate diagnosis is of extreme importance in order to make an effective therapy in the suppression of the tumour.

In the treatment of cancer cases by External Radiotherapy, the position of the organs as well as the information of the electronic density of the different tissues (necessary for the calculation of the dose distribution) are obtained from CT images. However, the contribution of this technique in the treatment plan in RE does not always provide sufficient information to be able to make a precise delineation of the volume to be treated. Furthermore, the patient is exposed to more ionizing radiation, although being almost insignificant, when compared with the doses received in the treatment with radiation.

This way, the use of MRI (in addition to other methods for obtaining image, such as the PET (positron emission tomography)), has been increasingly, bringing a significant value in the determination of tumours in soft tissues. In turn, the lack of information on the electronic density is one of the main obstacles associated with this method.

The symbiosis of the CT with the MR is already a fact, allowing to correct the inaccuracies obtained by the CT, which are compensated for by the MR and vice-versa. However, the merging of the two types of image is relatively complicated and leads in most cases to distortions.

Given all of these implications, some studies (Stanescu *et al.,* 2006, 2008; Chen *et al.,* 2004a, 2004b, 2007; Dowling *et al.,* 2011, 2012) have already been drawn up, and apply methods that allow the collection of information from the electronic density required and that in turn is coupled to MRI, allowing its exclusive use in TPS when it comes to injuries at the level of the brain, of gynecological tumours among others located in areas of soft tissue.

The feasibility of MRI, as single technique in the planning treatment for cancer patients in External Radiotherapy, in accordance with the anatomical region considered and pathology and the carrying out of tests which prove this situation is reflected in a strong motivation for the preparation of this work.

1.2 Objectives

The main goal of this thesis is studying the curt and feasibility of the exclusive application of Magnetic Resonance imaging in treatment plan in external radiotherapy.

The planned work will consist of four essential phases:

a) Make an approach to the construction methodologies of the electronic density distributions from images of MR;

b) Assign information to components outlined in MRI.

c) Make a comparison of dose distributions in the interior of tissues using the conventional approach (CT) with those obtained with the images of MR.

d) Check the applicability of this method in relation to the anatomical region considered and pathology.

This work will not have any implication with the treatments actually delivered to the patient, and in most cases, uses plans and images of patients who have already

been treated in the past at the External Radiotherapy Department of IPOPFG, EPE. It has been submitted to the IPOPFG Ethical Commission before the acquisition of the CT and MR images, which in turn authorized using these to perform this work.

1.3 Thesis organization

The work is structured into six distinct chapters. This being the first, where are contained: the introduction to the theme, the objectives set for the project and a brief description of the organization of the thesis.

The second chapter presents the theoretical foundations on the issues discussed, highlighting the key procedures followed along planning in External Radiotherapy.

The third chapter is devoted to the importance of images in TPS, referring to the physical principles of the two methods most commonly used in planning: CT and MR.

The fourth chapter is dedicated to the presentation of the materials and methods used where a detailed description is made of the entire experimental component of the work.

The presentation and analysis of the results of this investigation are made in the fifth chapter, which is described in detail the entire practical component developed in this project.

The conclusions structured according to the results found in the study and hypotheses, as well as suggestions for future works are presented in chapter six.

In the last part, are the references used in this study.

The Matlab™ (v.R2010b) script used, as well as several of the graphical results for the percentage of relative dose and the development of Hounsfield units is attached.

Chapter 2

BACKGROUND: “THEORETICAL FOUNDATIONS”

2. Background: “Theoretical Foundations”

In this chapter are described some theoretical notions of some concepts and processes which develop in the treatment by external radiotherapy, important for a better understanding of the work developed.

2.1 Radiotherapy – General Aspects

Radiotherapy is one of the main modalities used in the treatment of most cancer pathologies. In contrast with other medical specialities, which are based essentially on clinical knowledge and medical experience, radiotherapy, from the use of ionizing radiation for the treatment of cancer, depends also very much on modern technology.

The current advances in radiation oncology are mainly boosted by the technological development of procedures in radiotherapy equipment and the quality/accuracy of radiological imaging. These in turn allow improving the results of treatments, in particular, in terms of accuracy [Podgorsak, 2005].

Radiotherapy can be given in two different ways - from outside the body (external radiotherapy) or inside the body (internal radiotherapy).

External Radiotherapy usually involves using a machine called a linear accelerator (linac), which focuses high-energy radiation beams onto the area requiring treatment. External beam radiotherapy usually involves a series of daily treatments over a number of days or weeks [Podgorsak, 2005, Mayles *et al.,* 2007]. However, External Radiotherapy also comports the internal irradiation into the body, in a modality denominated as Intraoperative radiotherapy (IORT), which delivers a concentrated dose of radiation therapy to a tumor bed during surgery.

Internal Radiotherapy (known as Brachytherapy) can involve placing a small piece of radioactive material temporarily or permanently inside the body near the cancerous cells [Podgorsak, 2005, Mayles *et al.,* 2007].

2.1.1 Procedures in the planning of treatment in External Radiotherapy

The planning process of the treatment is crucial to achieve a better choice of the appropriate treatment for the patient.

The process is used to determine the number of radiation beams to be used to administer a given radiation dose to the patient, with the aim to control or remove a tumour [AAPM Task Group 53 Report, 1998].

The term 'planning of the treatment' has been sometimes interpreted as a process that is primarily designed for the analysis of dosimetric procedures, such as: computer calculations of the dose distribution, calculating the time of treatment and configurations of Monitor Units (*Monitor Units* - MU).

In reality, the planning of the treatment is a much more extensive method than just the realization of dose calculation, because it encompasses all the steps involved in patient plan [AAPM Task Group 53 Report, 1998].

It consists of three essential steps that will be described below, taking into account the diagram on figure 1.

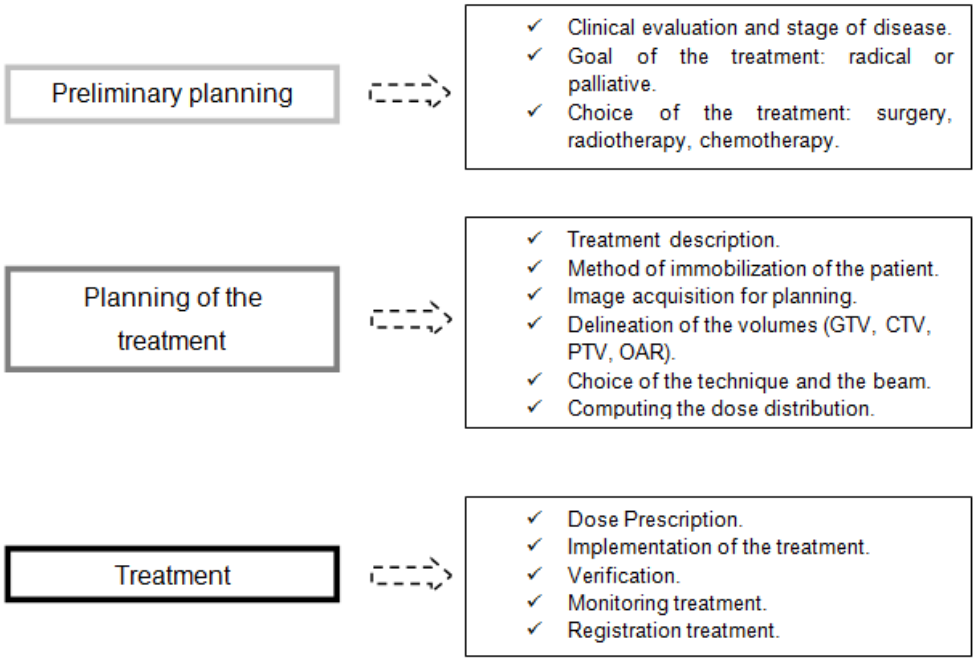

Fig. 2.1- Plan of Procedures in Radiotherapy [adapted from Doobs, 1999].

2.1.1.1 Preliminary Planning

In this first phase, the planning includes three basic stages that influence the entire treatment. Firstly proceeds to a clinical state of the patient's pathology, and then considering the problem in question, defines the goal of therapy. This step is very important because it influences the choice of the volume to be treated, the dose administered and the treatment technique. Finally made is the choice of the type of treatments to adopt (alone or concomitant): surgery, radiotherapy and chemotherapy.

2.1.1.2 Planning of the treatment

This is a crucial step in the whole process because the location of the tumour is determined, the volumes are defined and the technique and the beams are chosen, entrusting them to computing and dose distribution that will be administered on target volume.

Treatment planning is the process of determining the most appropriate way to irradiate the patient. It is a combination of the following five essential steps [Mayles *et al.,* 2007]:

1. Make sure the patient is positioned in the correct way taking into account the method of immobilization for the treatment to be feasible.
2. Define the tumoral volume and organs at risk
3. Choosing the appropriate type of beam;
4. Evaluation of the dose distribution;
5. Calculate and adjust the treatment machine settings to administer the absolute dose required.

Before carrying out the planning is important to determine the nature and extent of the tumour through various diagnostic techniques. Occasionally it is possible to perform a diagnostic test so that it contains the required information to the follow up of the planning. However, in most situations a new image is required for planning because the diagnosis and planning requirements are completely different. While for

the diagnosis it is required for an image without artefact and suitable enhancement of the tumour for a planning image it is indispensable a three-dimensional model, which is geometrically accurate in relation to the exact position of the patient in the treatment together with a mean of transference of the three-dimensional coordinate system for the therapy machine [Mayles *et al.,* 2007].

- **Image Acquisition / Definition of volumes**

The position, in which the image used for planning is acquired, will have to be maintained on the treatment, since the plan is done taking into account that position, hence the importance of this step in the whole process.

Taking this into consideration, it is the acquisition of the image where the size, extent and location of the tumour (target volume) are determined, as well as its relationship with so-called normal organs and external anatomy of the surface [AAPM Task Group 53 Report, 1998].

The accuracy of the data about the tumour, the target volumes and organs at risk are acquired under the same conditions, as those used for the subsequent treatment.

The techniques usually used are: CT, MRI, Ultrasound (US), image by positron emission tomography (PET) and CT image by emission of a single photon (SPECT). These methods offer a wide range of anatomical, functional and metabolic information on the tumour volume.

Most of times one resorts to fusion of some of these techniques with CT images to optimize the quality and the effectiveness of the treatment planning (standard technique used in the planning system in radiotherapy) [Doobs, 1999].

Having the images acquired, one proceeds to the delimitation of the volumes which is a significant pre-requisite for the planning of the treatment and for the accurate determination of the dose.

Report 50 from 1993 and Report 62 from 1999 of The International Committee on Radiation Units and Measurements (ICRU), define and describe the various target volumes and critical structures that help in the process of treatment planning and provide a basis for the comparison of the results of the treatments [BIR, 2003; Podgorsak, 2005].

Initially should be defined and delimited two volumes: GTV (Gross Tumor Volume) and the Clinical Target Volume (CTV). During the process of the planning of the treatment, other volumes are also determined: Planning Target Volume (PTV) and the organs at risk (Organs at Risk-OAR's).

Figure 2.2 shows how the different volumes are related to each other. As a result of the treatment planning, some more volumes could be defined: Volume Treaty (Treated Volume) and Irradiated Volume (Irradiated Volume).

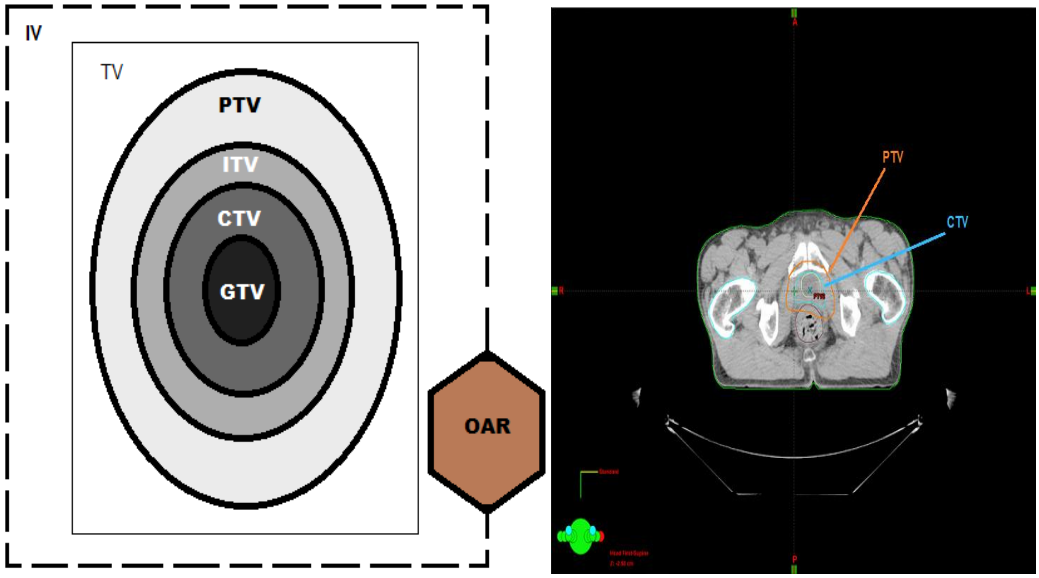

Fig. 2.2- **A**: Schematic representation of the relations between different volumes. GTV- gross tumour volume, CTV-clinical target volume, ITV-internal target volume, PTV-planning target volume, OAR-organs at risk. **B**: Axial planning CT slice showing PTV and CTV.

The Gross Tumour Volume (GTV) is the observable or palpable mass and it consists essentially of the primary tumour. The GTV almost always corresponds to parts of the malignant growth where the density of tumour cells is increased. Therefore, an appropriate dose should be delivered to the whole GTV [ICRU Report 50, 1993; ICRU Report 62, 1999].

The clinical target volume (CTV) is the volume of tissue containing GTV plus subclinical malignant tumour that should be eliminated. The CTV is, as the GTV, a merely anatomic and clinical concept and can be defined as a volume that includes

suspicious structures in addition to any tumour known[ICRU Report 50, 1993; ICRU Report 62, 1999].

The Internal Target Volume (ITV) is composed of the CTV plus an internal margin. The internal margin is designed to take into account the variations in the size and position of the CTV in relation to the frame of reference of the patient (usually defined by the bone anatomy), this is, the changes due to movements of organs such as respiration and the rectal and bladder content [ICRU Report 50, 1993; ICRU Report 62, 1999].

The Planning Target Volume (PTV) is a volumetric expansion taking into account the uncertainties in the position of the CTV from day to day. More specifically, an internal margin is added to compensate for the physiological changes in the size, shape and position of the internal anatomy. The PTV is therefore a geometric concept, and is used to ensure that the CTV receives the prescribed dose. In terms of planning, it is used to set the dose to be supplied during treatment. Its shape and size depend fundamentally on CTV and the technique used in the treatment [ICRU Report 50, 1993; ICRU Report 62, 1999].

The Treated Volume (TV) is the volume which is surrounded by an isodose defined by the oncologist, which is suitable to achieve the purpose of the treatment (e.g., curative, palliative). On the other hand, Irradiated Volume (Irradiated Volume) is defined as the entire volume of tissue which receives a dose that is considered significant in relation to the tolerance of the healthy tissue [ICRU Report 50, 1993; ICRU Report 62, 1999].

The OAR's are volumes which radiation sensitivity is such that the dose received from a treatment can be significant in comparison with its tolerance, which leads to a change in the arrangement of the beam or a change in the prescription of the dose. For example, in the case of prostate tumours, two of organs at risk will be the bladder and rectum [Podgorsak, 2005].

- **Choice of technique and beam**

An important goal of the planning of the treatment in radiotherapy is projecting a beam configuration which will provide a uniform dose on the target volume of planning (PTV) ensuring that the normal tissue receives a fairly lower dose and that the critical organs receive the lowest dose possible. This is achieved through the choice of: the type of treatment (electrons or photons), the energy beam, the beam arrangement, the use of wedges or blocks compensating etc [Mayles *et al*., 2007].

However, these goals are not always met, and sometimes it is necessary to a commitment, depending on the ultimate goal of every radiotherapy treatment. For example, if the treatment is palliative (where the aim is to decrease the symptoms due to the malignant disease, such as pain), radiation effects in the long run may not be a consideration and a simple beam arrangement will be enough. Moreover, if the treatment is radical, this is, aimed at controlling the tumour location; the long-term effects should be taken into account, which may result in a more complex scheme of radiotherapy [Mayles *et al*., 2007].

The equipment used in treatment, which is chosen in accordance with the energy of beam must then be selected according to certain characteristics, such as the percentage depth dose (Percentage Depth Dose, PDD) and the height / depth of the build-up region (maximum depth for which we have the maximum dose deposition), which vary with the energy and beam size (Table 2.1). Other factors such as the shade in the definition of the beam, the portal image, the existence of independent collimators or multi-leafs collimators should also be considered [Mayles *et al*., 2007].

Energy (MeV)	d_{max}(cm)	% Depth dose to 5cm	% Depth dose to 10cm
4	1.0	83.9	63.0
6	1.5	86.9	67.5
8	2.0	89.6	71.0
10	2.3	91.4	73.0
15	2.9	94.5	77.0
25	3.8	98.5	83.0

Tab. 2.1- Typical parameters of the beam from a field of $\mathbf{10} \times \mathbf{10}$cm and with a source-surface distance (Source-Surface Distance-SSD) of 100 cm [adapted from Mayles *et al.,* 2007].

With regard to the techniques of external radiotherapy, those that are usually used are:

- Conformal Radiotherapy,
- Intensity Modulated Radiation Therapy - IMRT,
- Volumetric Modulated Arc Therapy – VMAT,
- Stereotactic radiotherapy,
- Total Body Irradiation – TBI,
- Intra-operative radiotherapy,
- Etc.

Among those listed, there is an approach of the first four techniques that are more commonly used in the radiotherapy service where the work took place.

Conformal radiotherapy

Conformal radiotherapy uses the same radiotherapy machine as normal radiotherapy treatment. However, inside the machine is a device called a multi-leaf collimator (figure 2.3), which allows the beam of radiation to be shaped very precisely so that it 'conforms' to the area of the cancer. As a result, the healthy surrounding cells and nearby structures receive a lower dose of radiation, so the possibility of side effects is reduced.

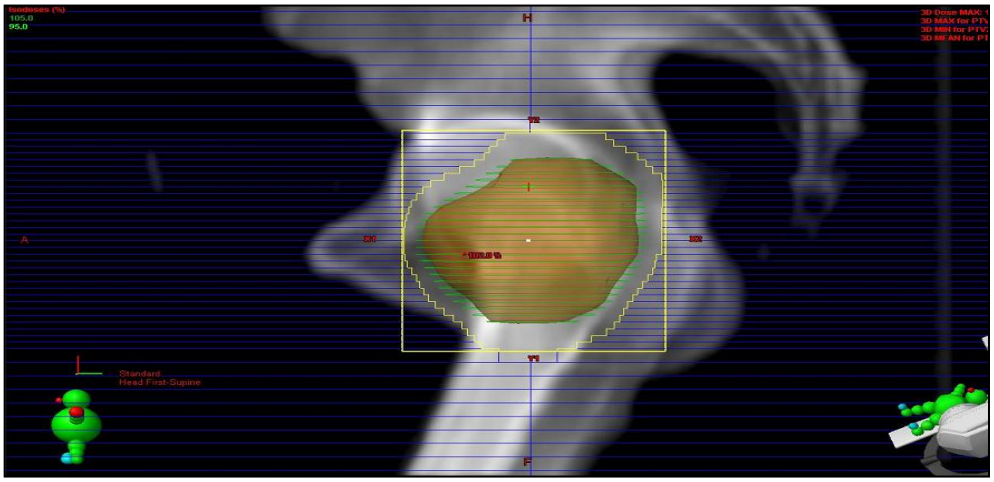

Fig. 2.3- Multi-leaf Collimator (MLC) in TPS (Prostate sagittal CT image).

This technique may be used to treat a number of different cancers, including cancers of the head and neck, prostate, esophagus, some types of lung cancer, breast cancer and brain tumours. It is especially useful if the tumour is close to important organs or structures in the body, because high doses of radiotherapy can be given with minimal risk to the healthy tissue. Although conformal radiotherapy is commonly used to treat some types of cancer, research is being carried out to see whether it can help to control other types of cancer better than standard radiotherapy, and cause fewer side effects [Podgorsak, 2005; Mayles *et al*., 2007].

IMRT

While in conformal radiotherapy the beam intensity is uniform, i.e. along the width of the beam the intensity does not vary, in the treatment with intensity modulated radiotherapy, as its name implies, the intensity is modelled according to the anatomical position of the tumour sparing healthy tissue areas (figure 2.4). In general, it is used about five to nine radiation fields oriented around the patient where the intensity adjustment is done through the use of the multi-leaf collimator. During this treatment, parts of the multi-leaf collimator are moved while the treatment is given [Podgorsak, 2005; Mayles et al., 2007].

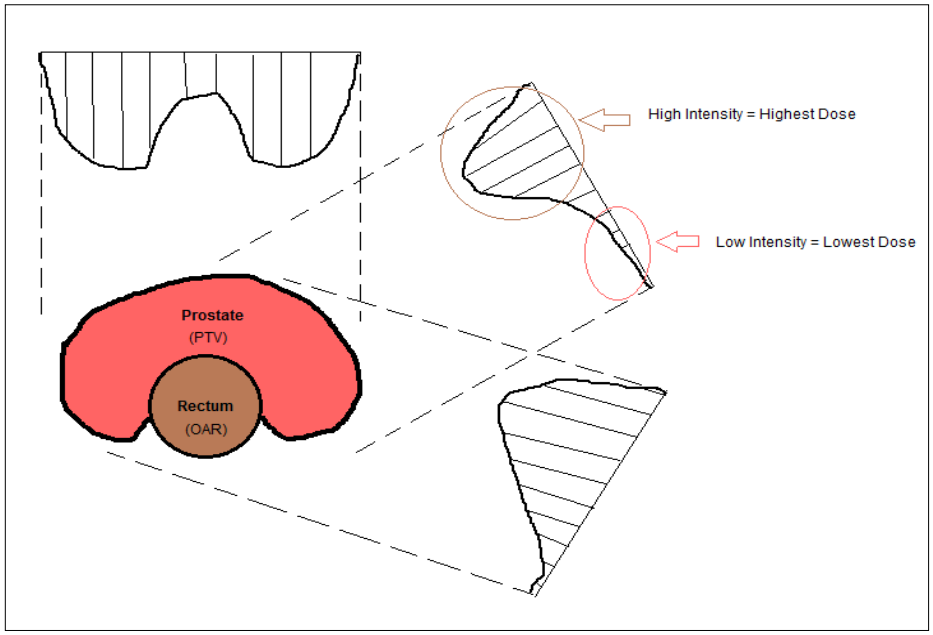

Fig. 2.4 - Drawing that illustrates the intensity modulated beam of radiation in prostate.

This enables the treatment beams to be shaped very precisely and allows the dose of radiotherapy to be altered in different parts of the treatment area. Again, the aim is to reduce the side effects of treatment.

The IMRT follows the inverse planning, in which minimum and maximum doses necessary for tumour control are prescribed to target volumes, in addition to being prescribed also maximum doses to organs at risk, based on well-established constraints probability of complications. With this, the dose distribution fits more precisely around the tumour or in target volumes in three dimensions, from the modulation or control of the radiation intensity in small multiple volumes of each field.

As it is possible to reduce the ratio between the dose and the volume irradiated in normal tissues, it is often allowed to administer higher and more effective doses to tumours with few side effects, if compared with conventional radiotherapy techniques.

Currently, the IMRT is mainly indicated for the treatment of prostate tumours and head and neck tumours, gynaecology, gastro-intestinal and tumours of the central nervous system.

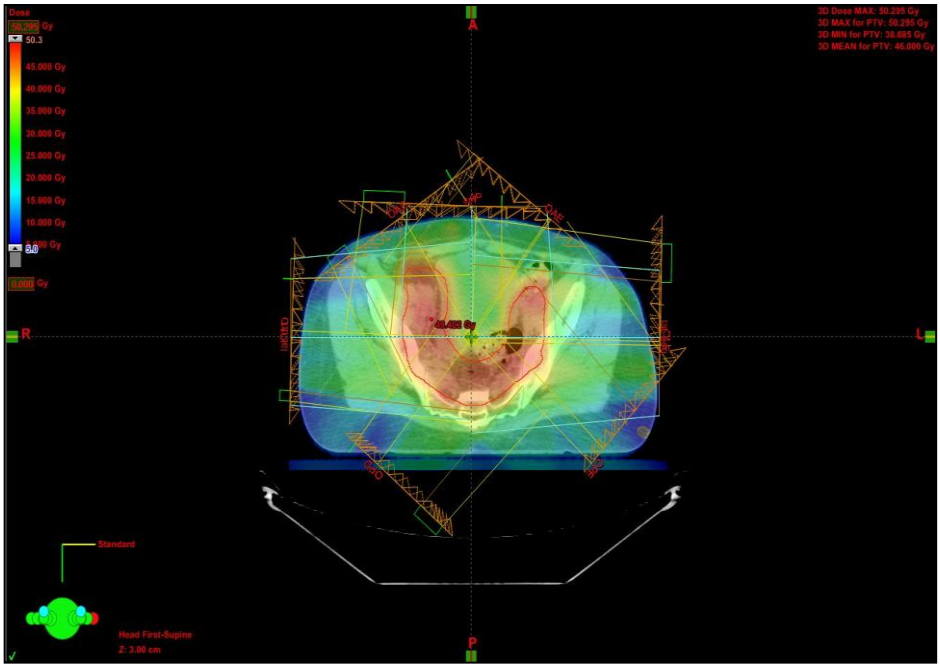

Fig. 2.5- Axial planning CT slice showing dose distribution of pelvis, with IMRT technique.

The radiotherapy per modelled intensity can be administered in two forms. On one hand, the Multiple-Static -Field (MSF) or step & shoot technique, in which each

field is subdivided into subfields, and for each one, the MLC leaves fit and radiate several times, adjusting to the shape of the tumour. Every time that the collimator is adjusted, the beam stops radiating. On the other hand, the dynamic multi-leaf collimator (DMLC) technique, in which for each field created, there is only one movement of the leaves, i.e. the MLC leaves adjust themselves without ever stopping the deposition of dose, hence the affirmation that it is a more homogeneous method and that saves time for treatment, in relation to MSF [Podgorsak, 2005; Mayles *et al.*, 2007].

Volumetric Modulated Arc Therapy – VMAT

The volumetric modulated arc therapy delivers a precisely sculpted 3D dose distribution with a single 360-degree rotation of the linear accelerator gantry. It is made possible by a treatment planning algorithm that simultaneously changes three parameters during treatment: rotation speed of the gantry, shape of the treatment aperture using the movement of multi-leaf collimator leaves, delivery dose rate (figure 2.6).

Several studies [Dobler *et al.*, 2010; Fogarty *et al.*, 2011; Verbakel *et al.*, 2009] have demonstrated the superiority of this technique in relation to the techniques that have already been referred to, by the fact of having a more homogeneous distribution of dose in a short treatment time, sparing also risk areas that should not be irradiated.

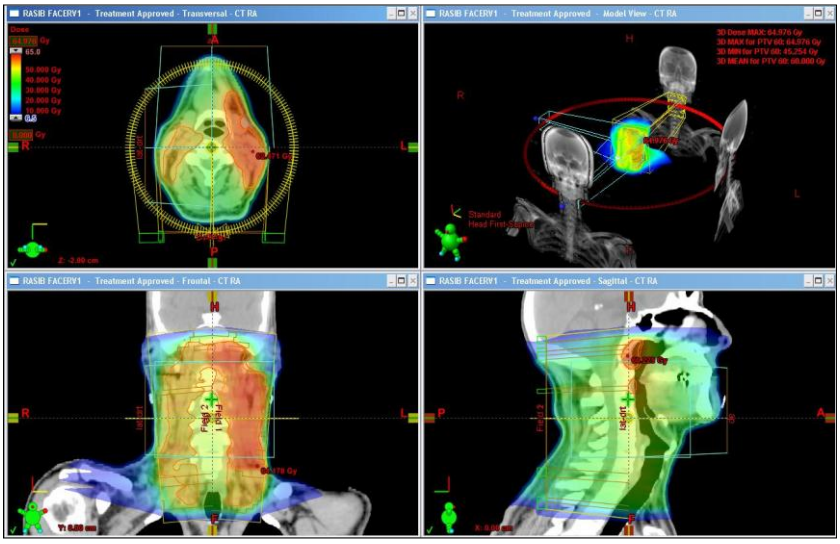

Fig. 2.6- Planning CT showing dose distribution of head and neck, with VMAT technique.

Stereotactic radiotherapy

This treatmentis a highly precise form of radiation therapy initially developed to treat small brain tumors and functional abnormalities of the brain. Stereotactic Radiotherapy includes the Stereotactic radiosurgery (SRS) and the Stereotactic Radiotherapy Fractionated. The principles of cranial SRS, namely high precision radiation where delivery is accurate to within one to two millimeters, are now being applied to the treatment of body tumors with a procedure known as stereotactic body radiotherapy (SBRT) [RadiologyInfo].

SRS involves the use of many beams of radiation, each giving a low dose (however the doses per session can be very high) to the tumour. This is used instead of normal treatment that uses just one or a few beams of radiation giving much higher doses [Wasik *et al*, 1999].

Again, the aim is to give a high dose of radiation to the cancer but a low dose to normal tissues, reducing side effects. There are also claims that the treatment targets the cancer more accurately than normal radiotherapy. The treatment is given by special types of radiotherapy machines, such as the *CyberKnife®, Gamma Knife®* and *NovalisTx™* (figure 2.7-B). The linear accelerator can perform Stereotactic Radiosurgery on larger tumors in a single session or during multiple sessions, which is called fractionated stereotactic radiotherapy.

As the name suggests, the equipment is stereotactic defining a fixed coordinate system [Minniti *et al*, 2010].Due to the high accuracy of treatment, this technique is usually applied in the treatment of brain injuries as well as in areas where the tumoral volume is very low, hence it is required a complete immobilization of the patient.

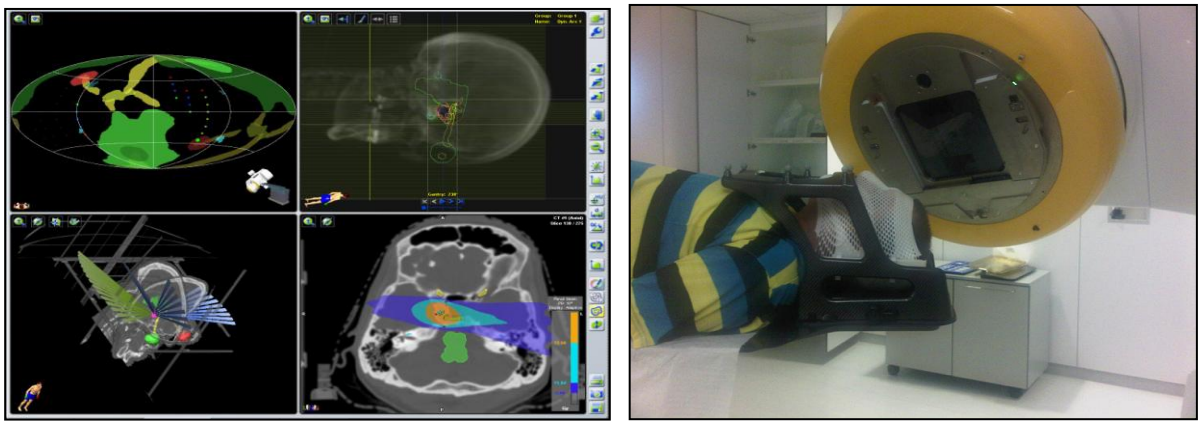

A **B**

Fig. 2.7- **A:** Stereotactic Radiosurgery (SRS) treatment planning; **B**: *Novalis Tx™* during the treatment with SRS technique.

- **Computing the dose distribution**

The computerized treatment planning systems (*Treatment Planning System* – TPS) are used in external radiotherapy to generate forms of beam and dose distributions with the aim of maximizing the tumoral control and minimize the complications in so-called healthy tissues. These systems allow the introduction of patient data, anatomical settings, configuration of the beam, calculation of the dose distribution, evaluation of planning in terms of dose, volume and effects, data output and its transfer to other units, such as the treatment machine [Podgorsak, 2005].

There are two essential objectives in the implementation of the algorithms for the calculation of dose distribution. In the first place, the dose calculation has to be fast to ensure that the process of planning of the treatment can be completed in clinically acceptable limits, and on the other hand, the result of the calculation of dose has to be precise enough so that the establishment of correlations between the dose delivered and the clinical effects remain reliable and significant [Dyk *et al.*, 2001].

The general approach of the principles for dose calculation covers a wide range of examples that are, primarily, a representation of the dose distribution in experimental models of physical basis which sculpt the transport of elementary particles since they are produced until the deposition of energy in the patient [Dyk *et al.*, 2001].

It is easily understood that the speed of calculation, usually means a decrease of accuracy (depending on the computer hardware). Therefore, the choice of the algorithm for dose calculation in a given occasion is, in large part, a commitment that should take into account the clinical impact of a greater inaccuracy in dose. Although it is a little difficult to organize, in practice, a good solution will have access to various algorithms and make the appropriate choice depending on the circumstances in question [Mayles *et al.*, 2007].

In the calculation of dose distribution it is essential that the algorithm takes into account the characteristics both of the anatomy of the patient and the beam having in mind the heterogeneous nature of the patient in three dimensions to determine the accuracy of dose dispersed in each point of calculation as well as the primary dose.

With respect to the anatomy of the patient in question the most effective representation is defined by a 3D array of voxels that derive from a CT image of the patient in the position in which he will be treated [Mayles *et al.*, 2007].

Ideally, the density of the tissue and the exact composition of each of these voxels must be considered. However, in practice, many simplifications have to be made.

The calculations of dose distribution have evolved from simple 2D models through 3D models, to techniques of Monte Carlo 3D with greater computing power in order to increase the speed of calculation.

The conventional plans and some 3D plans use a direct approach, i.e., the best planning is achieved by trial-and-error method. Another approach is to use the inverse planning in which the objectives and constraints are defined first and only then the beam configuration and the weights of the fields are determined by computer [Podgorsak, 2005].

As the majority of the treatments is done with beams of photons, and not with electron beams (which are used for superficial lesions, in regions with little bone tissue,…), one will only mention the calculation algorithms for beams of photons.

Among the various methods available for calculating the dose are only exposed in a very brief way, the two most commonly used in the Eclipse Treatment Planning Software from Varian Medical Systems (Palo Alto, CA) (software used in this work), Pencil Beam Convolution (PBC) and Analytical Anisotropic Algorithm (AAA).

As already mentioned, calculation algorithms have been incorporated into the treatment planning software to report for contributions from tissues of different densities that are near, far, and enclosing the site of interest. The heterogeneity corrections in the PBC model are based on dose values calculated in a water equivalent material multiplied by a heterogeneity correction factor generated from an electron density matrix derived from a CT value matrix [Carrasco *et al.*, 2004].

The AAPM Task Group 65 reported the observations by many investigators who demonstrated experimentally or by theoretical analysis that the PBC algorithm (path length based) does not work in regions of electron disequilibrium, and compute incorrect doses within or near to a low density medium, principally when the field size is small [AAPM Task Group 65 Report, 2004]. The recently published, AAPM Task Group 101 report recommends the utilization of algorithms that account for 3D scatter integration such as convolution/superposition, and algorithms that account for better photon and electron transport such as Monte Carlo [AAPM Task Group 101 Report, 2010].

The AAA is a pencil beam superposition-convolution algorithm for dose calculations [Ulmer *et al.*, 1996; Fogliata, *et al.*, 2006], available in the Eclipse treatment planning software, that has shown excellent accuracy overall and a great ability to handle small fields in inhomogeneous media. Dose distributions calculated by the AAA algorithm have been studied by several investigators [Cozzi *et al.*, 2008; Ronde *et a*l., 2009] and in the heterogeneous media; the AAA algorithm has been shown to be consistently more accurate than pencil beam convolution [Bragg *et al.*, 2008; Ronde *et al.*, 2009].

2.1.1.3 Treatment

After all the planning phases are completed, one proceeds to the treatment. During this period it is important to monitorize the treatment in order to verify the possibility of implementation during the treatment period.

There are several geometric factors that tend to compromise the quality of treatment, such as patient movement, tattoos by the labelling with respect to the internal anatomy and inaccurate beam alignment. In situations where the fields are more complex and the patient's anatomy which is less favourable, these problems tend to be more probable. Then, in order to avoid such situations, it uses the portal image, cone beam CT, among others, where it records an image serving as a reference for checking geometric allowing evaluating the degree to which the actual treatment corresponds to the treatment plan [AAPM Report No.24, Task Group 28, 2010].

If any change occurs in the patient, which influence any dosimetric parameter, one must modify the plan to ensure the probity of the therapy or correct the patient positioning.

2.1.2 Using MRI as an aid to External Radiotherapy Treatment Planning

The accurate delineation of tumour volumes and critical structures is a crucial component of treatment planning. The use of a single imaging study to accomplish the delineation is not always sufficient and it is necessary to resort to other types of image [Schlegel *et al.,* 2006].

MRI has been used for the diagnosis and monitoring of a wide range of conditions and treatments. MRI offers several advantages over other imaging techniques with particular reference to CT. As known widely, the MRI is devoid of harmful radiation when compared to CT scanning. This is of particular use in malignant tumor cases where repeated imaging may be necessary to monitor the progress of the disorder. Additional advantage is offered by the ability to directly obtain images in planes other than axially, as with CT. The high contrast resolution noted with MRI over CT offers better clarity and easier diagnosis and demarcation of soft tissues or lesions in most situations [Koshy *et al.*, 2011].

Currently, MRI is used for:

- Delineation of soft tissues;
- To determine extent and spread of disease;
- Staging of different tumors;
- Obtaining functional and metabolic information;
- Monitoring the response to treatment.

Nowadays, the planning systems have the ability to combine the information from different imaging studies using the process of image fusion or registration [Podgorsak, 2005].

Image registration is the process of superimposing two or more images from different imaging modalities, into one single image with just one coordinate (x, y and z) system. The original image is often referred to as the ‘reference image’ and the second image as the ‘target image’ [Cherry *et al*., 2009]. The process is simplified if external markers can be attached to the patient, using internal anatomic markers, e.g. the rib cage, ventricles, bone surfaces are more frequently used [Dougherty, 2009].

The high contrast in soft tissues, in some areas, such as the brain, causes the MRI is one of the most used techniques for image registration, allowing small lesions are seen more easily. CT/MR image registration or fusion (figure 2.8) combines the accurate volume definition from MR with the electron density information available from CT.

The MR data set is superimposed on the CT data set through a series of translations, rotations and scaling. This process allows the visualization of both studies side by side in the same imaging plane even if the patient has been scanned in a completely different treatment position [Podgorsak, 2005].

Magnetic resonance imaging has considerable potential for treatment planning. The superior soft tissues contrast provided by MR and the ability to vary contrast by manipulation of the imaging parameters facilitate optimal tumour evaluation. Together with its 3D multi-planar imaging capability, MR can provide advantages over reconstructed CT images.

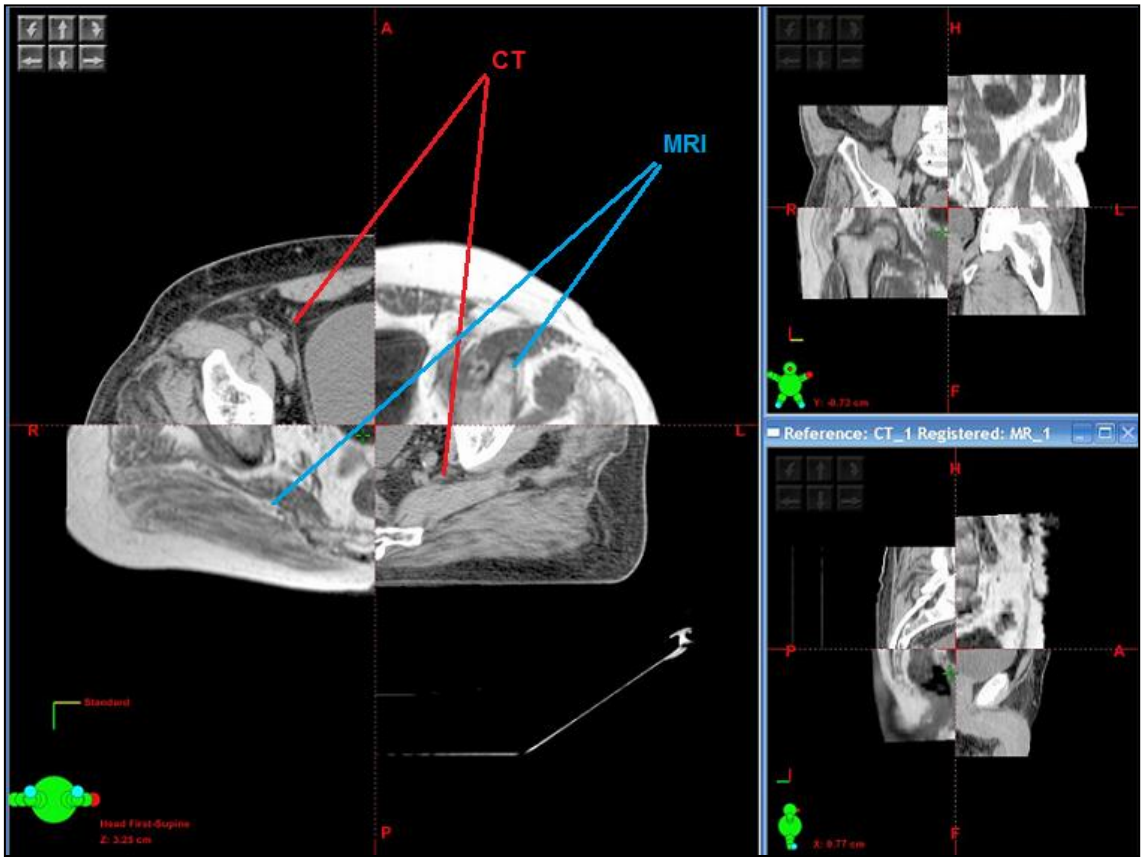

Fig. 2.8- Pelvic CT/MR image registration.

2.1.3 Using MRI alone in External Radiotherapy Treatment Planning

Introduction of newer methods of MRI, which offer better imaging options, have increased the popularity of MRI. MR imaging is now able to offer better options in terms of tumor delineation and identifying the extent, spread, and involvement of neighboring structures when compared to other modalities. While image distortion was one of the problems that commonly restricted the use of MRI, options such as phased array and faster sequences have reduced the disadvantages of MRI [Jacobs *et al.,* 2007].

Newer concepts such as diffusion-weighted and perfusion-weighted imaging and proton spectroscopy have changed the scenario of soft tissue imaging to a major extent [Jacobs *et al.,* 2007]. Further studies and further improvements in the field of imaging technology can enhance the use of MRI, making it the imaging modality of choice in almost all cancers in the body [Koshy *et al.*, 2011].

Today, the MRI is still a technique complementary imaging in treatment planning for external beam radiotherapy, and MRI alone cannot be used for radiotherapy planning, for several reasons [Podgorsak, 2005]:

- The physical dimensions of the MRI scanner and its accessories limit the use of immobilization devices and compromise treatment positions;

- There is no electron density information available for heterogeneity corrections on the dose calculations;

- MRI is prone to geometrical artefacts and distortions that may affect the accuracy of the dose distribution calculation and the treatment.

However, the use of MRI alone in the assessment of brain lesions, prostate tumors or gynecological for radiotherapy has been questioned by many [Stanescu *et al.*, 2006a, 2006b, 2008; Chen *et al.*,2004a, 2004b, Prabhakar *et al.,* 2007; Jonsson *et al.*, 2010].

CT is considered superior in certain aspects as MRI is associated with geometric distortion and MRI can neither provide information about bone structure nor help assess the electron density of the body tissues. But, MRI is superior in certain aspects. These include better contrast than CT when demarcating the soft tissues, more precise delineation of normal critical structures, and more accurate definition of treatment volumes.

In most of these cases, as it is soft tissue, it resorts, already referred to, fusion between CT and MRI. A particular reason for image fusion is that MR images are inherently prone to distortions that can alter the local topography targeted by the radiation treatment. Imprecise localization of the target may lead to an overall reduction in treatment accuracy and efficiency [Stanescu et al., 2008].

The replacement of the current CT/MRI-based RTP based procedure by MRI alone eliminates the sessions of CT (without exposure to x-rays) and, consequently, the image fusion process. Furthermore, any incidental errors caused by patient inter-procedure positioning and image fusion will be deleted. As a result, the improved target localization is expected to lead to a higher local tumor control and reduced normal tissue complications.

The MRI alone in treatment planning should result in a reduction in margins added to account for delineation uncertainties and less normal tissues irradiated, reducing treatment toxicity, and remove some systematic registration errors that occur when combining MR and CT.

Chapter 3

IMAGING MODALITIES IN RADIOTHERAPY

3. Imaging modalities in radiotherapy

In this chapter, it is held a brief exposure of the main types of image used in RTP, making reference to the physical principles of each one of them as well as the importance of its applicability.

The acquisition of medical images is one of the key procedures in the treatment plan in ER, having as purpose three important facts [Mayles *et al*, 2007]:

- The evaluation of the position and size of the target volume in relation to the remaining anatomical structures, in particular the components of risk;
- Acquisition of data required for an accurate calculation of the dose distribution;
- Obtaining accurate information for the set up of the patient during the treatment.

The guarantee of the quality of the image is essential to ensure the integrity between the planning and implementation of treatment.

As has already been explained in the previous chapter, the techniques commonly used in planning systems are: the CT, MRI, Ultrasound, image by positron emission (PET) and CT image by issuing a single photon (SPECT). As was also said, it is often made the fusion between them to get a greater efficiency in the treatment.

In accordance with the work carried out it is only made a description of the standard technique used (CT) and the MRI, complementary technique and that is intended to be implemented as practice in planning.

3.1 Computerized Tomography

3.1.1 Physical principles

There is an abundant literature on the whole physics that involves the CT [Bushberg *et al.*, 2002; Hsieh, 2009; Kak *et al.,* 2001; Kalender, 2011] and as such it would necessary more than one subsection of this work to detail all the information. However, it is described in a concise way the physical principles that derive from this technique of image acquisition, so that the process in question may be understood.

The X-rays were the first radiation to be used in medical equipment, and currently still have a huge importance at the clinical level [Bushberg *et al.,* 2002].

Furthermore, since the first medical images were obtained with X-rays, a large part of the concepts and techniques of image are directly conveyed from these devices.

Computed tomography (CT) is defined as a radiological technique of medical diagnosis that is based on the principle of operation of the X-rays, where the primary goal is to obtain two-dimensional images at different angles in order to achieve, by methods of reconstruction, three-dimensional images generated from multiple projections X-ray. These are acquired by a rapid rotation of the X-ray tube, 360 ° around the patient (figure 3.1). Radiation transmitted through this is collected by a ring of radiation-sensitive detectors [Hsieh, 2009].

This procedure allows, not only improving the contrast of the tissues, as also get in-depth information.

Thus, tissues with different compositions absorb radiation differently, this is, denser tissues (as the liver) or heavier elements (such as calcium in bones), absorb more radiation than the less dense tissues (such as the lung, which is filled with air), thus producing an anatomical image of the organs [Bushberg *et al*, 2002].

A **B**

Fig. 3.1- **A**: CT scanner (*GE Lightspeed*® scanner). **B**: Axial brain CT.

3.1.1.1 X-Ray Mass Attenuation Coefficients

The attenuation suffered by an X-ray beam in biological tissue occurs due to the interactions that occur in the middle (as, for example, Photoelectric Effect (PE) and/or effect of Compton (EC)).

Taking into account that the fraction of energy lost by a beam, when it exceeds a material, is proportional to its thickness dx:

$$\frac{dI}{I} = -\mu dx \tag{1}$$

One easily arrives at the following expression:

$$I(x) = I_0 e^{-\mu.x} \tag{2}$$

In which, μ represents the linear attenuation coefficient, x is the thickness of the object, I_0 is the initial intensity of the beam and I corresponds to the intensity of the beam after having crossed the material [Hsieh, 2009].

Using the transmitted intensity equation above, linear attenuation coefficients can be used to make a number of calculations [NDT Resource Center; NIST]. These include:

- The intensity of the energy transmitted through a material when the incident X-ray intensity, the material and the material thickness are known.
- The intensity of the incident x-ray energy when the transmitted X-ray intensity, material, and material thickness are known.
- The thickness of the material, when the incident and transmitted intensity, and the material are known.
- The material can be determined from the value of μ when the incident and transmitted intensity, and the material thickness are known.

The linear attenuation coefficient is useful when considering an absorbing material with the same density but of different thicknesses. A coefficient associated with it may have value when you want to include the material density ρ, is given by the mass attenuation coefficient, which is defined as $\frac{\mu}{\rho}$.

Then, a narrow beam of monoenergetic photons with incident intensity I_0, penetrating a layer of material with mass thickness x and density ρ, emerges with intensity I given by the exponential attenuation law (similar to the equation 2):

$$\frac{I}{I_0} = e^{-\left(\frac{\mu}{\rho}\right) \cdot x} \tag{3}$$

Equation 3 can be rewritten as:

$$\frac{\mu}{\rho} = x^{-1} \ln\left({}^{I_0}/_{I}\right) \tag{4}$$

From which $\frac{\mu}{\rho}$ can be obtained from measured values of I_0, I and x.

3.1.1.2 Hounsfield Units/ CT number

The attenuation coefficient, for each point of the image, is determined by the average of attenuation of all X-rays that pass on this point and is stored in a square matrix.

Each element of the matrix corresponds to one pixel of the image, which in reality represents a small volume (voxel). Each voxel is given a numeric value according to the degree of attenuation of X-rays in that same volume.

To reduce the dependence of the radiation energy, these numerical values are assigned according to the equation 5, shown below, which are called Hounsfield units (HU) or CT number [Dougherty, 2009]:

$$CT\ number\ or\ HU = \frac{(\mu - \mu_{H_2O})}{\mu_{H_2O}} \times 1000 \quad (5)$$

The HU values represent the attenuation coefficient of X-rays in various types of materials with respect to water. Thus, a scale is formed that correlates these coefficients with the densities, which in turn are converted to a scale of shades of gray.

The table 3.1 shows the typical CT numbers of various tissues. These values are displayed on a scale that varies between approximately -1000 HU to 3000 HU(for radiotherapy), where the -1000 corresponds to air, 0HU is the value assigned to the water, between -300 and 100 with respect to soft tissues, and the values that prowls the 3000 HU equivalent to the bone [Dougherty, 2009].

Tissue	CT number or HU
Bone	1000+
Liver	50-80
Muscle	44-59
Blood	42-58
Gray matter	32-44
White matter	24-36
Heart	24
Water	0
Fat	-20 to -100
Lung	-300
Air	-1000

Tab. 3.1- CT numbers of various tissues [adapted from Webster, 2006].

These units are very important in medical interpretation where it is necessary to determine the type of tissue that is to be analyzed. This is the way that it has to quantify electronic densities so that it is possible to calculate the dose, hence its importance for treatment planning.

The graph shown in figure 3.2 demonstrates the dependence/ratio of HU with the electron density. With increasing electron density, the HU tends to increase until it reaches a saturation value and in turn the dose also will increase it.

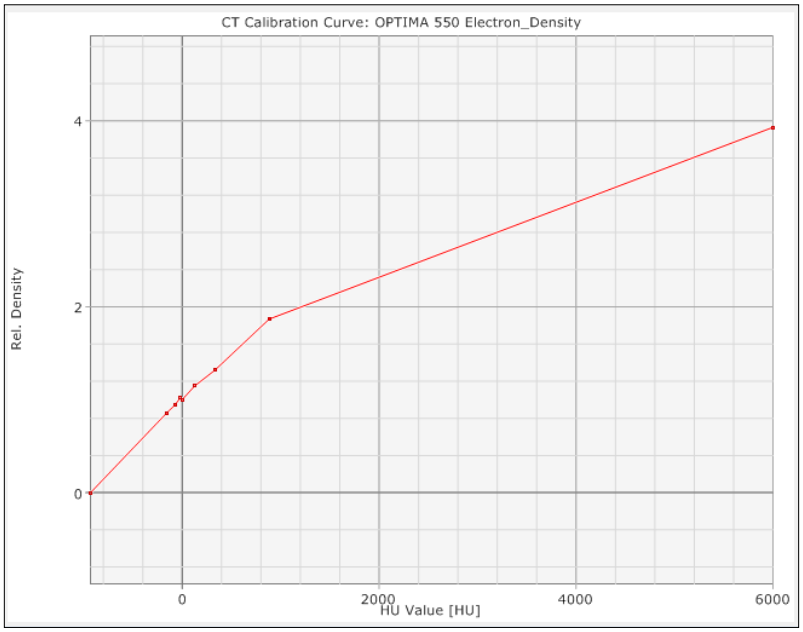

Fig. 3.2- CT Calibration Curve.

Usually the biological tissues are classified into four main types: fat, muscle tissue, bone, and air filled cavities. The physical characteristics of these compounds, such as electronic density, effective atomic number and mass density, are crucial for the dynamics of CT in a subsequent image interpretation with regard, for example, its contrast.

3.1.1.3 Relative predominance of individual effects

The probability for a photon to undergo any one of the various interaction phenomena with an attenuator depends on the energy *E* of the photon and on the atomic number *Z* of the attenuating material. In general, the Photoelectric Effect (PE) predominates at low photon energies, the Compton Effect (CE) at intermediate energies and pair production at high photon energies [Podgorsak, 2005]. Figure 3.2 shows the regions of relative predominance of the three most important individual effects with *E* and *Z* as parameters.

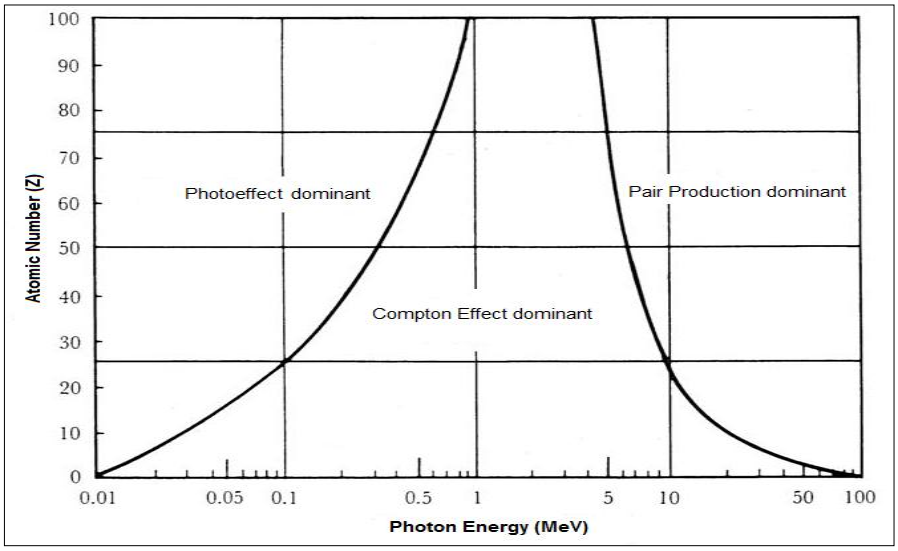

Fig. 3.3- Regions of relative predominance of the three main forms of photon interaction with matter. The left curve represents the region where the atomic coefficients for the photoelectric effect and Compton Effect are equal; the right curve is for the region where the atomic Compton coefficient equals the atomic pair production coefficient [adapted from Podgorsak, 2005].

Through the analysis of the graph depicted in figure 3.3, it is observed that from a certain value of energy, in the order of 75 KeV, the X-ray production occurs predominantly through the Compton Effect (being lower the likelihood of X-ray production from the Photoelectric Effect). Therefore, the images per CT derive its contrast from the influence of this type of interaction, having a good contrast for lower energies and a less reasonable contrast for higher energies.

In the region of higher energies, where the CE is dominant, the attenuation coefficient varies very little with the energy of X-rays. As this process is directly proportional to electronic density, this plays a dominant role in the formation of medical image in CT.

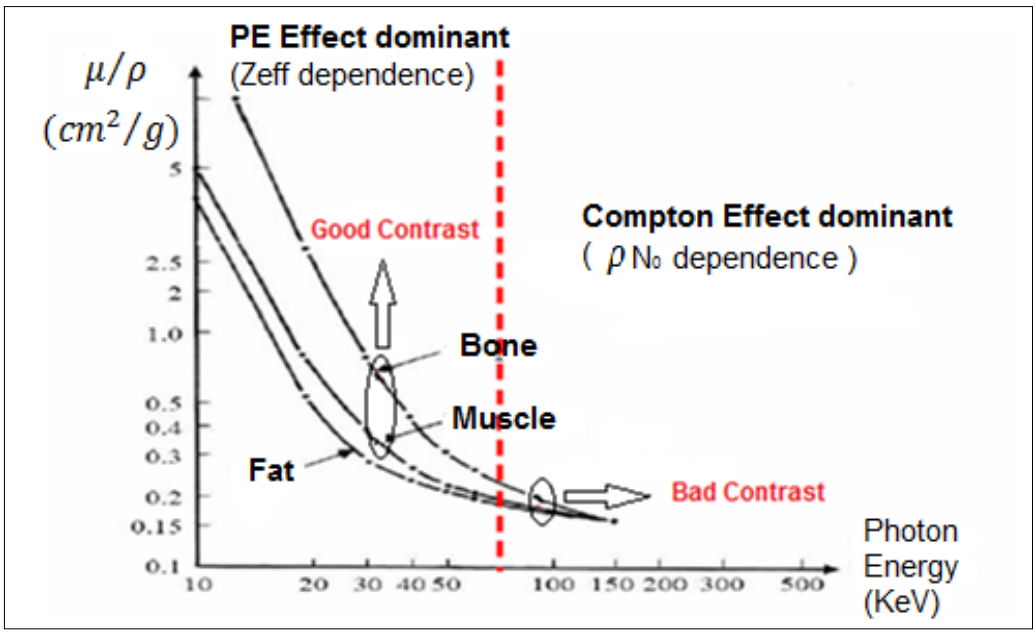

Fig. 3.4- Dependence of the material (effective atomic number and electronic density) [adapted from Webb, 2003].

3.1.1.4 CT Scanners Generations

To understand better this imaging modality is important to know its evolution over time, which allows not only their presentation, but also the reinforcement of several key concepts in CT imaging.

This section describes the evolution of CT scanners over the last 40 years.

- **First Generation**

The first generation of CT scanners employed a rotate/translate, pencil beam system in 1971. The x-ray source and detector were linearly translated to acquire individual measurements. After the linear measurements were completed, both the x-ray tube and the detector were rotated 1 deg to the next angular position to acquire the next set of measurements (figure 3.4) [Bushberg *et al.*, 2002; Hsieh, 2009].

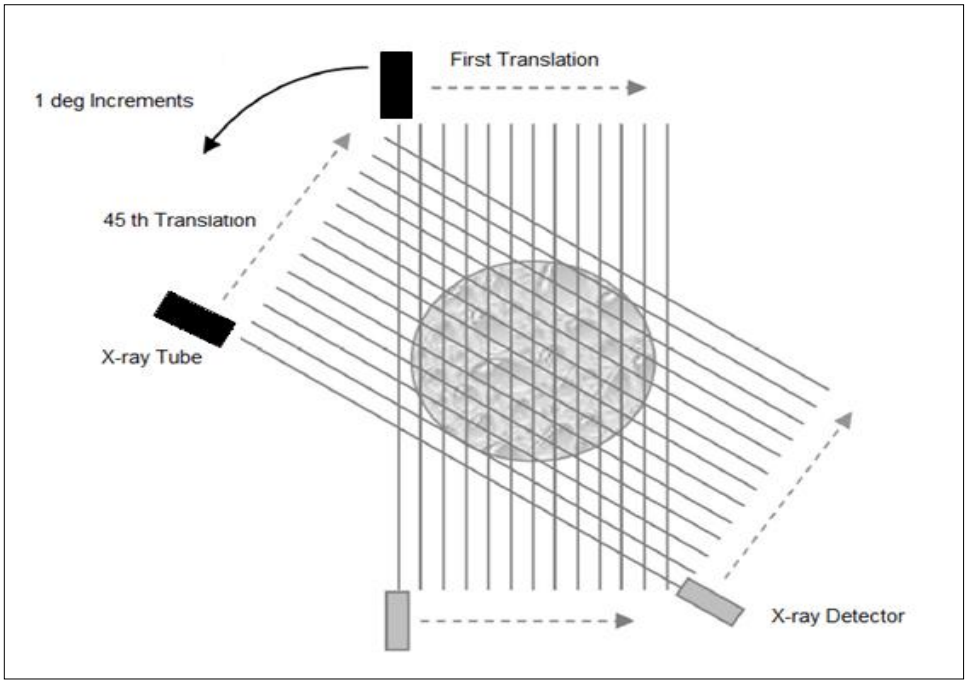

Fig. 3.5- First Generation CT scan geometry [adapted from Hsieh, 2009].

Although clinical results from the first-generation scanners were promising, there remained a serious image quality issue associated with patient motion during the 4-6 min data acquisition.

- **Second Generation**

In order to reduce the acquisition time comes the 2nd generation scanner in 1974. Although this was still a translation/rotation scanner, the number of rotation steps was reduced by the use of multiple pencil beams. A second-generation scanner with 3 narrow beams and 3 detectors is shown in figure 3.5 [Hsieh, 2009; Goldman, 2007].

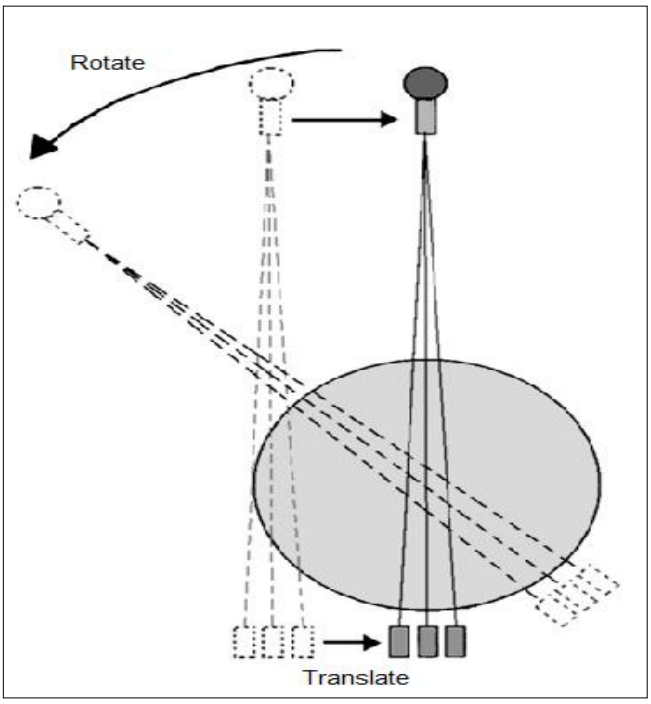

Fig. 3.6- Second Generation CT scan geometry [adapted from Goldman, 2007].

The shortest scan time with a second generation scanner was 18 seconds per slice, 15 times faster than with the first generation system. Incorporating an array of detectors instead of just one required the use of a narrow fan beam of radiation. Although a narrow fan beam provides excellent scatter rejection compared with plain film imaging, it does allow more scattered radiation to be detected than was the case with the pencil beam used in first generation CT [Bushberg *et al.*, 2002].

- **Third Generation**

The translational motion of first and second generation CT scanners was a fundamental impediment to fast scanning. Faster scans required the elimination of translation motion and the use of smoother and simpler pure rotational motion. This goal is accomplished by widening the x-ray beam into a fan beam encompassing the entire patient width and using an array of detectors to intercept the beam (Figure 3.6). The early third-generation CT scanners, was installed in late 1975. [Bushberg *et al.*, 2002: Hsieh, 2009; Goldman, 2007].

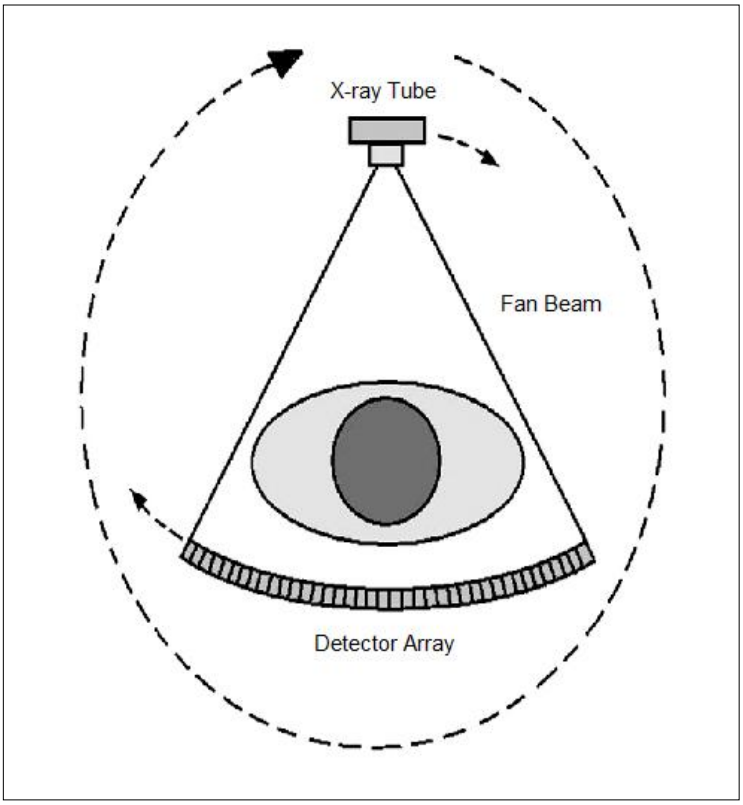

Fig. 3.7- Third Generation CT scan geometry [adapted from Goldman, 2007].

The detector array is rigidly linked to the x-ray tube, so that both the tube and the detectors rotate together around the patient. The motion of third generation CT is "rotate/rotate" referring to the rotation of the x-ray tube and the rotation of the detector array [Goldman, 2007].

Third-generation CT requires extremely high detector stability and matching of detector responses. First and second generation detectors were dynamically recalibrated at the beginning of each translation, before passing into the patient's shadow. Also, each detector measured rays passing through all voxels, so that any detector error or drift was spread evenly across the image and generally was not visible [Goldman, 2007].

The introduction of 'slip ring' technology was also a key to the success of helical or spiral CT. Due of the inherent advantages of the third-generation technology, nearly all of the state-of-the-art scanners on the market today are third generation [Hsieh, 2009].

- **Fourth Generation**

Several technology challenges in the design of the third-generation CT, including detector stability and aliasing, led to investigations, in 1976, of the fourth generation concept [Hsieh, 2009].

In this geometry, the detector forms an enclosed ring and remains stationary during the entire scan, while the x-ray tube rotates about the patient. Unlike the third generation scanner, a projection is formed with signals measured on a single detector as the x-ray beam sweeps across the object. The projection, therefore, forms a fan with its vertex at the detector, as shown by the shaded area in figure 3.7 [Hsieh, 2009].

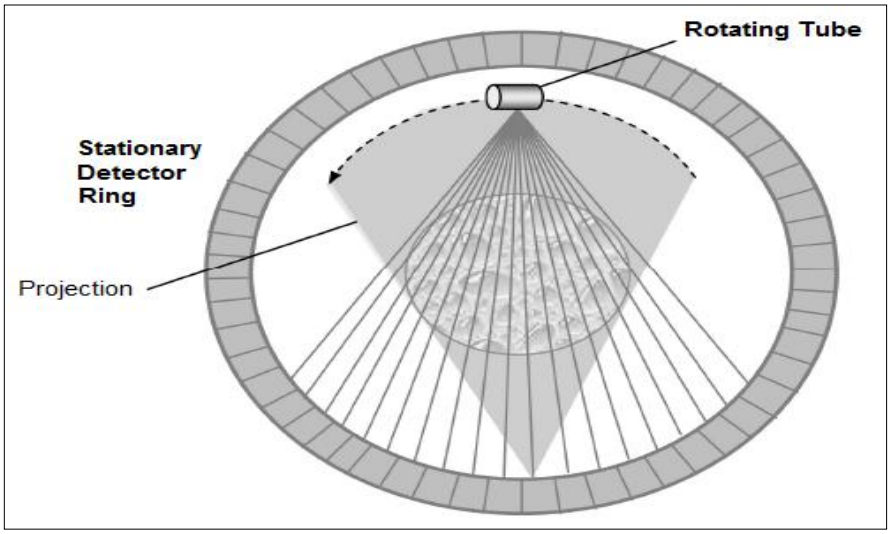

Fig. 3.8- Fourth Generation CT scan geometry [adapted from Hsieh, 2009].

Drawbacks of early fourth generation CT included size and geometric dose efficiency. Because the tube rotated inside the detector ring, a large ring diameter (170–180 cm) was needed to maintain acceptable tube–skin distances. On the other hand, acceptable spatial resolution limited detector apertures to ~4 mm. Consequently, even allowing for ~10% space between detectors, 1,200 or more detectors were needed to fill the ring, but cost considerations initially limited the number to 600. The result was gaps between detectors and low geometric dose efficiency (<50%). A later, alternate design used a smaller ring placed closer to the patient, with the tube rotating outside the ring; during tube rotation, the part of the ring between the tube and the patient would tilt out of the way of the x-ray beam (the peculiar wobbling motion of the ring was called nutation) [Goldman, 2007].

Another disadvantage of fourth generation geometry was scatter. The scatter-absorbing septa used in third generation designs could not be used, because the septa would necessarily be aimed at the center of the ring, which was the source of the scatter (patient's location); that is, they would preferentially transmit scatter rather than primary x-rays. The elimination of scatter was never truly solved in fourth generation designs [Goldman, 2007].

- **Fifth Generation**

The fifth generation scanner was known as the electron beam computed tomography (EBCT), or electron beam tomography (EBT), and was built between 1980 and 1984 for cardiac applications [Goldman, 2007; Hsieh, 2009]. To "freeze" cardiac motion, a complete set of projections must be collected within 20 to 50 ms. This is clearly very challenging for conventional third or fourth generation types of scanners due to the enormous centripetal force placed on the x-ray tube and the detector. In the electron-beam scanner, the rotation of the source is provided by the sweeping motion of the electron beam (instead of the mechanical motion of the x-ray tube), as show in figure 3.8 [Hsieh, 2009].

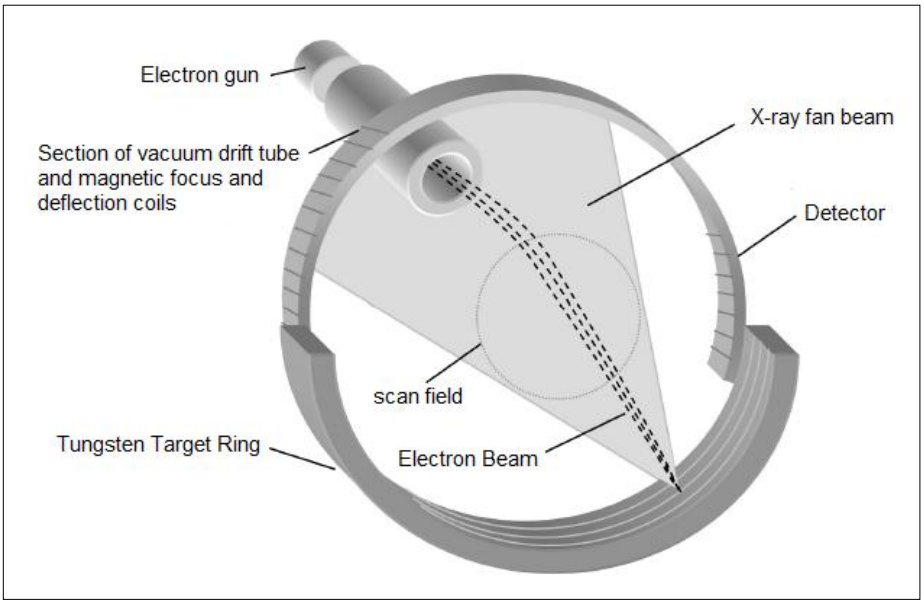

Fig. 3.9- Fifth Generation CT scan geometry (or Electron Beam Scanner) [adapted from Hsieh, 2009].

The X-rays are produced from the focal track as a high energy electron beam strikes the tungsten. There are no moving parts to this scanner gantry. The electron beam is produced in a cone-like structure (a vacuum enclosure) behind the gantry and is electronically steered around the patient so that it strikes the annular tungsten target [Bushberg *et al.*, 2002].

- **Sixth Generation**

In the early 1990s, the design of third and fourth generation scanners evolved to incorporate slip ring technology [Bushberg *et al.*, 2002]. A slip ring is a circular contact with sliding brushes that allows the gantry to rotate continually. The use of slip-ring technology eliminated the inertial limitations at the end of each slice acquisition, and the rotating gantry was free to rotate continuously throughout the entire patient examination. This design made it possible to achieve greater rotational velocities than with systems not using a slip ring, allowing shorter scan times [Bushberg *et al.*, 2002].

Helical CT (also inaccurately called spiral CT) scanners acquire data while the table is moving; as a result, the x-ray source moves in a helical pattern around the patient being scanned.

Helical CT scanners use either third or fourth generation slip-ring designs. By avoiding the time required to translate the patient table, the total scan time required to image the patient can be much shorter (e.g., 30 seconds for the entire abdomen). In some instances the entire scan can be performed within a single breath-hold of the patient, avoiding inconsistent levels of inspiration. With helical computed tomographic scanners, the x-ray tube rotates around the patient while the patient and the table are translated through the gantry. The net effect of these two motions results in the x-ray tube traveling in a helical path around the patient (figure 3.9).

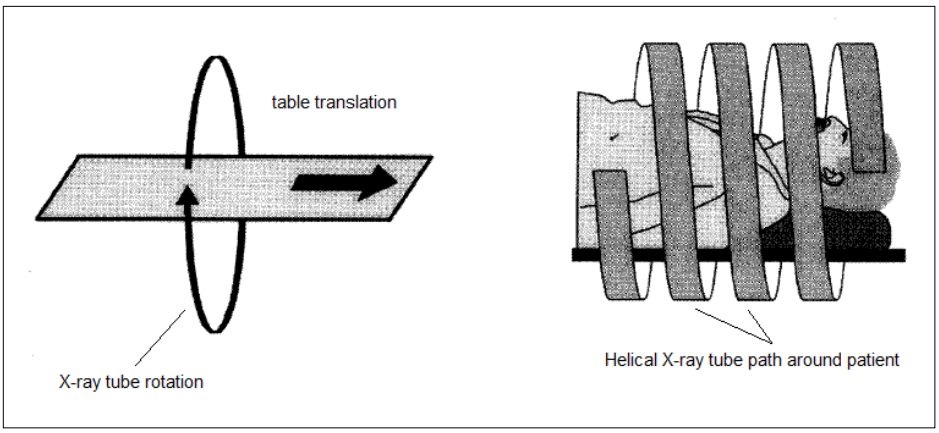

Fig. 3.10- Helical CT design [adapted from Bushberg *et al.*, 2002].

The commencement of helical scanning has introduced many different considerations for data acquisition. In order to produce reconstructions of planar sections of the patient, the raw data from the helical data set are interpolated to approximate the acquisition of planar reconstruction data [Bushberg *et al.*, 2002].

- **Seventh Generation**

The seventh generation of CT scanners is the last and new technology use in CT scanners, and is used as multiple detector arrays. This uses several, closely spaced, complete detector arrays. With no table translation (nonhelical acquisition), each detector array acquires a separate axial CT image. With a helical acquisition on a multiple detector array system, table speed and detector pitch can be increased, increasing the coverage for a given period of time [Bushberg *et al.*, 2002].

The X-ray tubes designed for CT have impressive heat storage and cooling capabilities, although the instantaneous production of x-rays (i.e., x-rays per mill-ampere-second) is constrained by the physics governing x-ray production. An approach to overcoming x-ray tube output limitations is to make better use of the x-rays that are produced by the x-ray tube. When multiple detector arrays are used (Figure 3.10), the collimator spacing is wider and therefore more of the x-rays that are produced by the x-ray tube are used in producing image data. With conventional, single detector array scanners, opening up the collimator increases the slice thickness, which is good for improving the utilization of the x-ray beam but reduces spatial resolution in the slice thickness dimension. With the introduction of multiple detector arrays, the slice thickness is determined by the detector size and not by the collimator. This represents a major shift in CT technology [Bushberg *et al.*, 2002].

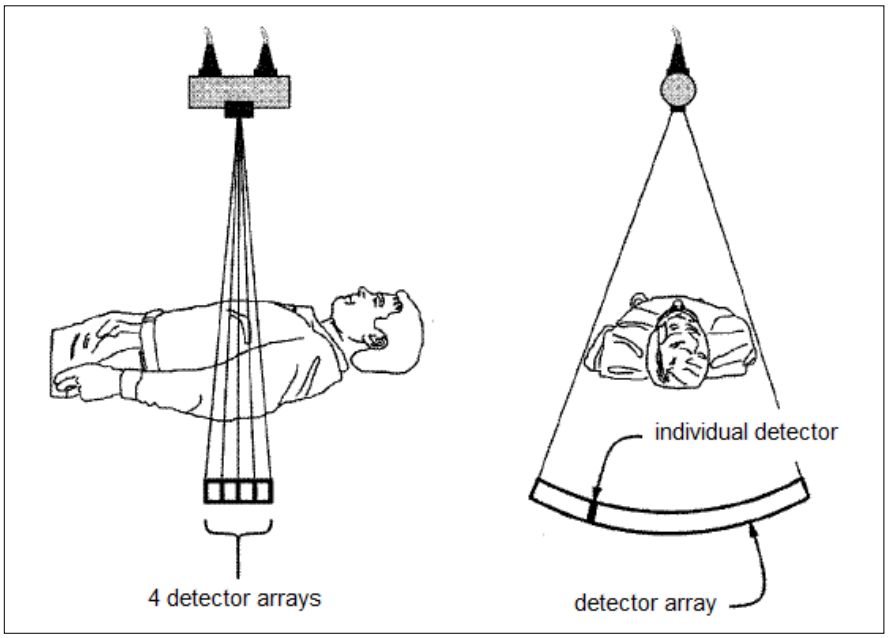

Fig. 3.11- Scheme of a multiple detector arrays of computed tomography scanners [adapted from Bushberg *et al.*, 2002].

3.1.2 Applicability in TPS

The CT is considered the gold standard technique in the planning system of treatment, due to the many advantages that it has, in particular, the geometric precision [Mayles *et al*,2007].

CT provides transverse slices of the human anatomy by reconstructing the attenuation of a narrow beam of X -rays through the different tissues, which contain anatomical images of very high resolution and contrast, based on the electron density, useful in the calculation of dose. CT images also give excellent soft tissue contrast, allowing for greatly improved tumors localization and definition. Patient contours can be obtained easily from the CT data on each transverse CT slice — in particular, the patient's skin contour, target and any organs of interest. The CT numbers associated with each pixel (reconstruction element) may be converted to electron density values.

The use of CT scans for treatment planning has become well established and has been shown to provide significant improvement in treatment accuracy [Podgosark, 2005; Cherry *et al*, 2009].

According to the pathology in question, a protocol is followed with the steps that must be taken to ensure that no failures occur on subsequent treatment.

Initially, the patient is placed on the stretcher/bed of the CT machine where one gets the first image for the positioning of the body and subsequent alignment of lasers.

Then, the most important phase of the acquisition comes, which is the marking with reference points on the skin (wire metal) and the appeal to masks and immobilization supports. These tags serve as guidance for the dosimetry allowing the location of the contours of the body. Typically, the wire is placed on the patient on the transverse plane parallel to the isocentre plane.

Immobilization devices are usually made of carbon fibre which allows that there is no disturbance of the dose distribution during the treatment. The mask is made individually for each patient being used during the entire treatment. Patients to be treated in the head and neck or brain areas are usually immobilized with a plastic mask that, when heated, can be moulded to the patient's contour. The mask is affixed directly on to the treatment table or to a plastic plate that lies under the patient, thereby preventing movement, as seen in figure 3.11.

As has already been mentioned this is one of the decisive steps in the entire treatment plan, since that the position that the patient has during the image acquisition should be the more identical as possible during the treatment, so that this is not compromised. Any adjustments which may be made in dosimetry, are practiced from these masks, hence its importance.

Completed all positioning adjustments, the final image is obtained, where the alignment is confirmed and the tattoo is made.

Following this, the data is sent to dosimetry to proceed with the treatment plan.

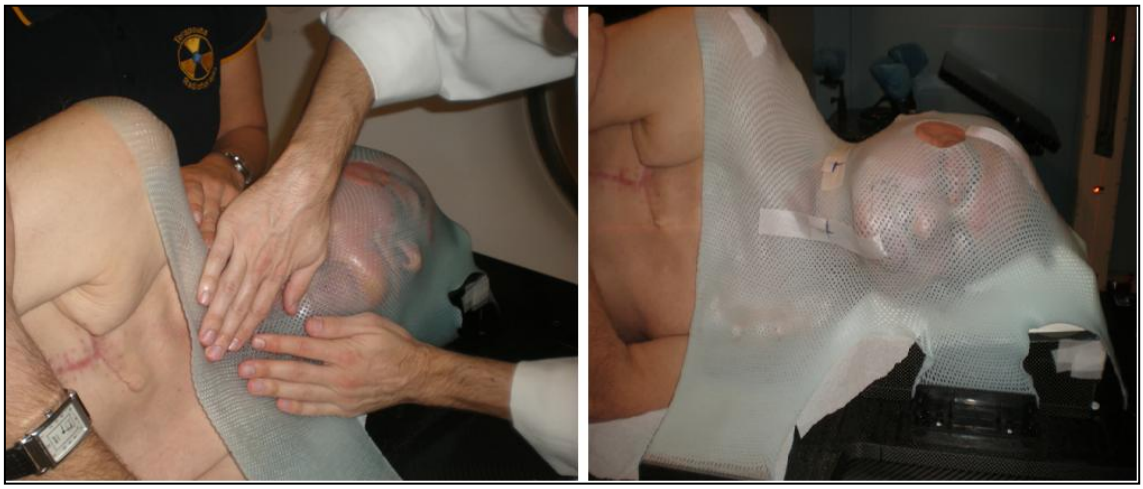

Fig. 3.12- Thermoplastic mask used for immobilization of brain and head and neck patients.

3.2 Magnetic Resonance Imaging

3.2.1 Physical principles

In the same manner as for the CT, devote only a chapter to MRI, is insufficient to understand, in an extended and rigorous way, all its entire mechanism. However, one intends only to clarify, from a general description, the functioning of this technique.

Magnetic resonance imaging (MRI) is a non-ionizing technique that uses radiofrequency (200MHz–2 GHz) electromagnetic radiation and large magnetic fields (around 1–2 tesla (T), compared with the Earth's magnetic field of about 0.5×10^{-4} T).

The large magnetic fields are produced by superconducting magnets; in which current is passed through coils of superconducting wire whose electrical resistance is virtually zero [Dougherty, 2009].

MRI images provide anatomical and physiological details, i.e. structure and function, with full three-dimensional capabilities, excellent soft tissue visualization, and high spatial resolution (~1mm). Like x-ray CT, it is a tomography imaging modality. Image reconstruction, while conceptually equivalent to that in CT, is obtained from the raw signals collected in frequency space. With sufficient slice images, the image data is practically three-dimensional and it is possible to reconstruct the data in different two-dimensional planes at will. Scans last several minutes, rather than a few seconds as in x-ray CT, so that patient motion can be a problem [Dougherty, 2009].

Furthermore, MRI scanners are several times as costly as a CT scanner because of the expensive superconducting magnet required.

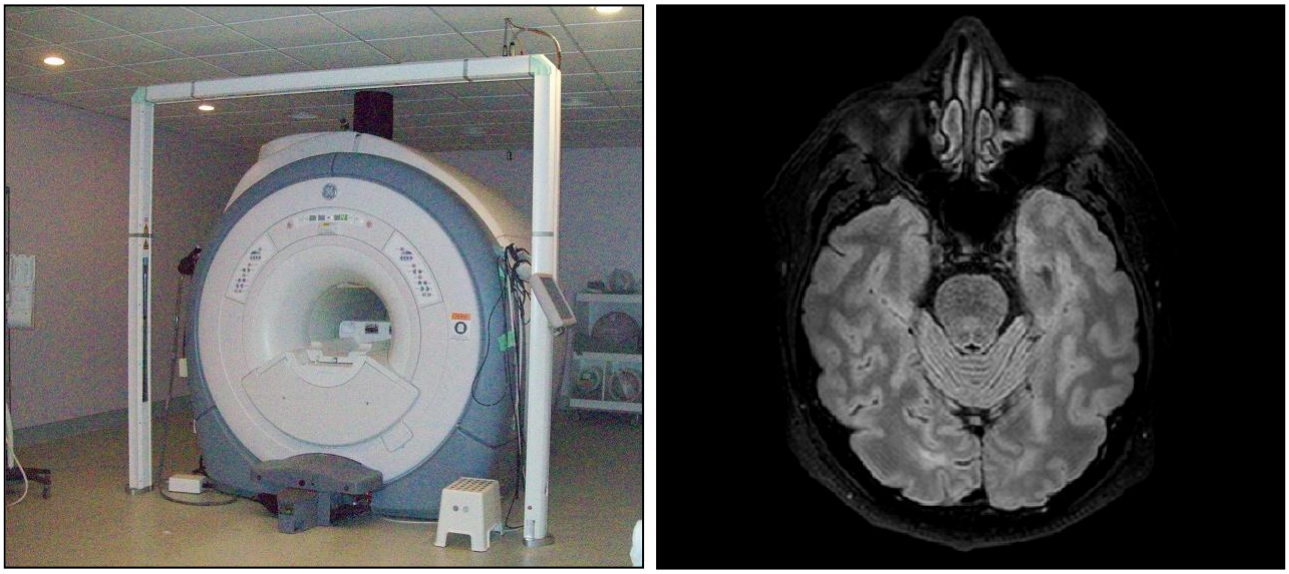

A **B**

Fig. 3.13- **A**: MR scanner (*GE Signa® HDxt 3.0T* scanner). **B**: Axial brain MRI.

3.2.1.1 Physics of Nuclear Magnetic Resonance

MRI imaging is based on nuclear magnetic resonance (NMR). Nuclei are composed of nucleons, either neutrons or protons. Nuclei with unpaired nucleons behave like small magnets, with an associated magnetic moment.

Among the most interesting nuclei for magnetic resonance imaging are 1H, 13C, 19F, 23Na, and 31P. All of these nuclei occur naturally in the body, with the proton (1H) being the most commonly used because the two major components of the human body are water and fat, both of which contain hydrogen. They all have magnetic properties which distinguish them from non magnetic isotopes. The hydrogen atom (1H) consists of a single positively charged proton which spins around its axis. Spinning charged particles create an electromagnetic field, analogous to that from a bar magnet. The term ‘spin magnet’ is used to describe them because they are in constant motion [Rinck, 2001].

When atomic nuclei with magnetic properties are placed in a magnetic field, they can absorb electromagnetic waves of characteristic frequencies. The exact frequency depends on the type of nucleus, the field strength, and the physical and chemical environment of the nucleus. The absorption and remission of such radio waves is the basic phenomenon utilized in MRI [Rinck, 2001].

3.2.1.2 Movement of precession - Larmor frequency

In the human body, the hydrogen protons are arranged in a random manner, this is, the magnetic moments do not have a defined spatial orientation, when subjected to the action of the low terrestrial magnetic field. This random arrangement causes the magnetization that results from a given tissue volume to be zero [Mazzola, 2009].

When the body is under the action of a high external magnetic field (1.5T), which we call B_0, the hydrogen protons tend to align themselves according to the direction of the applied field. However, the protons point either parallel or anti-parallel to the field [Dougherty, 2009].

Both orientations represent two levels of energy that the proton can occupy, matching the level of low power to parallel alignment and high energy level to anti-parallel alignment, as can be seen in figure 3.13.

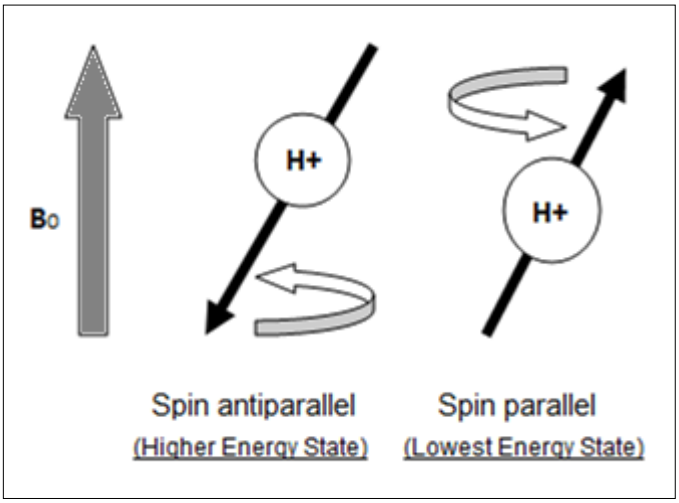

Fig. 3.14- Hydrogen protons under the action of an external magnetic field B_0 [adapted from Dougherty, 2009].

Nevertheless, to ensure that these protons remain in the anti-parallel state, it is necessary to provide more energy; hence they exist in greater in number, at steady state, spins in a parallel position to the external magnetic field. In this situation, the result of magnetization becomes different from zero and has a total magnetization (M_0) parallel to B_0.

As they are subject to a magnetic field, the hydrogen protons begin to make a motion of precession motion around B_0 at a given frequency w called Larmor frequency (given by the equation below), which is proportional to the applied field and the gyromagnetic constant γ for each one of the nuclei [Liang *et al*, 2000].

$$w = \gamma . B_0 \tag{6}$$

It is noted that any change in magnetic field will change the precession frequency.

Although there is a magnetization that is different from zero, this is not possible yet to be quantified, thus it is necessary to move the magnetization for a perpendicular axis to B_0, transverse axis. To be able to move the magnetization of the longitudinal axis to the transverse axis it is necessary to issue a wave of radio frequency (RF) with a magnetic field called B_1 and that in turn is parallel to B_0. The frequency which corresponds to the wavelength of RF is equal to B_0, i.e., it corresponds to the Larmor frequency. This describes the traditional resonance effect, where B_0 is canceled and the magnetization begins to suffer only the effect of field B_1, and in this way it makes a motion of precession around this, in the transverse axis, without ceasing to rotate around B_0 and with the Larmor frequency [Dougherty, 2009]. Figure 3.14 shows the effect of the pulsed radiofrequency in magnetization.

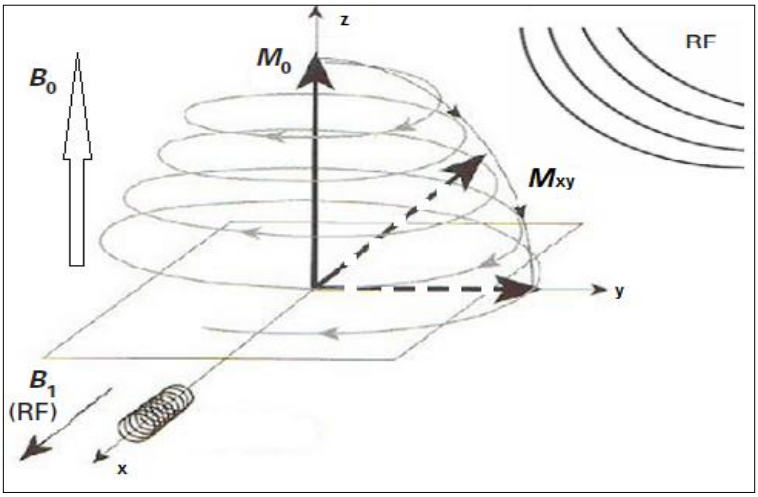

Fig. 3.15- The effect of a radiofrequency pulse, at the Larmor frequency, on the magnetization [adapted from Dougherty, 2009].

When the magnetization is in the transverse axis, the RF wave is turned off and from this moment in the magnetization is measured. The receiver that measures this magnetization notes down a current induced by the motion of precession around B_0, which fluctuates according to w and which amplitude decreases exponentially. This signal is known as Free Induction Decay (FID) [Liang *et al*, 2000].

The amplitude of this signal will decrease over time because of the relaxation process, during which the magnetization returns to its initial state of equilibrium and that depends on the chemical environment that involves the set of spins [Liang *et al*, 2000].

It is noted that in the state of balance the total magnetization (M_{total}) is oriented in accordance with the external magnetic field B_0 ($M_z=M_{total}=M_0$), therefore there is no transverse magnetization, i.e. M_{xy} is equal to zero.

3.2.1.3 The relaxation process time constants

During the relaxation process, two time constants are distinguished: T1, which corresponds to the longitudinal relaxation time ($M_z=M_{total}$), and T2 which is equivalent to the transverse relaxation time ($M_{xy}=0$). The constant T2 is always less than or equal to T1, therefore the transverse magnetization decreases more rapidly than the longitudinal, returning to the initial state. The duration of these times depends on the intensity of the interactions between the spins and the frequency with which these interactions are regulated. In its turn, both the relaxation constants are dependent on the properties of each tissue, being in this way possible to distinguish some tissues, such as: white matter, grey matter or fat [Dougherty, 2009].

Contrast is a factor of great importance for a correct interpretation of the image. The most important source of contrast in clinical MRI is the difference in relaxation times between different tissue types.

This depends on the manipulation of various parameters, such as the relaxation times T1 and T2, as well as the proton density structure of the tissue(s) being imaged [Liang *et al*, 2000]. For each anatomical volume that one wants to achieve, there are protocols with appropriate imaging sequences for image acquisition, and as such it is weights in the parameter that one wants to change. Imaging sequences can be conveniently characterised in terms of Spin-Echo (SE) or Gradient-Echo (GE) sequences.

A feature of MRI is that there is no standard, universally applied imaging sequence; there are an infinite set of combinations of possible timings and arrangements of the various imaging sequence components. In practice, sequences are often designed to give images that are weighted according to a particular relaxation time (i.e. T1-weighted or T2-weighted). Even when utilizing a particular type of weighting, there is flexibility and variability in the imaging parameters used.

Therefore, T1 weighted images acquired on different MR scanners are often obtained using slightly different values of the echo (TE) and repetition (TR) times, resulting in images with subtle differences in contrast [Mayles *et al.,* 2007].

Usually, when one wants to show a good anatomical delineation, a weight in T1 (short TE and TR) is made, if the interest is greater in the functional part weight is done at T2 (long TE and TR). For example, a T1-weighted image, tissues with long T1 appear with hypointense and tissues with short T1, with hyperintense. In T2 weighted images, tissues with short T2 appear hypointense and tissues with long T2 appear hyperintense [Liang et al, 2000].

To summarize, nuclear spins in the presence of an external magnetic field, B_0, align either with or opposed to the magnetic field. The parallel and anti-parallel spins almost cancel each other out, leaving a relatively small number of excess spins aligned parallel with the main magnetic field. If a radiofrequency signal is applied at the Larmor frequency, the individual spins resonate, absorbing the applied energy, and precess in phase. Depending on the magnetic field of the applied pulse and its length, the protons flip towards the x–y plane producing transverse magnetization. The transverse magnetization induces a voltage in an antenna or receiver coil in the x–y plane, often the same coil used to transmit the radiofrequency excitation pulse; this induced signal eventually becomes the MR signal. When the radiofrequency pulse is turned off, the protons de-phase as they try to realign with B_0. Two phenomena occur simultaneously. Transverse magnetization decreases (T2 decay), while longitudinal magnetization increases (T1 recovery) [Dougherty, 2009].

3.2.2 Applicability in TPS

Magnetic resonance imaging has considerable potential for treatment planning. Currently, the use of MRI has been frequent due not only to the high capacity that this technique has in highlighting areas of tumours and soft tissues, as well as its ability to vary the contrast of the image from the variation of their parameters.

Together with its 3D multi-planar imaging capability, MR can provide advantages over reconstructed CT images. Used in conjunction with CT, MRI can provide both complementary and supplementary information for the localization and characterization of tumours and surrounding normal tissues [Mayles *et al*, 2007].

The process of image fusion, between these two forms of acquisition, combines the exact definition of the tumour volume (obtained in MRI) with the information available from the density of electrons (acquired in CT). The data set of MRI is overlaid on the data of CT defined through a series of translations, rotations and scale. This process allows the visualization of both methods on the same image plane.

However, there is a high potential of introduction of problems during the registration of these two techniques, because it becomes difficult to coordinate the image sets, which may lead to a substantial disagreement about the target location, leading to errors in treatment.

The fact that the MRI does not submit information on the electronic density of the volumes in question, necessary to calculate the dose, is one of the most striking aspects that makes its exclusive use in TPS be rejected.

The introduction of MRI in RTP is also severely affected by distortions in geometry that are caused by the heterogeneity of the static magnetic field and by non-linearities of gradient magnetic fields from the magnetic resonance device, as well as by disturbances induced by the magnetic field of the object to be treated, in this case, the human body. These differences of the magnetic field and field gradient will lead to distortions in the image, which severity depends on the type of sequence of impulses and the manipulation of their parameters (constants of relaxation - T1 and T2, proton density, etc.) [Moerland, 1996].

Being the great aim of radiotherapy the administration of a large quantity of dose on tumour volume, thus sparing the surrounding healthy tissues, the exact region to be treated is of highest importance. Hence these distortions represent a major obstacle in the plan, since they will provide spatial information inaccurate, preventing a precise correlation of the image.

In addition to this problem there are others which undertake the use of MRI in the treatment plan, one of them being the lack of information about the electronic density required to dose calculation.

As the CT depends on the attenuation of RX by tissues as a function of the atomic number and electrons density, it can be automatically obtained by Hounsfield Units. The same does not happen with the MRI, which as has already been said, is derived from the density of protons and of constants of relaxation [Mayles *et al.*, 2007].

Another obstacle that arises is the low signal in the bone, which is important to limit the areas of heterogeneities as the interfaces bone-tissue and bone-air fundamental in dose calculation. On the other hand, as these are not visible as well as the landmarks, it leads to the limited registration of the image.

Taking into account all the aspects mentioned, the MRI has been used in TPS only as a complementary technique, but in spite of everything it holds a strong potential for further application in the treatment planning in radiotherapy.

3.3 Medical Imaging storage files - DICOM (Digital Imaging Communications in Medicine)

Throughout this chapter one has addressed two of the image techniques used in the system of planning in Radiotherapy. After the acquisition, the images are transferred to the system for subsequent planning and then follow for the treatment place.

The whole journey that the image suffers along the plane of procedures implies that there is, in addition to a communication system and network storage (Picture Achieving and Communication System-PACS), a common format that allows the correspondence between each station so that, in a safe manner, it is permitted the transference of data corresponding to each one of the patients.

This communication is safeguarded by a pattern called DICOM - *Digital Imaging and communications in Medicine.*

The DICOM format was published in 1993 taking into account the standard developed by the American College of Radiology (ACR) and the National Electrical Manufacturers Association (NEMA) who in 1983 formed a working group with the objective of developing a model that would allow the exchange of images. This standard is defined as a set of standards for treatment, storage and transfer of medical images and associated information, in an electronic format, and was created with the purpose of standardizing the formatting of diagnostic images allowing these to be exchanged between equipments, computers and hospitals [Medical-NEMA]. Compliance with this standard enables an open architecture for imaging systems, bridging hardware and software entities and allowing interoperability for the transfer of medical images and associated information between disparate systems [Dreyer *et al*., 2006].

3.3.1 DICOM Standard

The DICOM standard is divided into a number of parts each of which describes a particular component (figure 3.15).

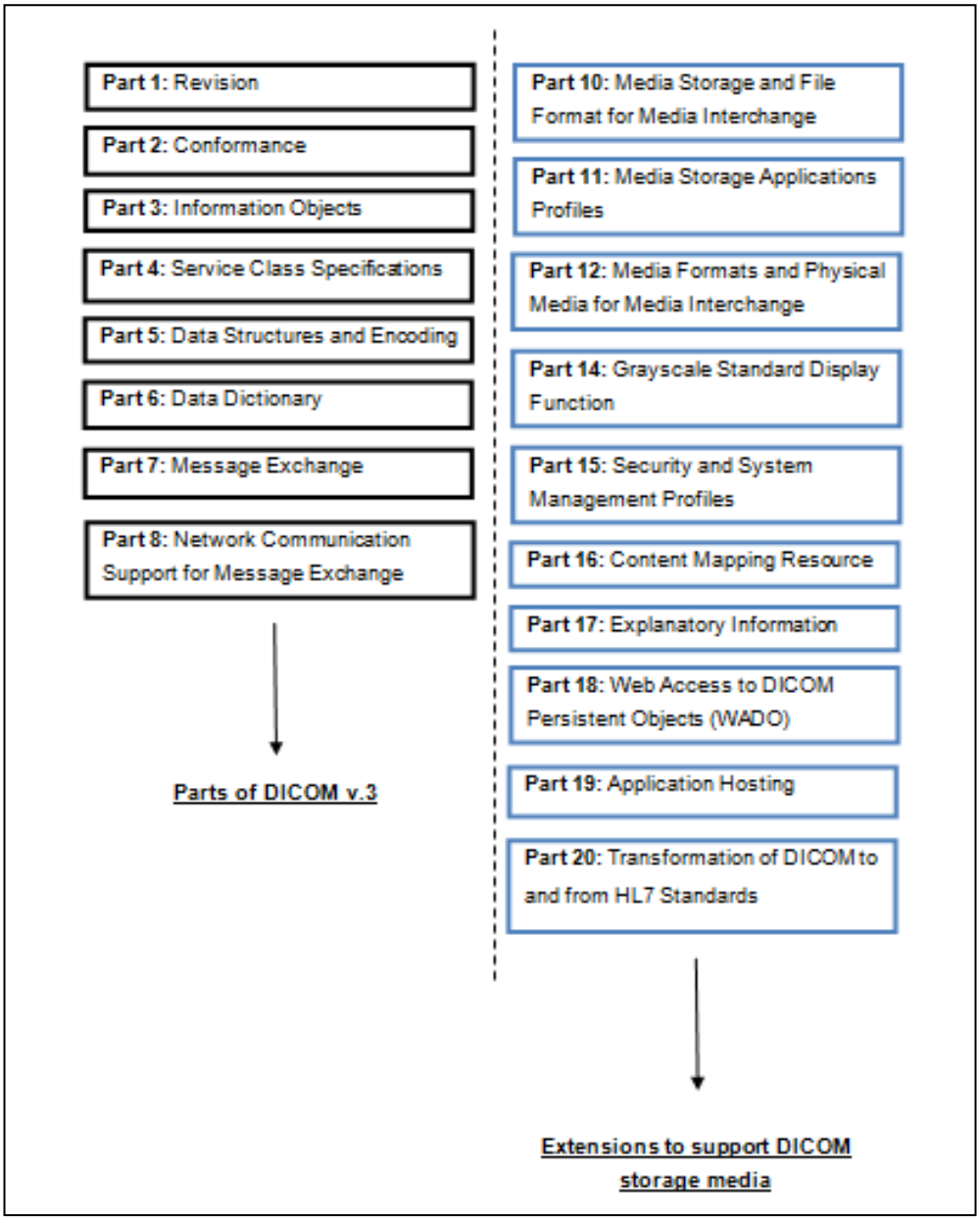

Fig. 3.16- Diagram of DICOM Standard [adapted from Medical-Nema].

The different parts [Alarcón, 2013] that comprise the DICOM Standard v.3 are interrelated and including a generally consist of:

- Part 1: provides an overview Standard general, its history, development and objectives, containing a brief description of the objectives of each part of it.

- Part 2: define the principles that must meet all the implementations who say they support the standard.

    - Requirements in accordance
    - Conformance statements
    - Although DICOM does not specify any validation procedure or test to ensure that conformity

- Part 3: specifies the number of information objects and classes. So information objects as classes provide abstract definition real entities, applicable for image communication medical and related information.

- Part 4: defines the number of classes of service. A service class associates one or more items of information with one or more commands, which were used on those objects.

- Part 5: specifies how DICOM applications must build and encoding the data set resulting from the use of objects information and service classes. Also specifies techniques supported by image compression standard.

- Part 6: Data Dictionary. Defines the collection of all elements DICOM.

- Part 7: Message Exchange. Specifies both the service and the protocol used by an application in medical imaging environment, to exchange messages.

- Part 8: Specifies the services and higher layer protocols, needed to support communication between DICOM applications a network environment.

The DICOM standard has become an essential component for the integration of systems of digital images in medicine, offering solutions for many applications related to network communication, as well as offline.

3.3.2 IOD – Information Objects

An object information (IOD) is a collection of pieces of information related, grouped into smaller entities called entities of information. Each of these entities contains information about an item, such as patient information (age, sex, ID), an image type and associated parameters (CT, MRI, US), etc. These are grouped in the form of a list of data, called attributes, and each one of these is given a reference number called tag (figure 3.16).

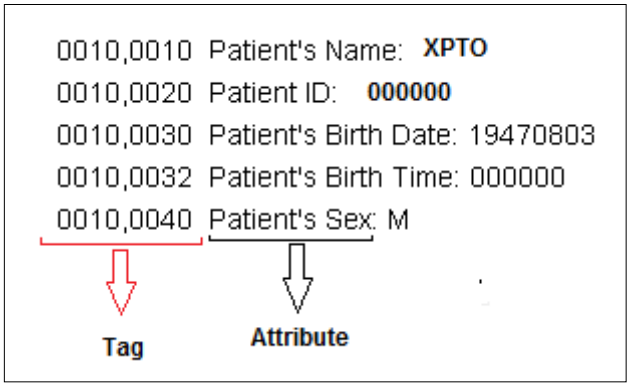

Fig. 3.17- Example of some attributes of a script from a DICOM image.

Two fundamental components of DICOM are the information object class and the service class. Information objects define the contents of a set of images and their relationship, and the service classes describe what to do with these objects. The service classes and information object classes are combined to form the fundamental units of DICOM, called service-object pairs (SOPs) [Huang, 2004].

According to the type of image, their attributes are different, for example, to differentiate a CT image of an MR image, there is a tag with a number (UID- Unique Identifier) that identifies the type of image in question. The attribute mentioned in the table below (table 3.2) with respect to the SOP Class UID and always have the same UID for the same class of imaging (CT, MRI, PET, etc.).

Tag	Attribute name	UID value	UID name
(0002,0002)	Media Storage SOP Class UID	1.2.840.10008.5.1.4.1.1.2	CT Image Storage
		1.2.840.10008.5.1.4.1.1.4	MR Image Storage

Tab. 3.2- The UID values that are registered and used throughout the Parts of the DICOM Standard to CT and MRI [adapted from DICOM-Dictionary].

However, it is necessary to understand that all the attributes that are distinguished with the termination UID are unique and characteristic of a single image, and there is no other value equal to the same tag in another image.

There are three important attributes that define the uniqueness of a picture, i.e. are unique and work as an ID and are designated by Study Roots Identifiers. These in their turn are distinguished into three levels: Study, Series and Image (table 3.3).

Name	Tag
STUDY level	
Study Instance UID	(0020,000D)
SERIES level	
Series Instance UID	(0020,000E)
IMAGE level	
SOP Instance UID	(0008,0018)

Tab. 3.3- Study Roots Identifiers [adapted from DICOM-Conformance].

With the exception of the Study Instance UID, which remains equal for the same case study, this is, for the same patient, for the remaining, the UID value will vary from image to image, even if they belong to the same class (CT, MRI, etc.).

In addition, for each modality, the DICOM defines precisely the data elements that are mandatory, optional (i.e., can be omitted) or required under certain circumstances, this is, in the case of a CT image, for example, the attribute that affects the current in the X-ray tube (tag: 0018,1151) will not be present in the script of an MR image. In the same way that the echo time (tag: 0018, 0081) that appears in the script of the MRI does not appear in CT image.

3.3.3 Conformance Statements

It is important to understand that the DICOM requires that there is a declaration of conformity [DICOM Conformance Statement] that must explain what DICOM services and options are supported, which extensions and peculiarities were implemented by the supplier, and how the device communicates with other DICOM systems. In theory, when comparing two declarations of conformity it is possible to determine if the two devices compatible with DICOM are capable of fully communicate with each other or not [DICOM-offis, DICOM-Conformance].

This document describes:

- SOP supported.
- Syntax transfer.
- Paper to perform in each.
- A way to implement the network with the exceptions that could be, and if there is a possibility of a physical link
- Describe the configurable elements of implementation:
  - Application name.
  - Presentation Management.
- If the system supports extended character sets.

Generally, these documents include more information with more detailed description. The more complete the information will be easier to achieve connectivity and interoperability implementation.

In practice, however, the declarations of conformity are only understandable by specialists since they are complex and require a thorough knowledge of these resources.

Chapter 4

MATERIALS AND METHODS

4. Materials and Methods

4.1 Overview

One of the core objectives of the planning system is to estimate what dose can be deposited in tumour volume, while delivering the minimum dose possible in healthy tissues. The only technique of image acquisition that allows this situation is the CT, hence it is the reference image used, being the remainder considered complementary techniques, once they serve only to aid in limiting the organs/tissues.

The information on the electronic density that comes from CT allows the achievement of the values of Hounsfield Units on which the algorithms for dose calculation depend on. Thus, the planning software only recognizes CT for this purpose.

The use of CT for treatment planning, however, is not straightforward. The extra costs associated with multiple imaging modalities have motivated several groups to study the possibility of developing treatment plans using only MR images [Beavis *et al*., 1998, Pasquier *et al*., 2006]. Others refer to the additional uncertainty introduced with the registrations between CT and MR as a motivation for treatment planning that directly uses MRI [Pasquier *et al*., 2006; Prabhakar *et al*., 2007]. Errors introduced in the registration will affect the treatment systematically throughout the entire treatment period. Prostate and gynecological patients are especially problematic as the patients can have different rectal and bladder filling during the different imaging sessions. This implies that the registration result can significantly depend on the surrounding tissues and in itself introduce significant uncertainty [Nyholm *et al*., 2009; Roberson *et al*., 2005].

Replacing the current CT/MRI-based RTP procedure with MRI simulation will eliminate the CT scanning sessions (no x-ray exposure) and consequently the image fusion process. Moreover, any incidental errors caused by patient inter-procedure positioning and image fusion would be eliminated. As a consequence, the improved target localization is expected to lead to a higher local tumour control and reduced normal tissue complications [Stanescu *et al.*, 2008].

The exclusive application of images of MR on treatment planning system is not trivial and there are still some obstacles to be overcome.

In addition to the geometric distortion and the marking of the patient in order to maintain a correct positioning during the subsequent treatment, the absence of information on the electronic density of the tissues, indispensable in the calculation of the dose is one of the most evident problems which present itself.

For MRI simulation it is required that different electron density information (i.e. CT values or HU's) be correlated or assigned to MR images and the image distortions be addressed [Chen *et al.*, 2004b, Doran *et al.,* 2005, Stanescu *et al*., 2006a, 2006b].

There is no apparent correlation between MR tissue signal intensity and CT numbers as different tissues may exhibit similar signal values, e.g. hard bone and air show as dark regions. To compensate for this limitation, MR images can be prepared for dose calculations by assigning bulk CT values to the voxels corresponding to segmented volumes of interest (VOIs) [Chen *et al.*, 2004a, Stanescu *et al*., 2006a]. These VOIs represent certain tissue types relevant to dosimetric calculations such as bone, lungs (air) and soft tissue.

Having in mind all these aspects and managing to overcome some of these problems, it will demonstrate that the implementation of MRI only-based RTP is increasingly a certainty.

4.2 Methodology

For this study two approaches were established: a first plan which is based on the standard procedure of RTP with the use of the CT image, i.e. a CT-based RTP and the second plan which exclusively uses MRI-based RTP (figure 4.1).

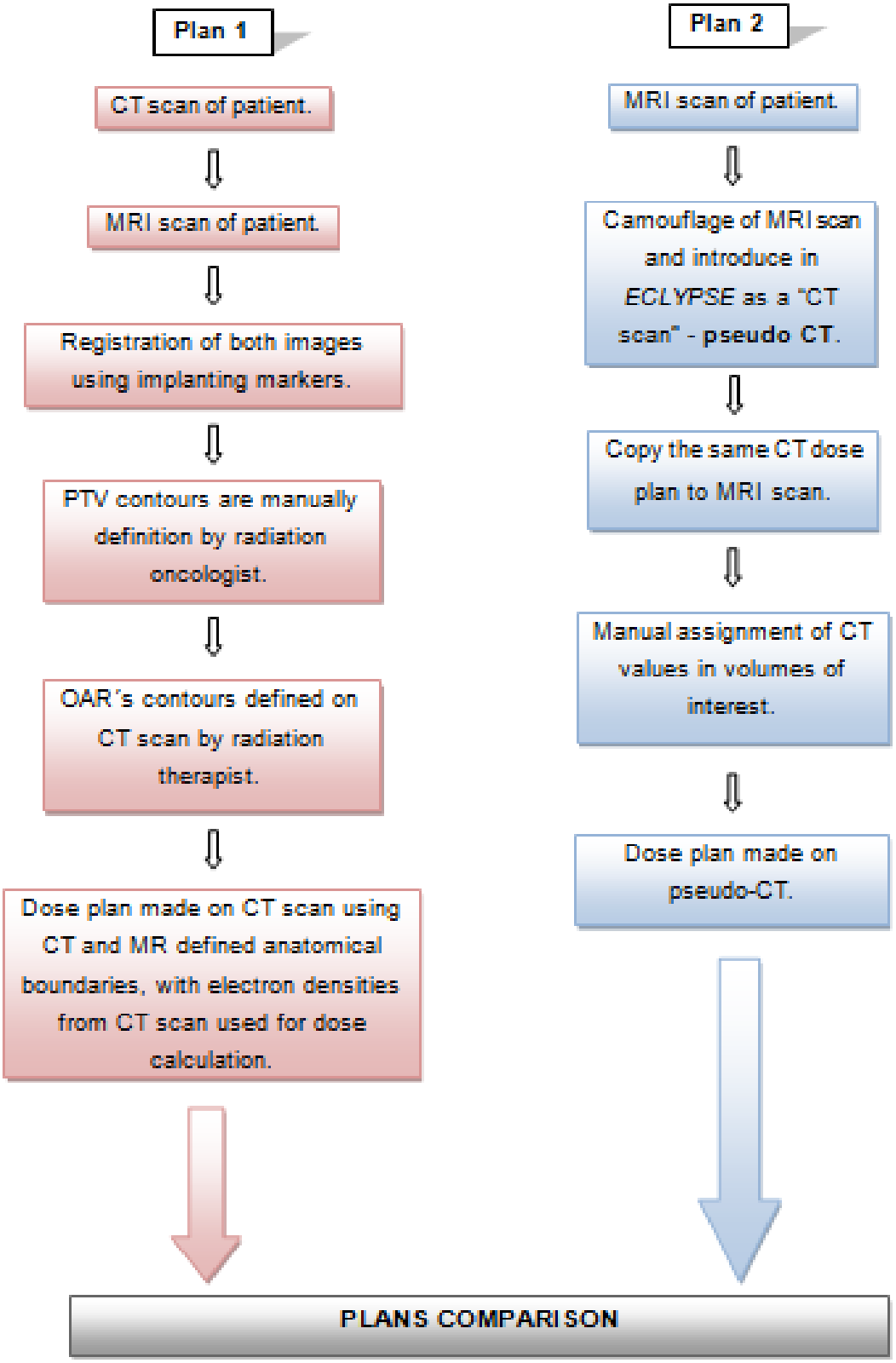

Fig. 4.1- Plan 1: Steps in the conventional radiotherapy workflow with CT and MRI; and Plan 2: the proposed new radiotherapy workflow based on MRI only.

4.2.1 Subjects

The aim of this study was to assess each plan (plan 1 and plan 2 – figure 4.1) using images of patients already treated without influence on treatment plan. However, during the time that the study was performed, this situation was not possible, since no patient was in these conditions.

In order to overcome this problem, one has resorted to the use of a phantom created by a student with the intent to be used in Nuclear Medicine Service. This had different volumes with inhomogeneities, and so decided to use it as an object of study.

The procedures that would be used for a patient were exactly the same as those used in the phantom.

The phantom simulates the chest (lung, spine) with an inner tube, between the lungs, with a volume, which simulates the tumor lesion.

The material that simulates the spine was Teflon, commonly used to simulate bone in Nuclear Medicine. Inside the lungs of the phantom has styrofoam (polystyrene) and copper sulphate ($CuSO_4$) dissolved in water, where in about 20 liters of water were dissolved, approximately 700 grams of $CuSO_4$. This compound exhibits paramagnetic properties that lead to an increase of the value of the intensity of the magnetic field, thereby obtaining an hyperintense on the MRI images.

The rest of the phantom was filled with only water with copper sulphate, which appears with bluish colour, as seen in Figure 4.2.

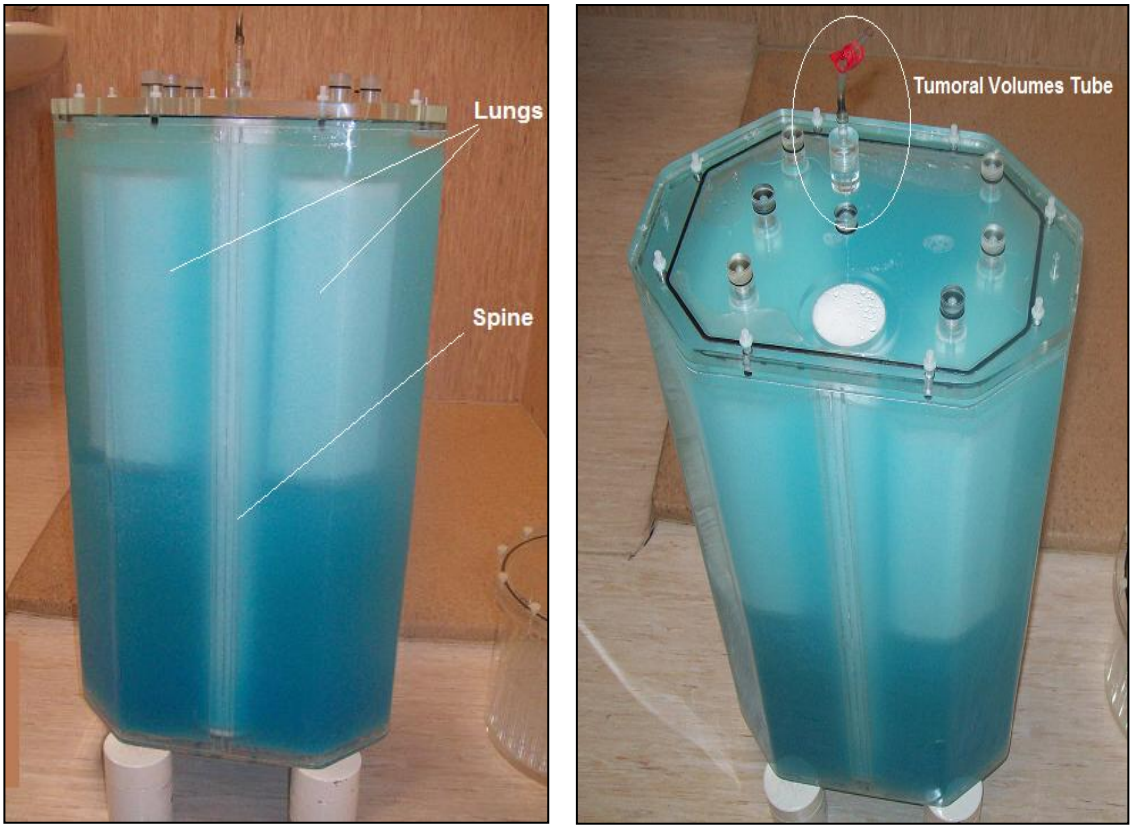

Fig. 4.2- Phantom used in the study.

4.2.2 Imaging

Initially, the images were acquired on a *GE Lightspeed*® CT scanner with 2.5mm and 120 kVp, which followed directly to the TPS.

Then, it proceeded to the acquisition of MRI Images. At this stage it was necessary to place markers were possible to be visible in the images without causing artifact.

Likewise, would have a similar size and positioning[1] of the metallic markers used in the CT images, so that the source of the images were the same in each of the two modes.

The markers used were made with a hematocrit tube with vaseline and sealed at both extremities as shown in figure 4.3.

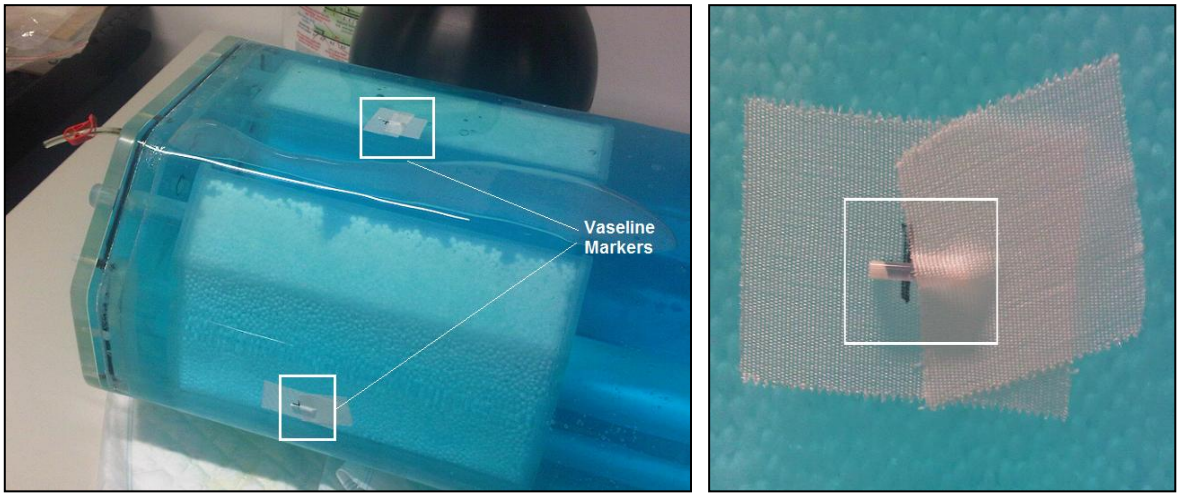

Fig. 4.3- Vaseline markers in the phantom.

Two sequences were acquired for MR images on a *GE Signa*® *HDxt* 3.0T scanner. A T1-weighted with Fast Relaxation Fast Spin Echo sequence (FRFSE) and a T2-weighted with Fast Spin Echo sequence (FSE). However, for further planning, we used the T1-weighted images, because these images emphasized better markers.Both reference scans were imported via DICOM into the treatment planning system, Eclipse™ v. 10.0 (Varian Medical Systems, Palo Alto, CA).

[1] The positioning of the phantom was made with recourse to external lasers (LAP™). However, these lasers are never used. Their existence is due to the possibility of a future use utilize "MRI only" in TPS.

One important aspect that has been mentioned is the fact the Eclipse supports multi-modality (CT, MRI, PET) image registration using a mutual information algorithm. However, only accepts CT images for the calculation of the dose distribution.

To overcome this problem, the MRI reference scan was camouflaged as a CT scan by modifying several attributes in the DICOM header.

Changing the parameters of the DICOM header was done in MATLAB™ (v.R2010b) with the adaptation of a script given by Sune K. Buhl (Department of Oncology (52AA), Herlev Ringvej University Hospital, Copenhagen).

To understand, more precisely, this process of "camouflage", the script was divided into four fundamental parts:

1. Setting of the paths of the MRI and CT folders;

2. Loading data from DICOM header of a CT image, which are then copied to the pseudo-CT;

3. Saving MRI variables to be added to the pseudo-CT images;

4. Changing information on the pseudo-CT and save the final images.

The main changes occurred in the parameters with new unique identifiers-UID (because with this identification tags are unique to a particular type of image). Thus, from the *dicomuid* command generated three new UID's to the *SeriesInstaceUID*, the *StudyInstanceUID* and the *SOPInsstanceUID* attributes.

Moreover, tags such as (0002,0002) corresponding to the *Media Storage SOP Class UID*, which takes a different value according to the image mode in question has also been necessary to modify by changing the value of MR image (1.2. 840.10008.5.1.4.1.1.**4**) to the value of a CT image (1.2.840.10008.5.1.4.1.1.**2**).

As can see in the attached script (appendix A), other parameters were changed/added, which is the case of those which relate exclusively to CT images.

Thus, the MRI scan appeared throughout the system as a CT scan.

4.2.3 Structure definition and treatment plan

4.2.3.1 CT based RTP

With the images in Eclipse started by mark the reference point (origin) taking into account the metallic markers.

Then proceeded to limit the volumes of interest (lungs, spine and CTV) have been obtained automatically from each electronic density. The exception was the marking of the PTV which was done manually from the standard margins between CTV and PTV (~1mm).

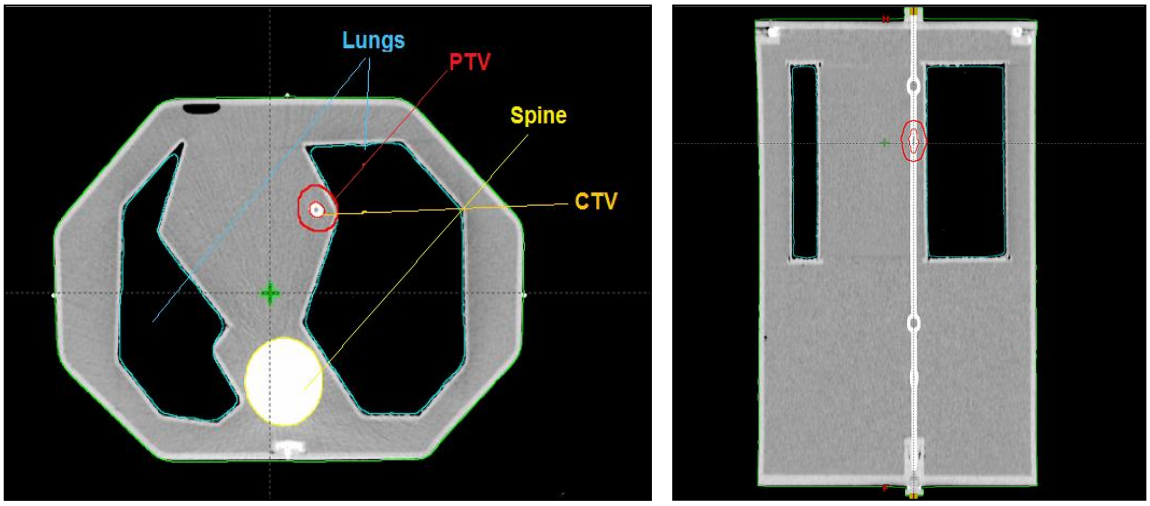

A **B**

Fig. 4.4- A: Axial CT volumes; B: Sagittal CT volumes.

The next step was the setting of the beam angles that was made in a simplified form as it is a phantom.

In the choice of treatment technique there were not any special criteria, thus opted by applying the technique of conformal radiotherapy, creating four fields at 0 º, 80 º, 130 º and 330 º as seen in Figure 4.6. The energy of the beams was 6 MeV which used a *Trilogy* linac.

4.2.3.2 MRI-only based RTP

Initially, when importing the pseudo-CT (MRI) for the planning system, this had made an automatic registration of images. This process would facilitate the marking of the contours in the images, causing them to stay exactly the same position in both images.

However, due to some artifact generated in the MRI image, the image appeared slightly distorted, which made the structures would not be positioned correctly. Then, the external contours (body) and the internal contours as used in CT-based treatment planning were used for MRI based treatment planning by manually copying target and critical structure contours from CT to MRI, and adjust according the same coordinates of CT. The plan transfer is done with regard to the isocenter, which was set to be at the center of mass of the PTV.

Although manually transferring internal contours could introduce some small errors, it was considered to be more reliable to use the same internal structure contours for our plan comparison than using new contours generated independently on MRI because this would introduce additional and potentially more significant uncertainties in the contours between MRI-only based and CT-based treatment planning.

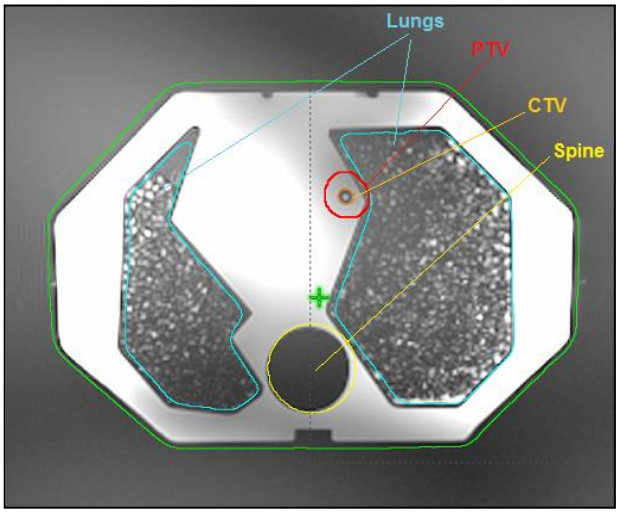

Fig. 4.5- Axial MRI volumes.

The next step was the treatment plan, the main objective is to compare the two techniques, and it then proceeded to exact copy of the plan madein CT (keeping the same beam, the same weights, etc.) for MRI.

Being, in reality, an MR image and not a CT image, there is no information about the electron density of the structures.

Therefore, then became the assignment of the CT values or Hounsfield Units; it was possible to calculate the dose distribution in this plane.

We created two plans equal to CT-based treatment planning, only changing the HU:

- ✓ In the first plan (plan 2), which is called the plane MRI-based HU mean, the HU is given, taking into account the mean HU values of each of the volumes in the CT images. For lungs the average value was -650 HU for the spine was 890 HU for the CTV was 1000HU and body was 20HU.

- ✓ In the second plane (plane 3), MRI-based wba (w-water, b-bone and a-air) differentiated three types of materials: water, bone and air, with the respective values: 0 HU, 1000HU and -1000HU. Thus it is considered air into the lungs, bone for the spine, and water for the remaining structures (PTV, CTV and body).

4.2.4 Dose calculation and plan comparison

Once the images and all contours of interest are available and the assign de CT values, to proceeded the dose calculation.

The dose calculation was performed using Anisotropic Analytical Algorithm (AAA) v. 10.0.28 with four fields to the both three plans:

- Plan 1: CT-based treatment planning;
- Plan 2: MRI-based treatment planning HU mean;
- Plan 3: MRI-based treatment planning wba.

The evaluation of the plans was made by comparing the Dose-Volume Histograms (DVH) as well as from Isodose curves.

4.2.4.1 CT-based plan VS MRI-based plan with HU mean

In Figure 4.6 depicts the Isodose curves between the CT-based plan and the MRI-based plan with HU mean. It can be seen that the two plans look very similar in terms of Isodose distributions and they are acceptable according to clinical criteria.

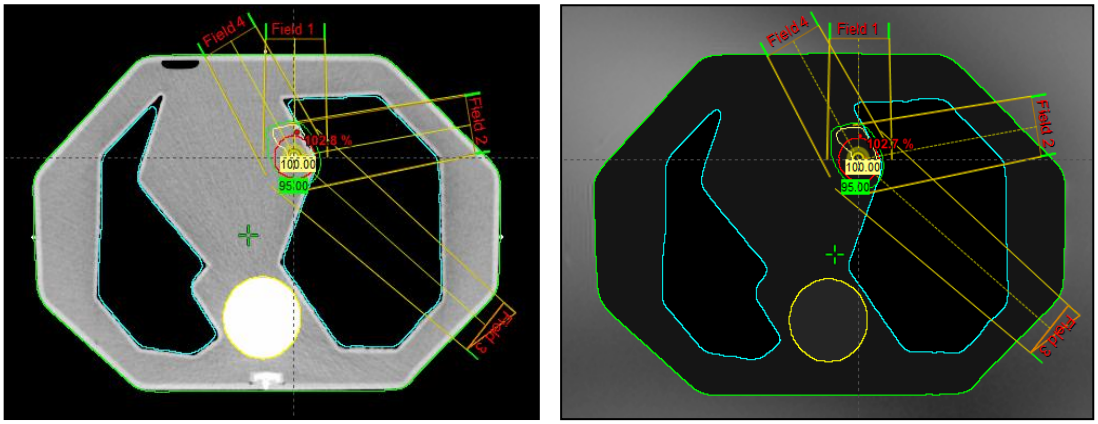

A **B**

Fig. 4.6- Comparison of Isodose distributions between: **A**-CT based plan and **B**-MRI based plan (HU mean).

The DVH's are shown below for the same plans. The histogram is represents in terms of percentage of relative dose. The differences for de spine are most evident, but the lines of the other volumes are coincident for both plans. Again the differences are clinically insignificant.

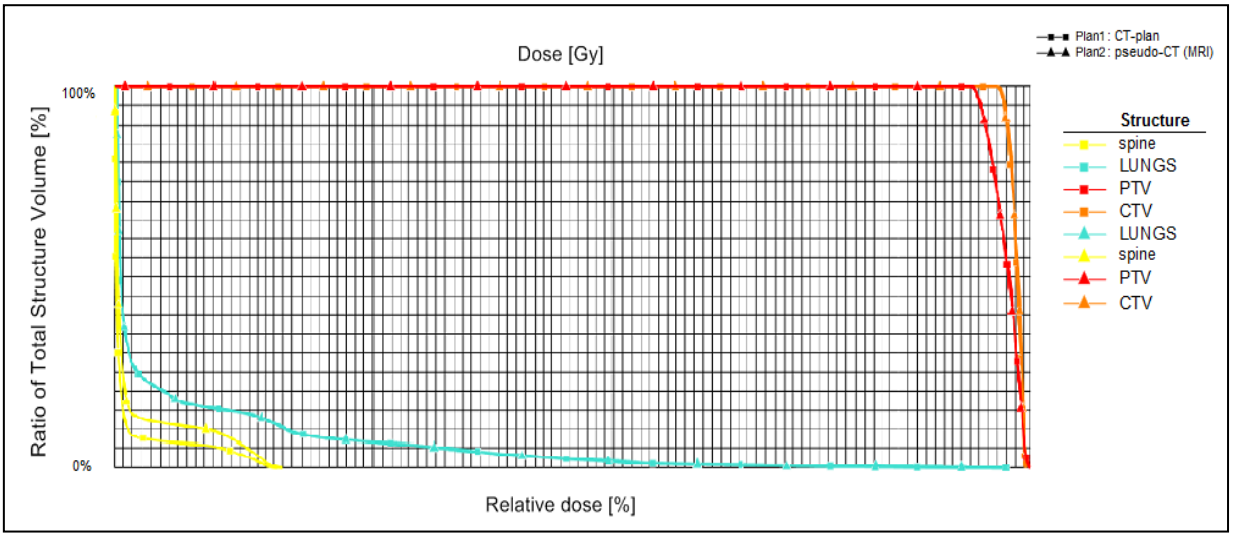

Fig. 4.7- Dose–Volume histograms for Spine, Lungs, planning target volume (PTV) and Clinical Target Volume (CTV) between CT–based plan (plan 1) and MRI–based (HU mean) plan (plan 2).

4.2.4.2 CT-based plan VS MRI-based plan with wba

As the above comparison, results are also quite similar between the CT-based plan and the MRI-based plan with wba, in terms of isodose curves (figure 4.8) and for appreciation from the DVH's (figure 4.9).

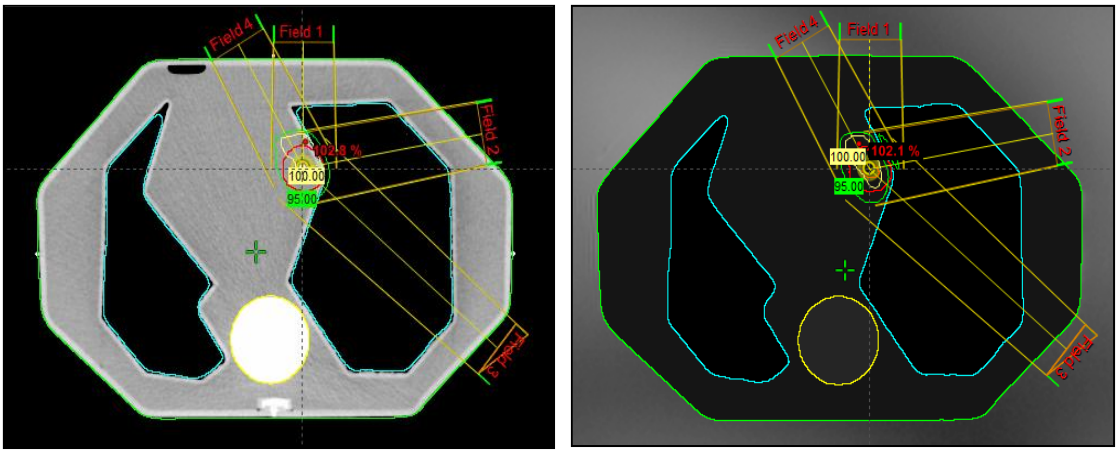

A **B**

Fig. 4.8- Comparison of Isodose distributions between: **A**-CT based plan and **B**-MRI based plan (wba).

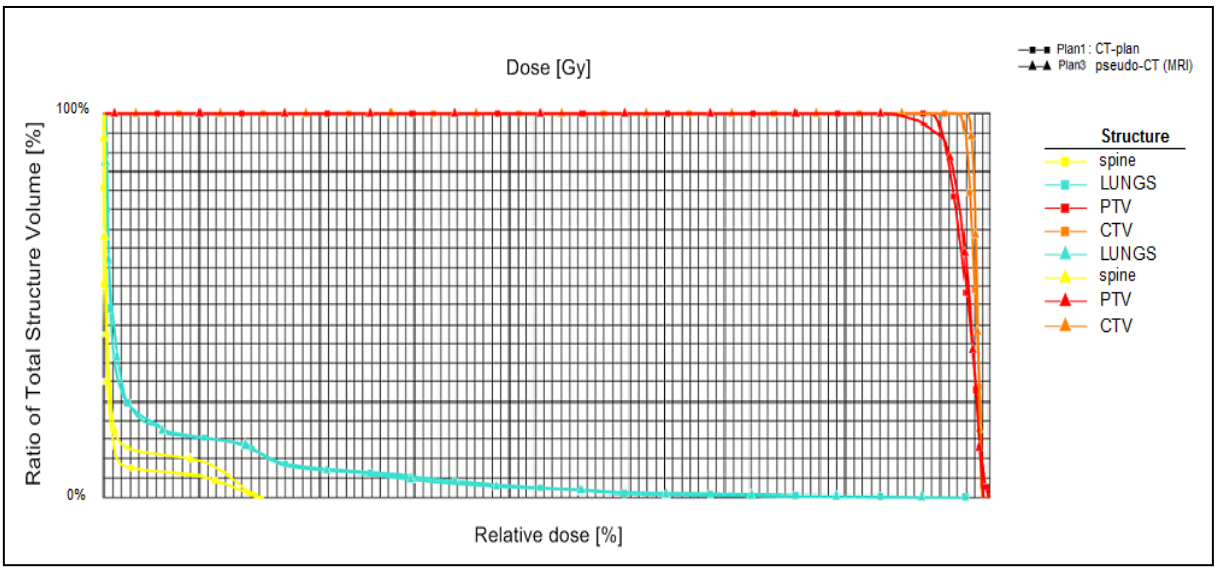

Fig. 4.9- Dose–Volume histograms for Spine, Lungs, planning target volume (PTV) and Clinical Target Volume (CTV) between CT–based plan (plan 1) and MRI–based (wba) plan (plan 3).

Chapter 5

RESULTS AND DISCUSSION

5. Results and discussion

Throughout this project, one of the aspects that most curiosity was aroused to understand what would be the best way to assign the HU distribution in MR images, i.e., on what fundament was based on the choice of the values that were as close as possible the real values obtained from the CT images.

So, one decided to perform two different approaches, in studying real cases of patients already treated: five patients with brain lesions and two with lesions in the prostate (table 5.1), using only the CT images.

Patient No.	Brain	Prostate
1	30	73
2	55	77
3	59	-
4	65	-
5	74	-

Tab. 5.1- Age of patients used in the study.

With planning already done, then were created two new plans, corresponding to each of the approaches, exactly equal to the original plan, which only made the change of HU's.

In the first approach was started by differentiating means, taking into account the three types of materials: water, bone and air, 0HU, 1000HU, and -1000HU, respectively. In this plan was designated CT-wba.

Likewise, the second plane (CT-HU (mean)) has moved the HU, but this time by assigning the mean value of HU. These values were obtained as follows: for each patient and for each of the respective structures was acquired a significant number of HU's along the series of original CT slices, then proceeded to calculate the average of those values . These values were obtained not only for the patients used in the calculation of the dose, but to a larger sample of patients.

In the following figures are presented two graphs which show the HU mean values from each patient: one of these graphics concerns a brain volume (figure 5.1) and the other corresponds to the prostate (figure 5.2). The graphs corresponding to the remaining volumes can be found in appendix B.

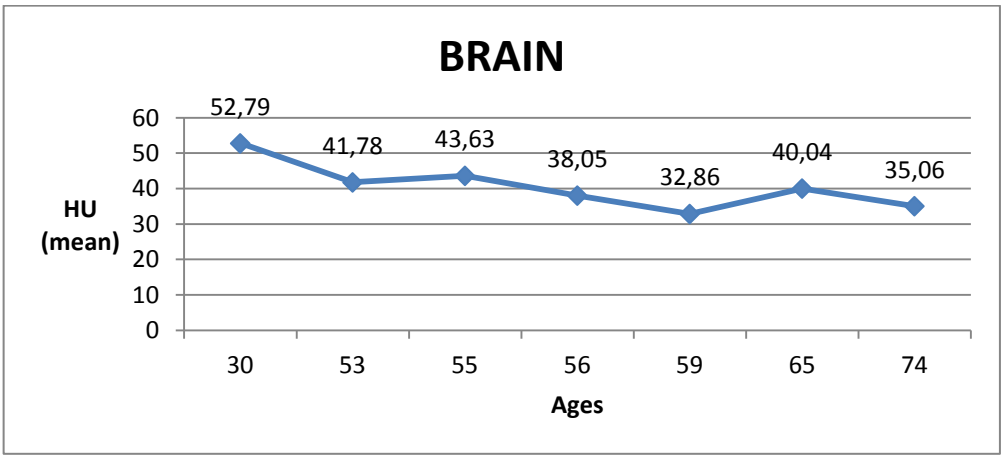

Fig. 5.1- Variation of Hounsfield Units for the brain.

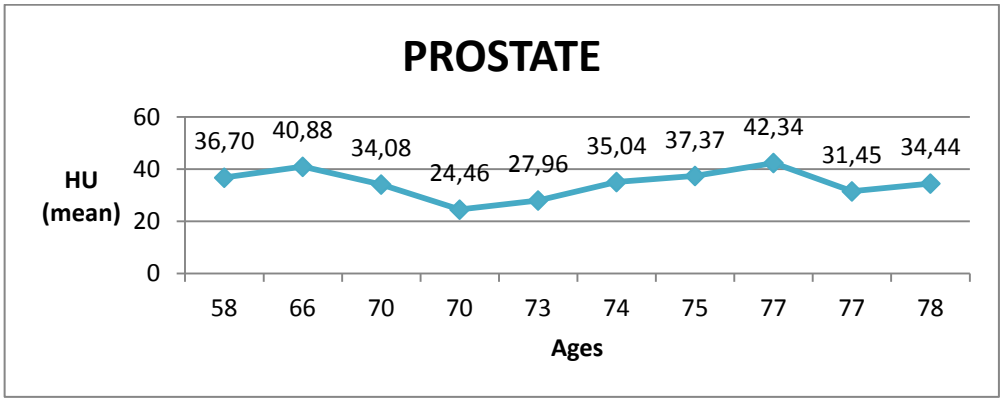

Fig. 5.2- Variation of Hounsfield Units for the prostate.

Considering just the two plans, CT-wba and CT-HU (mean), proceeded to the respective dose calculation, applying the algorithm for calculating AAA.

The results show that both planes have very similar results to those obtained in original CT when referring to the percentage of minimum, maximum and mean dose relative.

The following graphs refer to the results in terms of mean dose for patients with brain lesions. Again, only three volumes are exposed, and the remainders are attached.

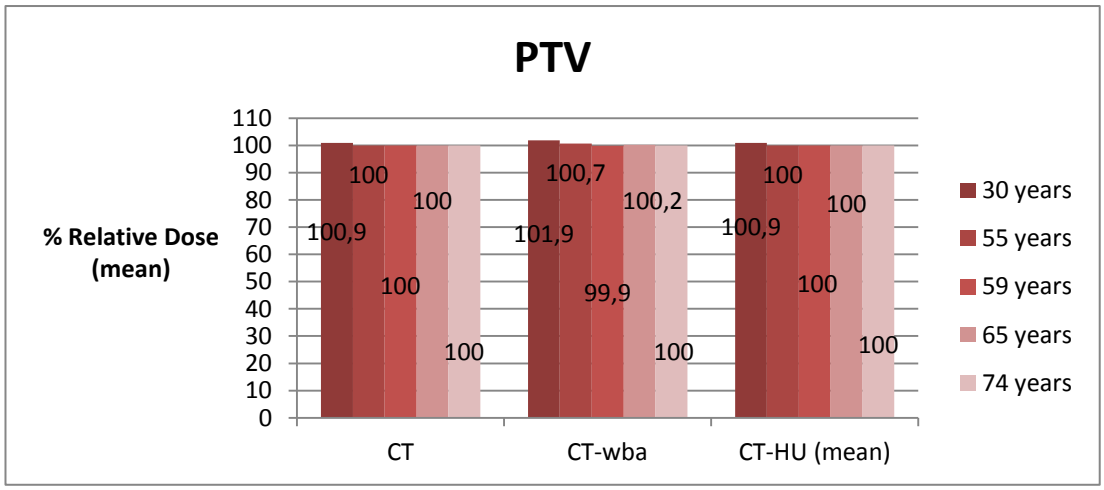

Fig. 5.3- Percentage of Relative Mean Dose between CT, CT-wba and CT-HU (mean) of the PTV in brain lesions.

In the PTV, comparing each one of patients individually, one verifies that the plan using the CT-HU and the CT-wba presents similar results when compared with the one from the original CT.

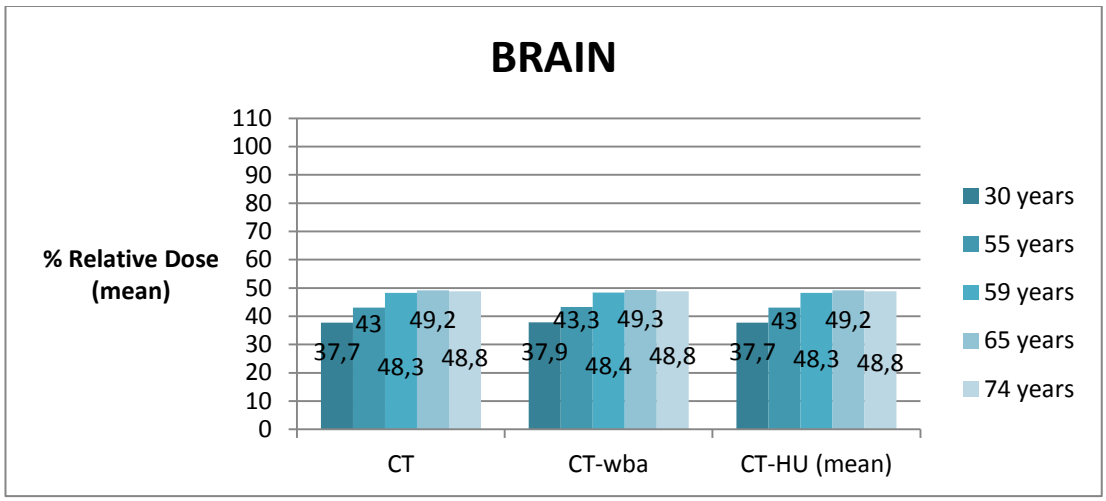

Fig. 5.4- Percentage of Relative Mean Dose between CT, CT-wba and CT-HU (mean) of the brain.

The dose distribution is similar on all the plans for the brain (figure 5.4). Again the differences seem to be clinically insignificant, according with the clinical acceptance criteria of this service, this is, less than 2%.

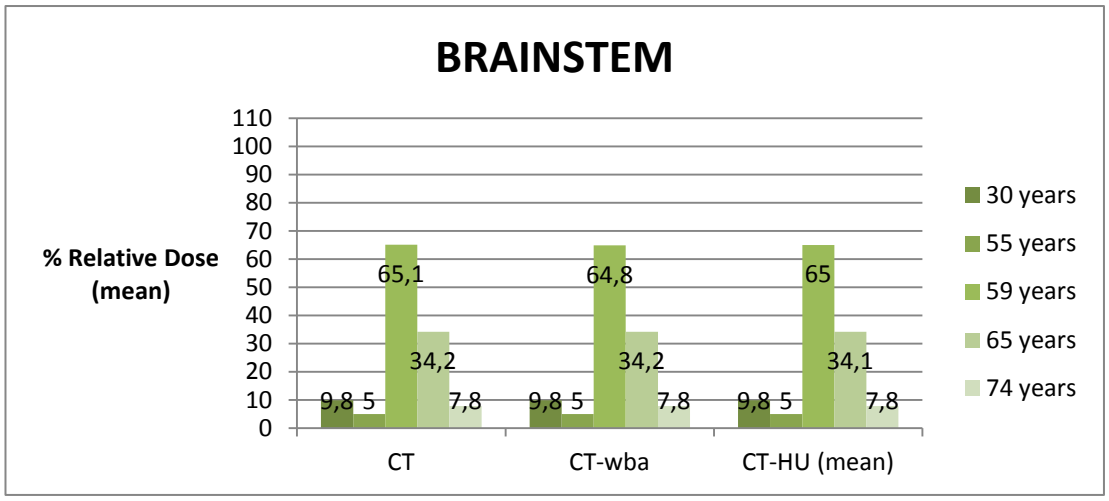

Fig. 5.5- Percentage of Relative Mean Dose between CT, CT-wba and CT-HU (mean) of the brainstem.

In this volume (figure 5.5), one notices that there are no significant differences between the three plans (CT, CT-wba and CT-HU). When compared between patients, the relative dose values present a more pronounced discrepancy due to the different location of the target volume in each patient.

The results in lesions of the prostate show the same conclusions as those obtained in brain lesions (see appendix B).

In general, in all of them it is possible to see that both the plan with segmentation of water, bone and air and the plan by assigning mean HU have negligible differences.

The dose change of the true CT into the modified one (CT-wba and CT-HU) is less than 0.5% in all structures and ~1% at the PTV.

Taking into account all the previous analysis, the methods used in the study followed the same consistency, as seen in the previous chapter. However, the application has been made in the phantom.

The results are listed in table 5.2 for each of the plans performed in terms of percentage relative dose.

Volumes	**Dmin (%)**			**Dmax (%)**			**Dmean (%)**		
	Plan 1	**Plan 2**	**Plan 3**	**Plan 1**	**Plan 2**	**Plan 3**	**Plan 1**	**Plan 2**	**Plan 3**
Lungs	0,1	0,1	0	100,2	98,2	98,3	5,8	5,8	5,7
Spine	0	0	0	18,5	19	18,6	1,2	2	1,9
PTV	95,6	96,1	89,9	102,8	102,7	102,1	100	100	100
CTV	98,6	98,8	100	102,2	102,4	102	98,8	101,2	101,3

Tab. 5.2- Percentage of Relative dose (minimum, maximum and mean) obtained in each of the plans: plan 1-CT, plan 2-MRI (HU mean) and plan 3-MRI (wba).

The analysis of the table, noting the mean relative dose and with reference to the plane 1 (CT-based treatment planning), it is found that:

- ✓ On the second plan the lungs and PTV have the same value, while as for the spine the difference is 0.8%. In the CTV the discrepancy is more significant, about 2.4%. This is due to the fact that the delineation of this structure has been done manually in the pseudo-CT, did not correspond accurately, the positioning of CTV in one plane.

- ✓ In plan 3, the results are different except in the PTV. However, the values move apart more than the values of the plan 2, because the plan 3, allocating the assignment of the HU is not true to the type of material in question.

Considering other studies referenced throughout this work, we note that most of these, overcomes the problem of lack of information from HU, considering the homogeneous environment, which facilitates the assignment of these values during the planning process.

When a comparison is made on the CT –based plan with MRI-based plan, the differences are around about 2% -5% of mean dose for prostate pathologies [Chen *et al.*, 2004], for example.

In this work, assuming the heterogeneities of the environment for pulmonary pathology, the percentage of mean dose values are below 1%, which demonstrates that these results are promising.

This study prove that, for the pathology in question, the manual assignment of values HU or the segmentation of the image into water, bone and air, does not change significantly the results of the dose distribution, indicating that, for the dose calculation algorithm used (AAA), organ differentiation does not seem to be critical for “MRI only” based external radiotherapy treatment planning.

Chapter 6

CONCLUSION AND FUTURE WORK

6. Conclusion and Future Work

The evolution of technology over the years has allowed a substantial improvement in the quality of care in Radiotherapy. It was with this intention that this work emerged.

Increasingly focuses on the quality of images in order to make an accurate treatment planning, eliminating the entire tumor volume, while preserving the quality of life of the patient.

The investigation of the state of the art enabled realizes that there are few published articles on the subject as well as diverse approaches in other countries. Most of them prove that this procedure can be successfully applied. Likewise, the results obtained with the realization of this study confirm precisely the same.

MRI has proven to be the best imaging technique in precise delineation of target volumes, notably in areas of soft tissue.

A major obstacle in the use of MRI in TPS was the lack of information on the electronic density of the tissues, which is essential for calculating the dose. This work demonstrated that this problem can be easily overcome with the manual assignment of Hounsfield Units values.

Nevertheless, there are still some adversities, such as deformities due to inhomogeneities in the image field and the lack of reference images (portal image, OBI ...) during treatment, which must be ascertained that there are no objections to the application.

The results are focused on the feasibility of implementation of MRI as a exclusive technique for the treatment planning dosimetry in external beam radiotherapy, saving an additional CT examination.

The implementation of MRI as an exclusive technique in the treatment plan in External Radiotherapy is still a possibility, not a certainty, in most radiotherapy services in Portugal.

More studies should be conducted in phantoms and real patients for this technique could become integrated into international protocols radiotherapy.

This is the idea that is intended retain, i.e., which extends the study trying to perfect the method, so that, in the very near future, the "MRI only" be applicable in the treatment planning in External Radiotherapy.

REFERENCES

References

Alarcón J I J, *Introducción al Control de Calidad en Radiología Digital: Conectividad DICOM (Tema 5).* Spanish Society of Medical Physics, 2013.

Beavis A W, Gibbs P, Dealey R A, Whitton V J, *Radiotherapy treatment planning of brain tumours using MRI alone*, Br. J. Radiol., 71:544-548, 1998.

Benedict S H, Yenice K M, Followill D, Galvin J M, Hinson W, Kavanagh B, *et al*., *American Association of Physicists in Medicine Radiation Therapy Committee **Task Group 101**: Stereotactic body radiation therapy*, Medical Physics, 37:4078-101, 2010.

Bragg C M, Wingate K, Conway J, *Clinical implications of the anisotropic analytical algorithm for IMRT treatment planning and verification*. Radiother Oncology, 86:276-84, 2008.

Bushberg J T, Seibert J A, Edwin M L, Boone J M, *The Essential Physics of Medical Imaging*, 2nd Edition, Lippincott, Williams and Wilkins, 2002. ISBN: 0-683-30118-7.

Carrasco P, Jornet N, Duch M A, Weber L, Ginjaume M, Eudaldo T, *Comparison of dose calculation algorithms in phantom with lung equivalent heterogeneities under conditions of lateral disequilibrium,* Medical Physics, 31:2899-911, 2004.

Chen L, Price RA Jr, Wang L, Li J, Qin L, McNeeley S, Ma CM, Freedman GM, Pollack A, *MRI-based treatment planning for radiotherapy: dosimetric verification for prostate IMRT*, Int J Radiat Oncol Biol Phys, 60(2):636-647, 2004a.

Chen L, Price RA Jr, Nguyen TB, Wang L, Li JS, Qin L, Ding M, Palacio E, Ma CM, Pollack A. *Dosimetric evaluation of MRI-based treatment planning for prostate cancer,* Phys. Med. Biol., 49(22):5157–70, 2004b.

Chen L, Thai-Binh N, Elan M S, Chen Z, Wei L, Lu W, Price R A, Pollack A and Ma C, *Magnetic resonance based treatment planning for prostate intensity-modulated radiotherapy: creation of digitally reconstructed radiographs*, Int. J. Radiat. Oncol. Biol. Phys. 68(3): 903–911, 2007.

Cherry P, Duxbury A M, *Practical radiotherapy: physics and equipment*, 2nd Edition, Blackwell Publishing Ltd, 2009. ISBN: 978-1-4051-8426-7.

Cozzi L, Nicolini G, Vanetti E, Clivio A, Glashörster M, Schiefer H, *et al.*, *Basic dosimetric verification in water of the anisotropic analytical algorithm for Varian, Elekta and Siemens Linacs,* Medical Physics, 18:128–35, 2008.

DICOM@Offis - Introduction to the DICOM Standard. Available at: http://dicom.offis.de/dcmintro.php.en, Accessed on March, 2013.

Dobler B, Weidner K, Koelbl O, *Application of volumetric modulated arc therapy (VMAT) in a dual-vendor environment*, Radiation Oncology, 5:95, 2010.

Doobs J, Barrett A, Ash D, *Practical Radiotherapy Planning*, 3rd Edition, 1999. ISBN-10: 0340706317.

Doran S J, Charles-Edwards L, Reinsberg S A, Leach M O, *A complete distortion correction for MR images: I. Gradient warps correction,* Phys. Med. Biol. 50:1343–61, 2005.

Dougherty G, *Digital Image Processing for Medical Applications*, Cambridge University Press, 2009. ISBN-13 978-0-521-86085-7.

Dowling J A, Lambert J, Parker J, Salvado O, Fripp J, Capp A, Wratten C, Denham J W, Greer P B, *An Atlas-Based Electron Density Mapping Method for Magnetic Resonance Imaging (MRI)-Alone Treatment Planning and Adaptive MRI-Based Prostate Radiation Therapy*, Int. J. Radiat. Oncol. Biol. Phys. 83(1):e5-e11, 2012.

Dreyer K J, Hirschorn D S, Thrall J H, Mehta A, *PACS: A guide to the digital revolution*, 2nd Edition, Springer, 2006. ISBN-10: 0-387-26010-2.

Dyk J V, Barnett R B, Battista J J, *Modern Technology in Radiation Oncology*, Chapter 8, 2001.

Fogarty G B, Diana Ng, Guilin Liu, Haydu L and Bhandari N, *Volumetric modulated arc therapy is superior to conventional intensity modulated radiotherapy - a comparison among prostate cancer patients treated in an Australian centre,* Radiation Oncology, 6:108, 2011.

Fogliata A, Nicolini G, Vanetti E, Clivio A, Cozzi L, *Dosimetric validation of the anisotropic analytical algorithm for photon dose calculation: Fundamental characterization in water*, Int. J. Radiat. Oncol. Biol. Phys., 51:1421-38, 2006.

Fraass B, Doppke *K*, Hunt M, Kutcher G, Starkschall G, Stern R, Dyk J V, *American Association of Physicists in Medicine Radiation Therapy Committee Task Group 53: Quality assurance for clinical radiotherapy treatment planning*, Medical Physics, Vol. 25, No. 10, 1773-1829,October 1998.

Goldman L W, *Principles of CT and CT Technology,* J Nucl. Med. Technol. 35:115–128, 2007.

Hsieh J, *Computed Tomography: Principles, Design, Artifacts and Recent Advances*, 2nd Edition, John Wiley & Sons, Inc. and SPIE, 2009. ISBN: 978-0-8194-7533-6.

Huang H, *PACS and Imaging Informatics: basic principles and applications,* John Wiley & Sons, Inc, 2004. ISBN: 0-471-25123-2.

International Commission on Radiation Units and Measurements: **ICRU Report No.50.** Prescribing, recording and reporting photon beam therapy. Bethesda, MD: ICRU, 1993.

International Commission on Radiation Units and Measurements: **ICRU Report No.62**. (Supplement to ICRU Report 50). Prescribing, recording and reporting photon beam therapy. Bethesda, MD: ICRU, 1999.

Jacobs M A, Ibrahim T S, Ouwerkerk R, *MR Imaging: Brief Overview and Emerging Applications,* RadioGraphics, 27:1213–1229. 2007

Jonsson J A, Karlsson M G, Karlsson M, Nyholm T, *Treatment planning using MRI data: an analysis of the dose calculation accuracy for different treatment regions*, Radiation Oncology, 5:62, 2010.

Kak A, Slaney M, *Principals of Computerized Tomography Imaging*, SIAM-IEEE Press, 2001. ISBN-10:0-89871-494-X.

Kalender W A, *Computed Tomography: Fundamentals, System technology, Image quality, Applications*, 3rd Edition, Publicis Publishing, 2011. ISBN: 978-3-89578-317-3.

Karlsson M, Karlsson M G, Nyholm T, Amies C, Zackrisson B, *Dedicated Magnetic Resonance Imaging in the Radiotherapy Clinic,* Int. J. Radiation Oncology Biol. Phys., Vol. 74, No. 2, pp. 644–651, 2009.

Koshy M, Pentaleri M, Paryani S, *et al*.,*The Role of MRI in Radiation Therapy Planning*, Siemens Medical Solutions USA, Inc. 2011.

Liang Z-P, Lauterbur P C, *Principles of Magnetic Resonance Imaging: a signal processing perspective*, IEEE Press, 2000. ISBN: 0-7803-4723-4.

Mayles P, Nahum A, Rosenwald J C, *Handbook of radiotherapy physics: Theory and Practice*, Taylor & Francis Group, 2007. ISBN-10: 0-7503-0860-5.

Mazzola A, *Magnetic resonance: principles of image formation and applications in functional imaging*, Revista Brasileira de Física Médica, 3(1):117-29, 2009.

Minniti G, Valeriani M, Clarke E, D'Arienzo M, Ciotti M, Montagnoli R, Saporetti F and Enrici R, *Fractionated stereotactic radiotherapy for skull base tumors: analysis of treatment accuracy using a stereotactic mask fixation system*, Radiation Oncology, 5:1, 2010.

Moerland M A, *Magnetic Resonance Imaging in Radiotherapy Treatment Planning*, Thesis for obtaining the PhD degree at the University of Utrech, Netherlands, 1996.

National Electrical Manufacturers Association (NEMA) -DICOM: Digital Imaging and Communications in Medicine. Available at: http://medical.nema.org/Dicom, Accessed on March, 2013.

NDT Resource Center. Available at: http://www.ndt-ed.org/EducationResources/CommunityCollege/Radiography/Physics/attenuationCoef.htm . Accessed on August, 2013.

Nyholm T, Nyberg M, Karlsson M G, Karlsson M, *Systematisation of spatial uncertainties for comparison between a MR and a CT-based radiotherapy workflow for prostate treatments,* Radiat Oncol, 4:54, 2009.

Papanikolaou N, Battista J, Boyer A, Kappas C, Klein E, Mackie T R, *et al.* *American Association of Physicists in Medicine Radiation Therapy Committee Report no. 85: Tissue inhomogeneity corrections for megavoltage photon beams,* ***Report of Task Group 65*** *of the Radiation Therapy Committee of the American Association of Physicists in Medicine*, 2004.

Pasquier D, Betrouni N, Vermandel M, Lacornerie T, Lartigau E, Rousseau J, *MRI alone simulation for conformal radiation therapy of prostate cancer: technical aspects*, Conf Proc IEEE Eng Med Biol Soc, 1:160-163, 2006.

Podgosark E B, *Radiation oncology physics: a handbook for teachers and students,* Vienna: International Atomic Energy Agency, 2005. ISBN: 92-0-107304-6.

Prabhakar R, Julka P K, Ganesh T, Munshi A, Joshi R C, Rath G K, *Feasibility of using MRI alone for 3D radiation treatment planning in brain tumors*, Jpn J Clin Oncol, 37:405-411, 2007.

RadiologyInfo: *Stereotactic Radiosurgery (SRS) and Stereotactic Body Radiotherapy (SBRT),* Available at: http://www.radiologyinfo.org/en/info.cfm?pg=stereotactic. Accessed on June, 2013.

Reinstein, L E, Amols H I, Biggs, P J, Droege, R T, et al., *American Association of Physicists in Medicine Radiation Therapy Committee Report* No. 24: *Radiotherapy Portal Imaging Quality*, ***Report of Task Group No. 28***, 1988.

Rinck P A, *Magnetic Resonance in Medicine: The Basic Textbook of the European Magnetic Resonance Forum*, Blackwell Science, 4th Edition, 2001.ISBN: 0-632-05986-9.

Roberson P L, McLaughlin P W, Narayana V, Troyer S, Hixson G V, Kessler M L, *Use and uncertainties of mutual information for computed tomography/ magnetic resonance (CT/MR) registration post permanent implant of the prostate*. Med Phys, 32:473-482, 2005.

Ronde H, Hoffmann L, *Validation of Varian's AAA algorithm with focus on lung treatments,* Acta Oncol. 48:209-15, 2009.

Schlegel W, Bortfeld T, Grosu A-L, *Medical Radiology-Diagnostic Imaging and Radiation Oncology: New Technologies in Radiation Oncology*, Springer-Verlag Berlin Heidelberg, 2006. ISBN: 978-3-540-00321-2.

Stanescu T, Jans H and Fallone B G, *Investigation of a 3D MR distortion correction protocol,* Proc. 52nd Annual Meeting of Canadian Organization of Medical Physicists (COMP) (Saskatoon, Canada) pp 36–8, 2006b.

Stanescu T, Jans H S, Pervez N, Stavrev P, Fallone B G, *A study on the magnetic resonance imaging (MRI)-based radiation treatment planning of intracranial lesions,* Phys. Med. Biol. 53:3579–3593, 2008.

Stanescu T, Jans H S, Stavrev P, Fallone B G, *3T MR-based treatment planning for radiotherapy of brain lesions*, Radiol. Oncol. 40(2):125–32, 2006a.

The British Institute of Radiology, *Geometric Uncertainties in Radiotherapy: Defining the Planning Target Volume,* Chapter 1- *Clinical overview of geometric uncertainties in radiotherapy* by J.Doobs, T. Landberg, 2003. ISBN: 0-905749-53-7.

THE DICOM 3.0 STANDARD, *Part 2: Conformance,* ACR-NEMA, PS 3.2-2011.

THE DICOM 3.0 STANDARD, *Part 6: Data Dictionary,* ACR-NEMA, PS 3.6-2011.

The National Institute of Standards and Technology (NIST – Medical Measurement Laboratory) – Hubbell J H and Seltzer S M, *Tables of X-Ray Mass Attenuation Coefficients and Mass Energy-Absorption Coefficients from 1 KeV to 20 MeV for Elements Z = 1 to 92 and 48 Additional Substances of Dosimetric Interest,* NISTIR 5632, 1989, 1990, 1996. Available at: http://www.nist.gov/pml/data/xraycoef/ . Accessed on August, 2013.

Ulmer W, Harder D, *Applications of a triple gaussian pencil beam model for photon beam treatment planning,* Medical Physics, 6:68-74, 1996.

Verbakel W F, Cuijpers J P, Hoffmans D, Bieker M, Slotman B J, Senan S, *Volumetric intensity-modulated arc therapy vs. conventional IMRT in head-and-neck cancer: a comparative planning and dosimetric study*, Int. J. Radiat. Oncol. Biol. Phys., 74(1):252-259, 2009.

Wasik M W, Rudoler S , Preston P E, Hauck W W, Downes B M , Leeper D, Andrews D, Corn B W, Curran W J, *Immediate side effects of stereotactic radiotherapy and radiosurgery,* Int. J. Radiat. Oncol. Biol. Phys., 43(2):299-304, 1999.

Webb A G, *Introduction to Biomedical Imaging,* Wiley-IEEE Press, 2003.ISBN: 978-0-471-23766-2.

Webster J G, *Encyclopedia of Medical Devices and Instrumentation*, Wiley, 6 Volume Set, 2nd Edition, 2006. ISBN: 978-0-471-26358-6.

APPENDIX

APPENDIX A

A.1 Script for 'Camouflage' MR images in CT images

```
%%%%%%%%%%%%%%%%%%%%%%%%%%%%%%%%%%%%%%%%%%%%%%%%%%%%%%%%%%%%%%%%%%%%%%%
%                                                                     %
%                                                                     %
%              Script for 'Camouflage' MR images in CT images         %
%                                                                     %
%                                                                     %
%                                                                     %
%Using Magnetic Resonance Images for planning treatments in External %
%                                                                     %
%     Radiotherapy- validation procedures for planning "MRI only      %
%                                                                     %
%                                                                     %
%                                                                     %
%   Ana Catarina Freire Moreira, Master's degree in Medical Physics  %
%                                                                     %
%                  FCUP & IPO PORTO, EPE  2013                        %
%                                                                     %
%                                                                     %
%                                                                     %
%                                                                     %
%%%%%%%%%%%%%%%%%%%%%%%%%%%%%%%%%%%%%%%%%%%%%%%%%%%%%%%%%%%%%%%%%%%%%%%
%                                                                     %
% Adapted from: 'Create-data.m' by Anne Katrine Duun-Christensen and %
% Sune                                                                %
% Kristian Buhl                                                       %
%                                                                     %
%        Technical University of Denmark / University of Copenhage   %
%                                                                     %
%%%%%%%%%%%%%%%%%%%%%%%%%%%%%%%%%%%%%%%%%%%%%%%%%%%%%%%%%%%%%%%%%%%%%%%

clc, clear all, close all

% Set path for the CT and MRI scans:
path_CT = 'C:\Users\Utilizador\Desktop\SE0\CT';
path_MR= 'C:\Users\Utilizador\Desktop\SE0\MR';

% Set path for temp folder:
path(path, 'C:\Users\Utilizador\Desktop\SE0\temp');

% Set patient and scanning ID variables:
  ID = '111111';
  GivenName = 'FICTITIOUS';
  FamilyName = 'FICTITIOUS';
  Study_date = '2013';
  Series_date = '2013';
  Study_time = '111111';

% Setting variable used through the code:
path(path, path_CT);
inputdir_CT = path_CT;
```

```
path(path, path_MR);
inputdir_MR = path_MR;

Dicomfiles_CT = dir(fullfile(inputdir_CT,'*.dcm'));
Dicomfiles_MR = dir(fullfile(inputdir_MR,'*.dcm'));

% Loading local CTtemplate.dcm:
originalCT = dicominfo('IM1ct.dcm');

% Creating new UNIQUE dicom UID's:
uid1 = dicomuid;
uid2 = dicomuid;
uid3 = dicomuid;

% Loading original MR-images and saving (via Dicomwrite) with the CT-
dicom:

for p = 1:length(Dicomfiles_MR)
    fname = Dicomfiles_MR(p).name;
    info = dicominfo(fname); %Reading dicom info
    t = (dicomread(fname));
    s = info.InstanceNumber;
    dicomwrite(t,['C:\Users\Utilizador\Desktop\SE0\temp\temp'
num2str(s) '.dcm'],originalCT,'CreateMode','create');

   % Saving MRI variables to be added to the MRasCT images:
    BitDepth = info.BitDepth;
    BitsStored = info.BitsStored;
    HighBit = info.HighBit;
    coor = info.ImagePositionPatient;
    orien = info.ImageOrientationPatient;
    location = info.SliceLocation;
    pixelspace=info.PixelSpacing;
    slicethickness = info.SliceThickness;
    SeriesTime_MR=info.SeriesTime;
    SeriesNumber_MR=info.SeriesNumber;
    StudyID_MR=info.StudyID;
    PatientBirthDate_MR=info.PatientBirthDate;
    PatientSex_MR=info.PatientSex;
    StudyDescription_MR=info.StudyDescription;
    PatientID_MR=info.PatientID;
    PatientName_MR=info.PatientName;
    %FamilyName_MR=info.FamilyName;


    % Loading info on the 'CT' (MR) images:
    infoMR_to_CT = dicominfo(['temp' num2str(s) '.dcm']);

    % Setting MRasCT variables:

    infoMR_to_CT.PatientID=PatientID_MR;
    infoMR_to_CT.PatientName=PatientName_MR;
    infoMR_to_CT.FamilyName=FamilyName_MR;
    infoMR_to_CT.StudyDescription=StudyDescription_MR;
    infoMR_to_CT.PatientSex = PatientSex_MR;
    infoMR_to_CT.PatientBirthDate = PatientBirthDate_MR;
    infoMR_to_CT.SeriesTime = SeriesTime_MR;
    infoMR_to_CT.SeriesNumber = SeriesNumber_MR;
    infoMR_to_CT.PatientID = ID;
```

```
    infoMR_to_CT.PatientName.GivenName = GivenName;
    infoMR_to_CT.PatientName.FamilyName = FamilyName;
    infoMR_to_CT.StudyID = StudyID_MR;
    infoMR_to_CT.SeriesInstanceUID = uid1;
    infoMR_to_CT.StudyInstanceUID = uid2;
    infoMR_to_CT.SOPInstanceUID = uid3;
    infoMR_to_CT.MediaStorageSOPClassUID ='1.2.840.10008.5.1.4.1.1.2';
    infoMR_to_CT.MediaStorageSOPInstanceUID = uid3;
    infoMR_to_CT.SliceLocation = location;
    infoMR_to_CT.SliceThickness = slicethickness;
    infoMR_to_CT.ImagePositionPatient = coor;
    infoMR_to_CT.ImageOrientationPatatient = orien;
    infoMR_to_CT.BitDepth = BitDepth;
    infoMR_to_CT.PixelSpacing = pixelspace;
    infoMR_to_CT.BitsStored = BitsStored;
    infoMR_to_CT.HighBit = HighBit;
    infoMR_to_CT.RescaleIntercept = 0;
    infoMR_to_CT.RescaleSlope = 9;

    % Saving final MRasCT images:
    dicomwrite(t,['C:\Users\Utilizador\Desktop\SE0\CT\'
num2str(s)'.dcm'],infoMR_to_CT,'CreateMode','create');


end
```

APPENDIX B

B.1 Graphics

B.1.1 Percentage of Relative Dose (mean)

B.1.1.1 Prostate Tumors

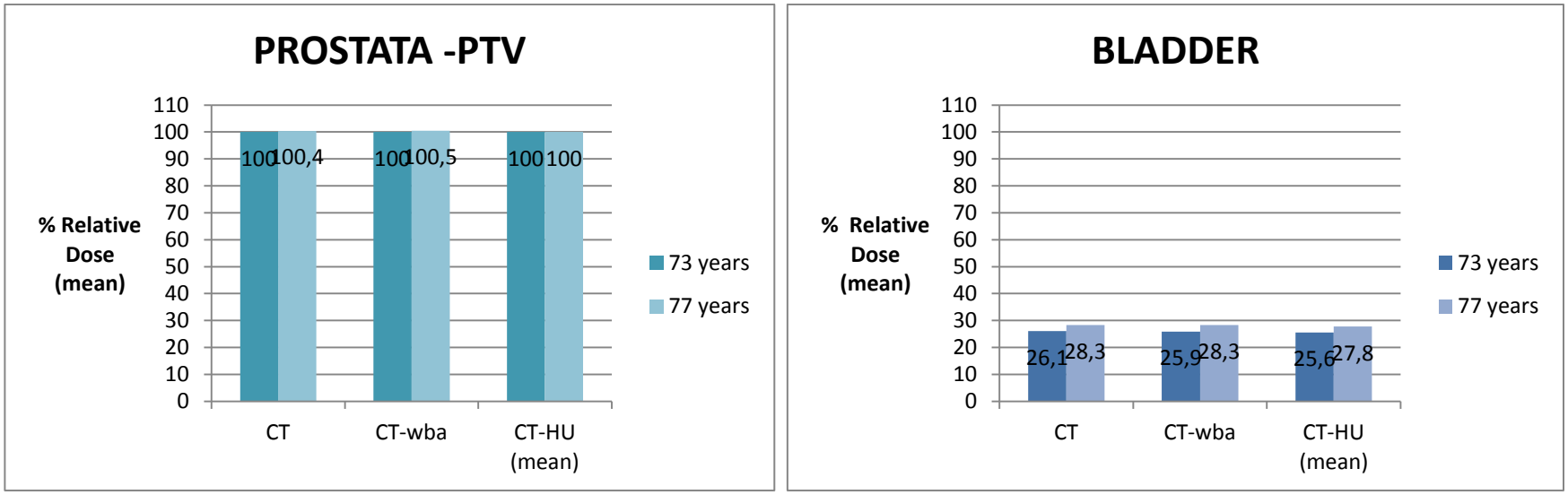

Graphs 1- Percentage of Relative Mean Dose between CT, CT-wba and CT-HU (mean) of the prostate and the bladder.

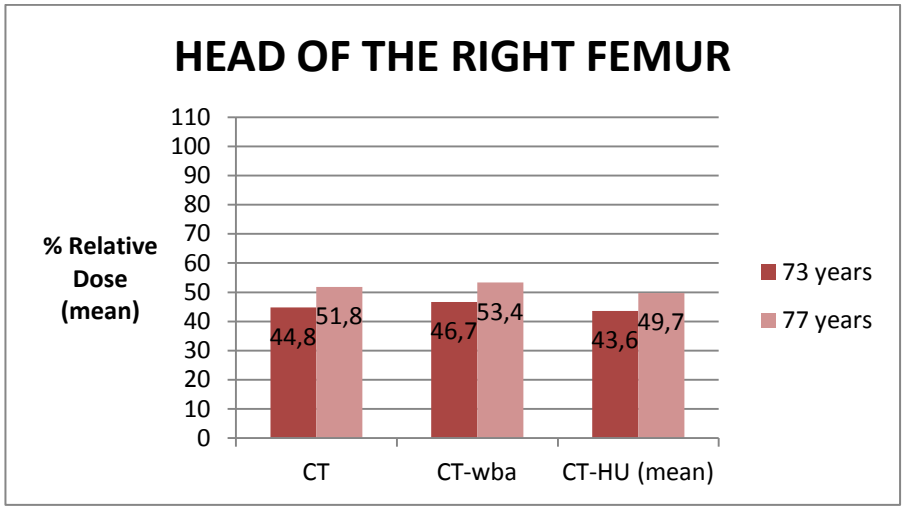

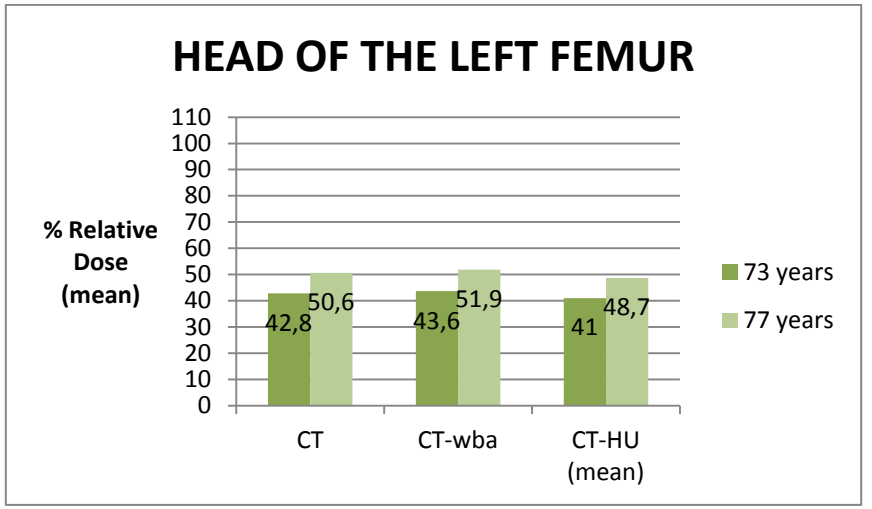

Graphs 2- Percentage of Relative Mean Dose between CT, CT-wba and CT-HU (mean) of the head of right and left femur.

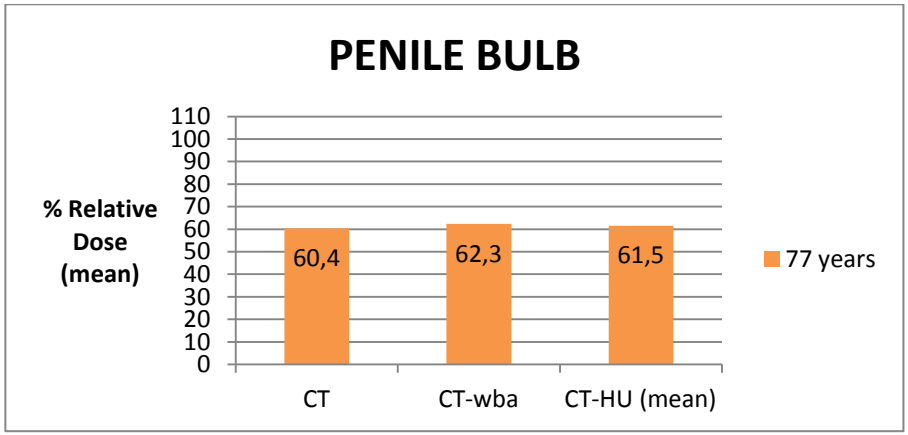

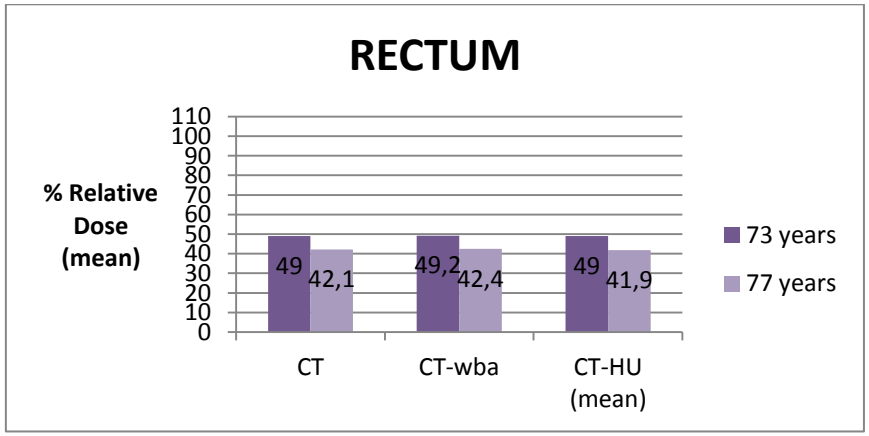

Graphs 3- Percentage of Relative Mean Dose between CT, CT-wba and CT-HU (mean) of the penile bulb and the rectum.

B.1.1.2 Brain Tumors

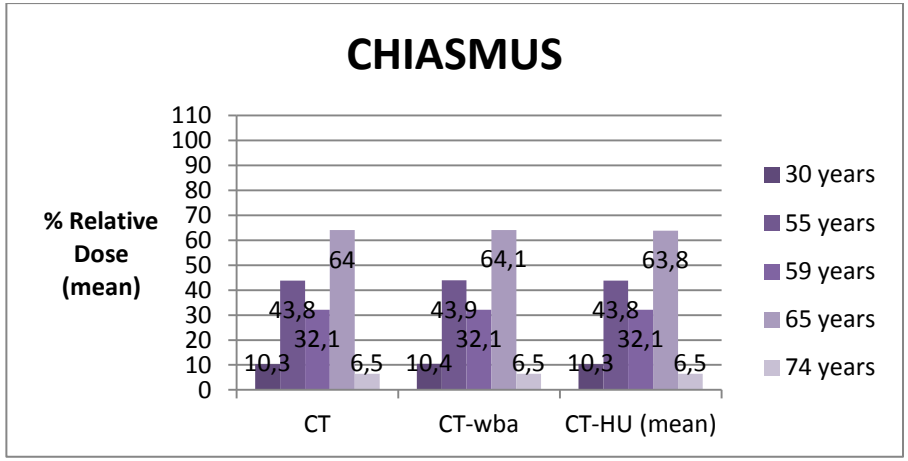

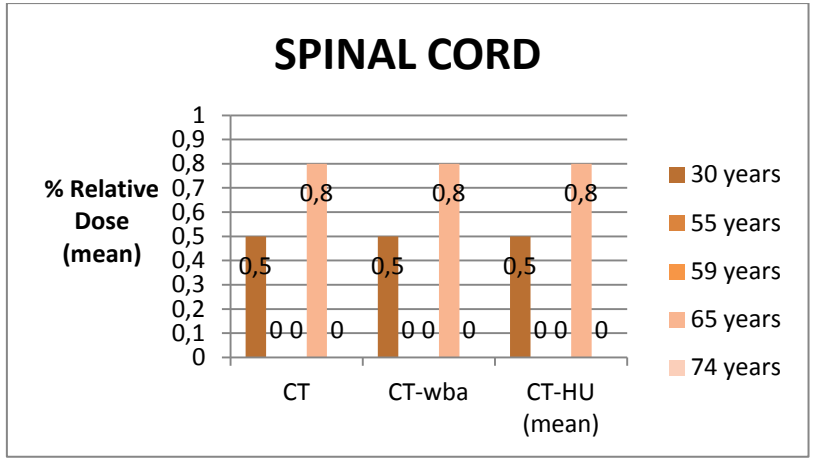

Graphs 4- Percentage of Relative Mean Dose between CT, CT-wba and CT-HU (mean) of the chiasmus and the spinal cord.

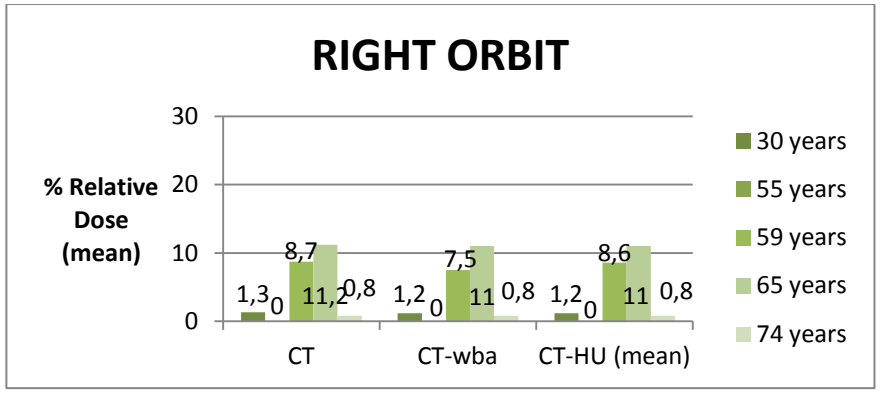

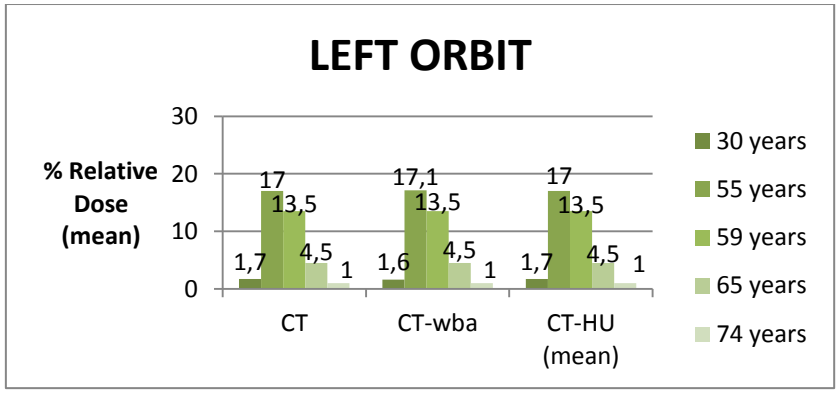

Graphs 5- Percentage of Relative Mean Dose between CT, CT-wba and CT-HU (mean) of the right and left orbit.

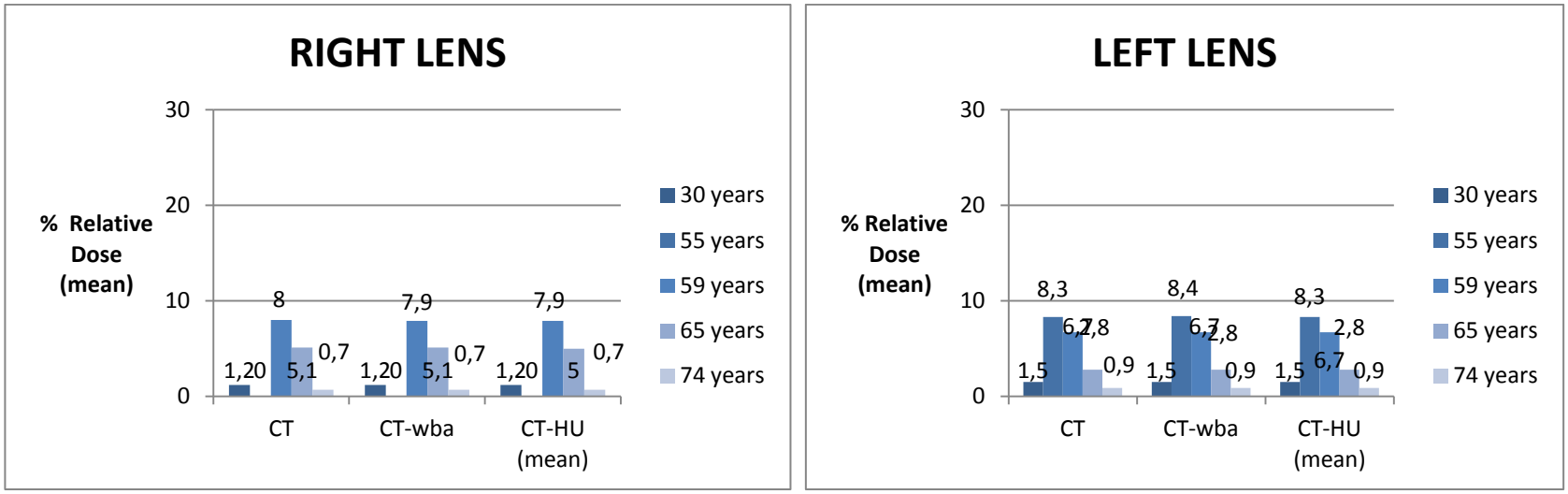

Graphs 6- Percentage of Relative Mean Dose between CT, CT-wba and CT-HU (mean) of the right and left lens.

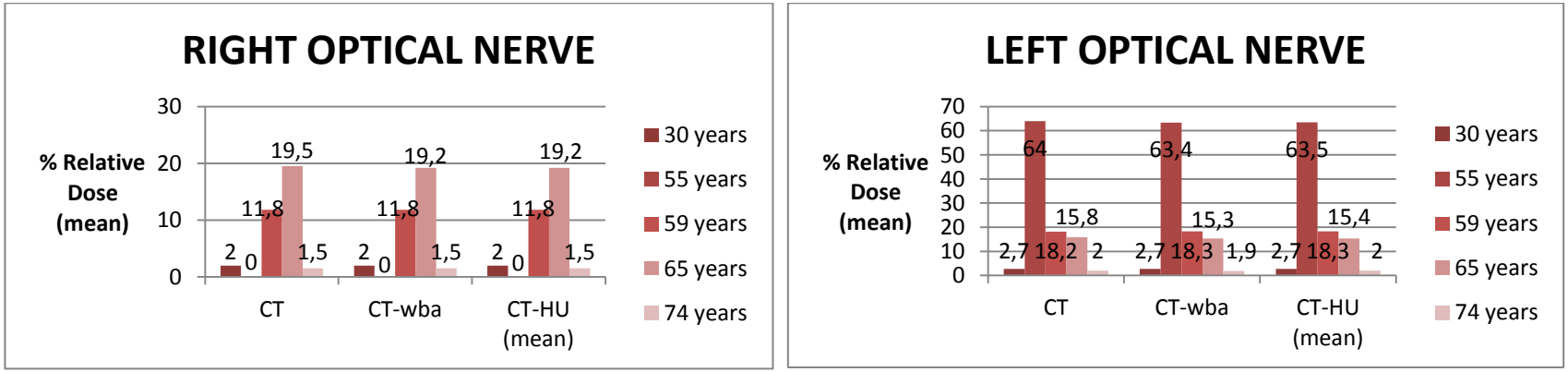

Graphs 7- Percentage of Relative Mean Dose between CT, CT-wba and CT-HU (mean) of the right and left optical nerve.

B.1.2 Variation of Hounsfield Units according to the patients' age

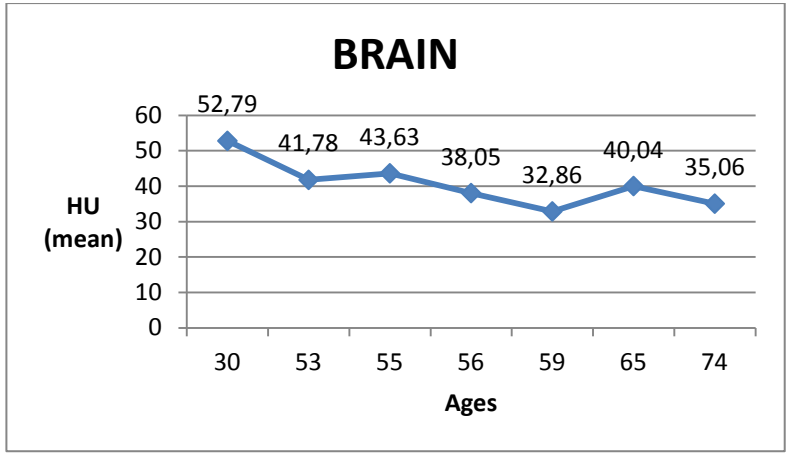

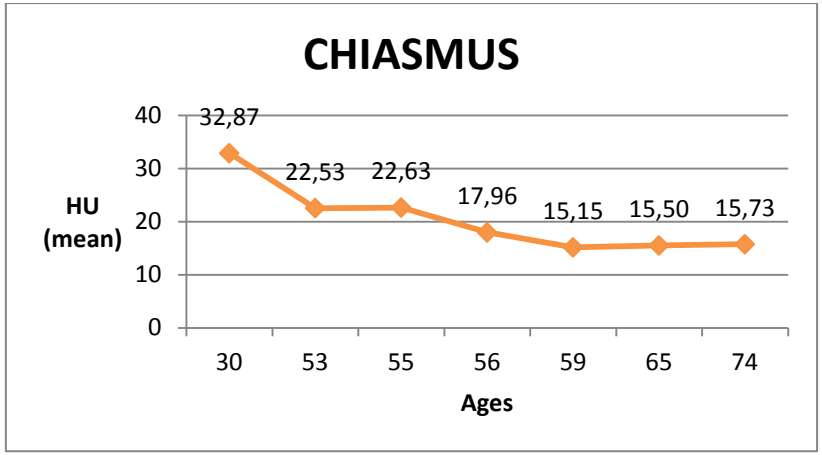

Graphs 8- Variation of Hounsfield Units of the brain and the chiasmus.

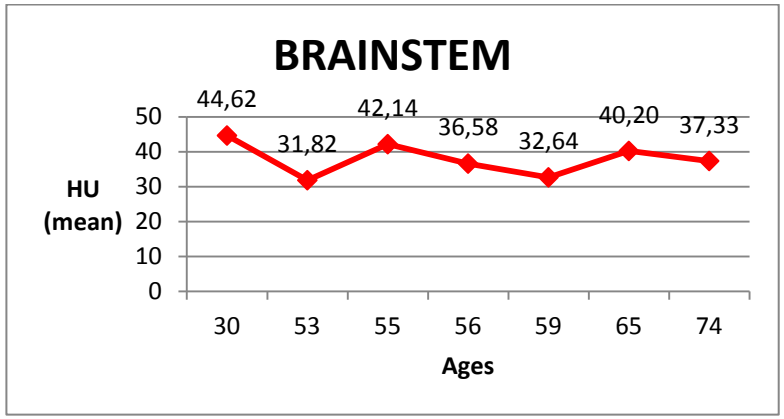

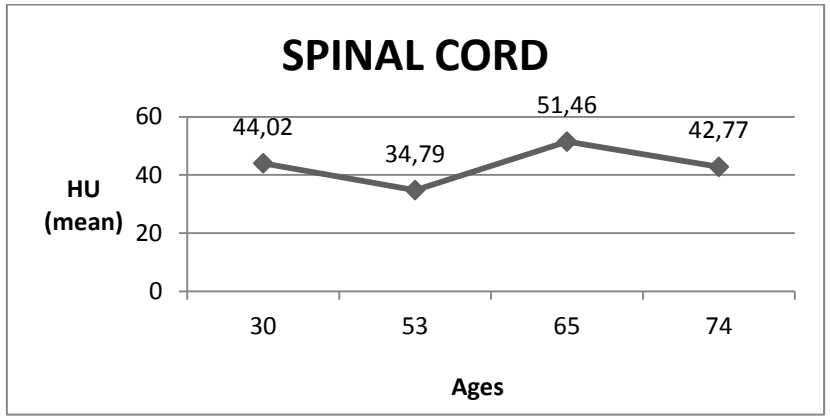

Graphs 9- Variation of Hounsfield Units of the brainstem and the spinal cord.

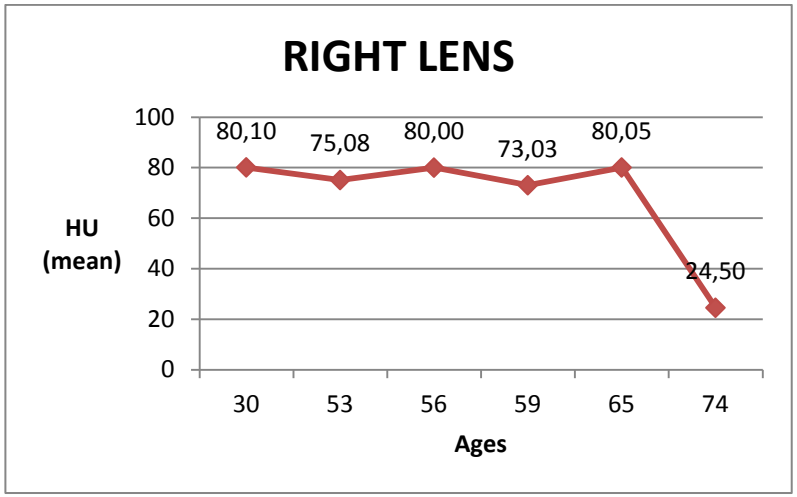

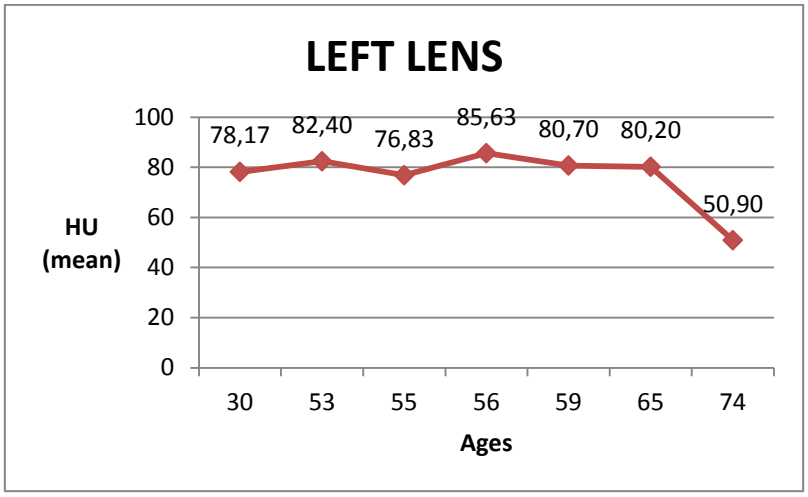

Graphs 10- Variation of Hounsfield Units of the right and left lens.

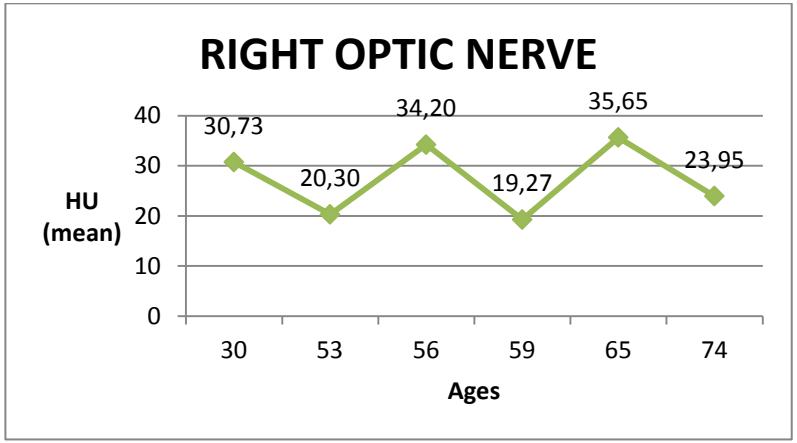

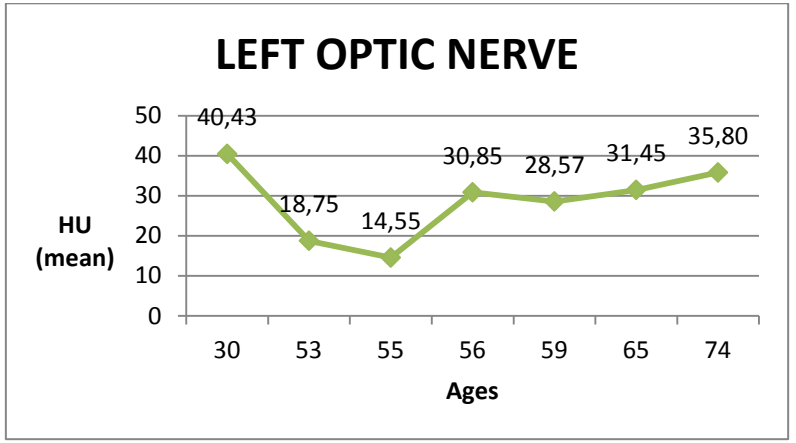

Graphs 11- Variation of Hounsfield Units of the right and left optic nerve.

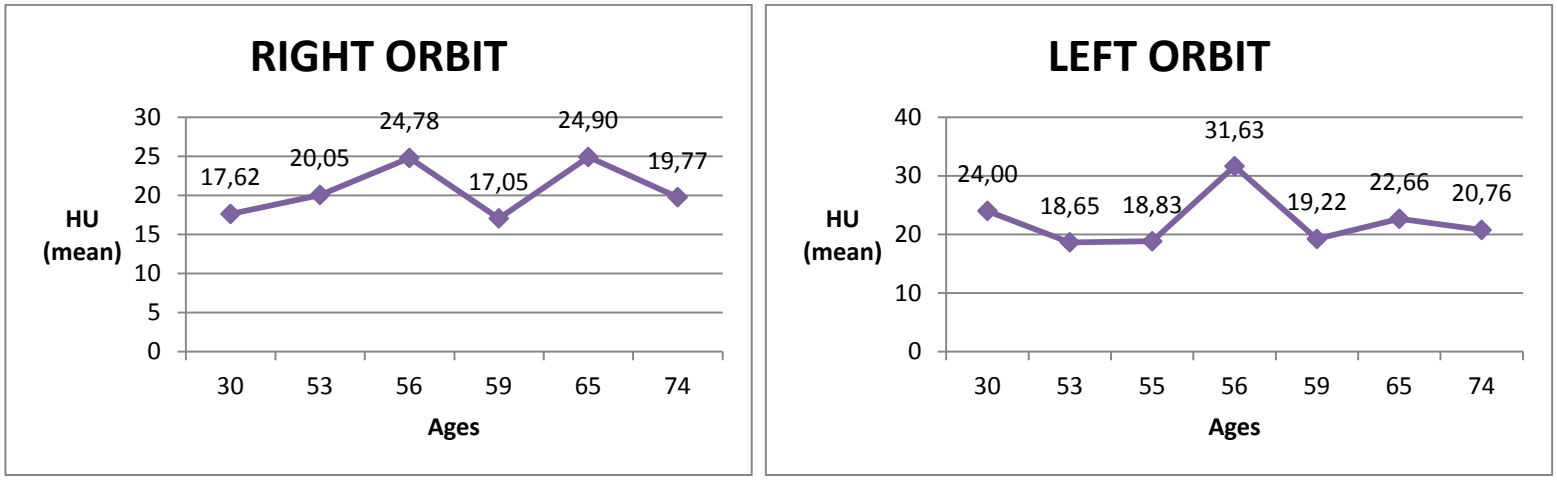

Graphs 12- Variation of Hounsfield Units of the right and left orbit.

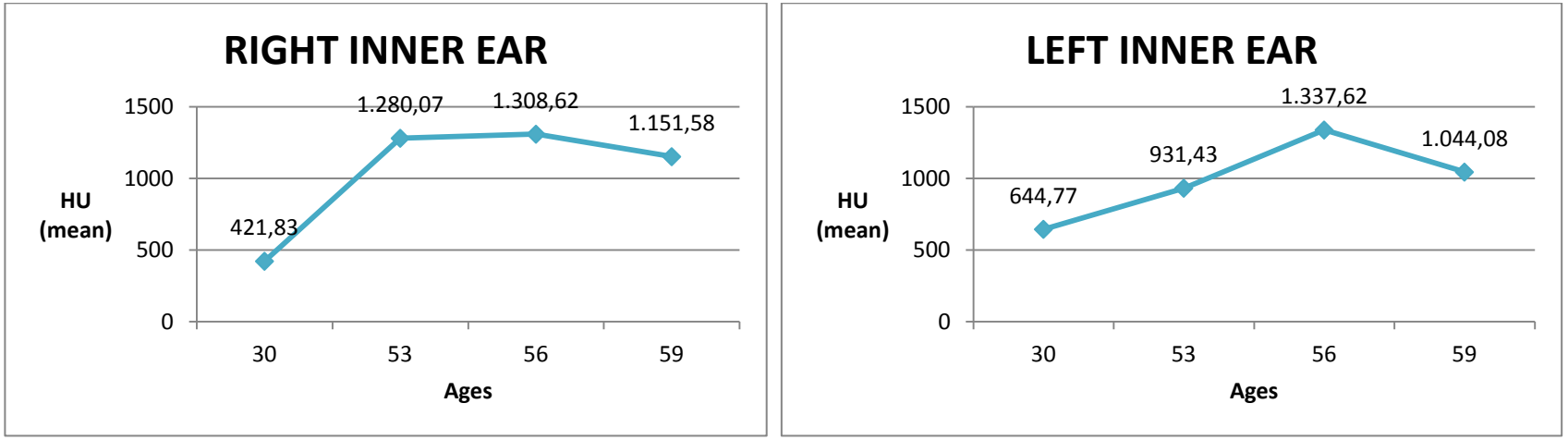

Graphs 13- Variation of Hounsfield Units of the right and left inner ear.

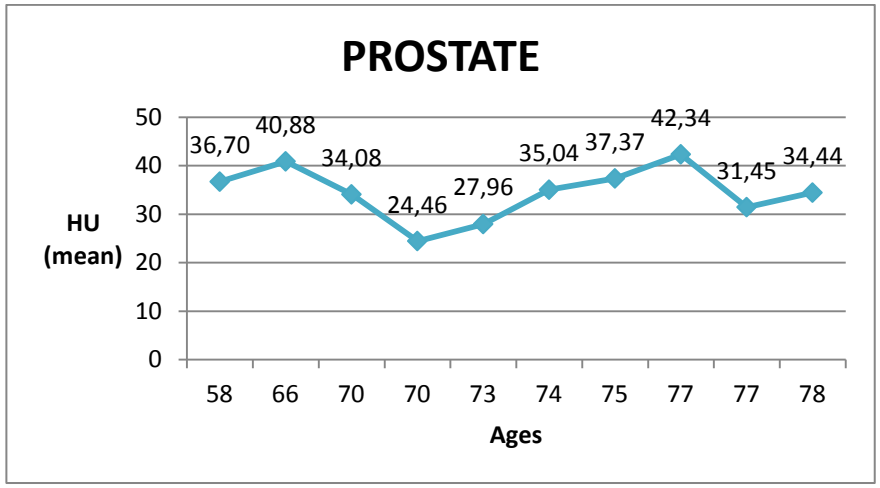

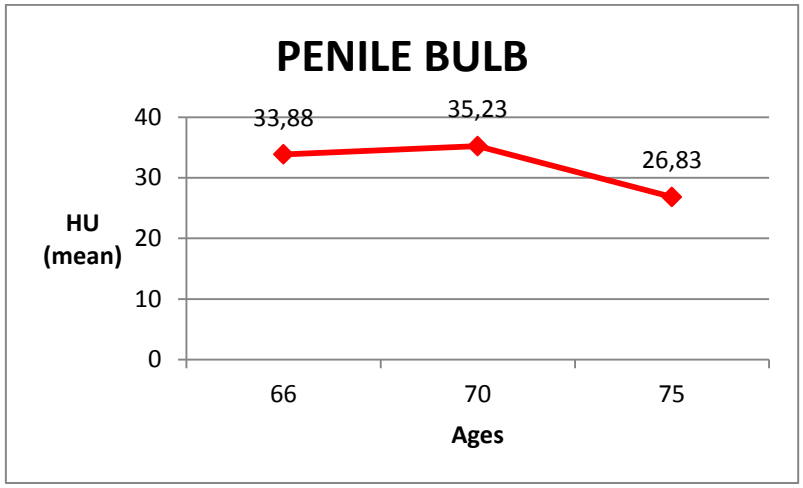

Graphs 14- Variation of Hounsfield Units of the prostate and the penile bulb.

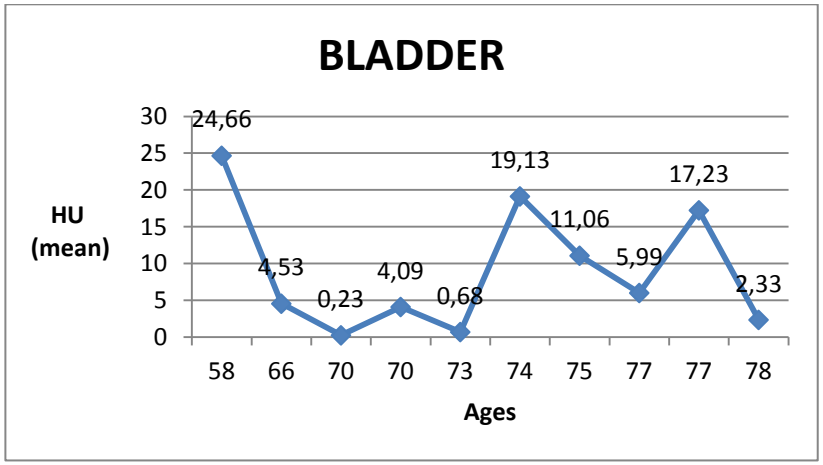

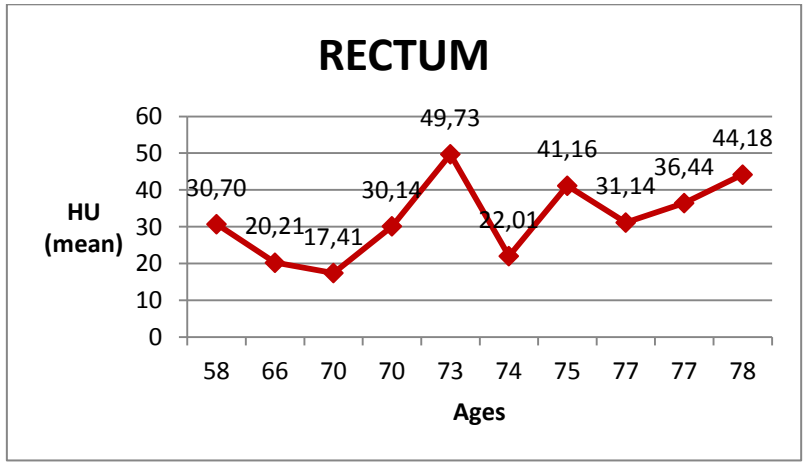

Graphs 15- Variation of Hounsfield Units of the bladder and the rectum.

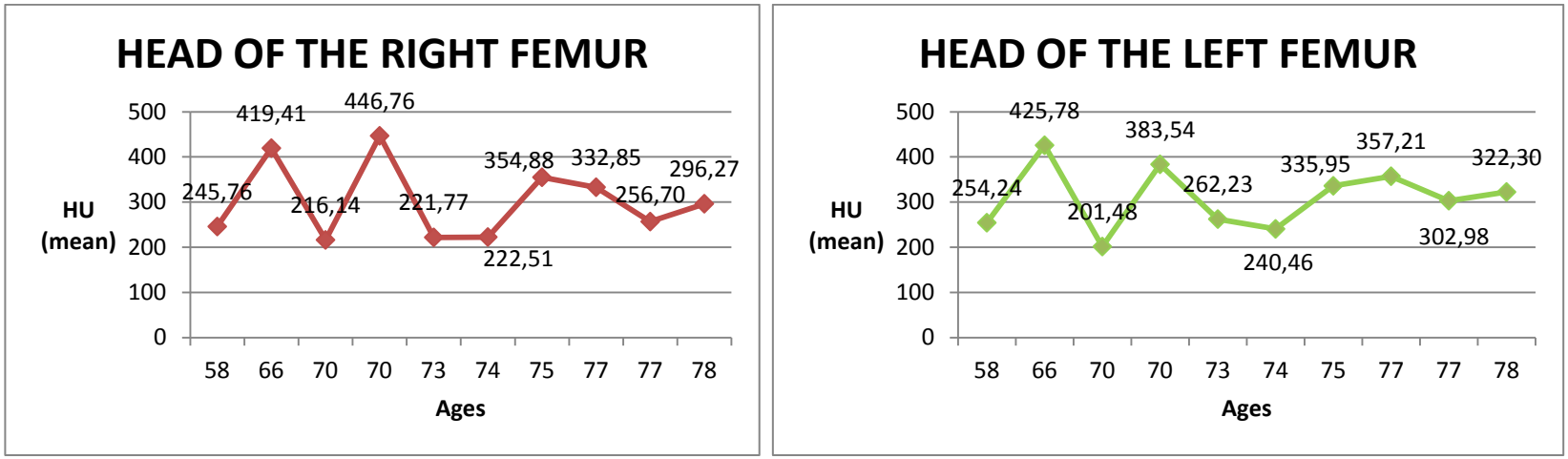

Graphs 16- Variation of Hounsfield Units of the head of the right and left femur.